FFI-rapport 2015/02324

Fragmentation of 40 mm shell with 6 different compositions – 4 melt cast and 2 press filled

Gunnar Ove Nevstad

FFI Forsvarets forskningsinstitutt

FFI-rapport 2015/02324

Fragmentation of 40 mm shell with 6 different compositions – 4 melt cast and 2 press filled

Gunnar Ove Nevstad

Norwegian Defence Research Establishment (FFI)

2 December 2015

FFI-rapport 2015/02324

120503

P: ISBN 978-82-464-2794-2
E: ISBN 978-82-464-2795-9

Keywords

Testing

Fragmentering

Approved by

Ivar Sollien	Research Manager
Jon Eilif Skjervold	Director

English summary

In the EDA project B-0585-GEM2-GC “Formulation and Production of New Energetic Materials” different nitropyrazoles for use in melt cast compositions have been studied, in addition to GA/BAMO polymers, for use as binder in propellants and pressed explosive charges. Norway’s main activity was in synthesis of GA/BAMO polymers to coat nitramine crystals, coated crystals or granules applied for press filling of munition units or production of pressed charges.

Norway was the only country that used their energetic binders for explosive compositions. Italy and Germany used their polymers in propellant formulations. The compositions we have studied with high content of HMX will have their primary application as boosters or as main fillings for shaped charges. France, Sweden and the Czech Republic studied melt cast compositions based on pyrazoles to replace TNT. To study the performance of these compositions, generic testing was required. Selected test vehicles were for propellants 2inch rocket motors, and for melt cast compositions 40 mm shells. With our pressed fillings Norway joined the group performing fragmentation testing.

Ten 40 mm shells filled with six different compositions have been detonated to study the fragmentation ability. Four melt cast compositions, two containing DNAN and two containing TNT, have been tested. The last two compositions were press filled HMX compositions with energetic GA/BAMO binder. The HMX content for Sats 400/13 was 94.7 wt. % and for Sats 432/13 it was 94.3 wt. %. These two compositions contained an energetic binder developed at FFI. The four melt cast compositions were developed and filled by Chemring Nobel. Their names and nominal content was MCX-6002 TNT/NTO/RDX (34/51/15), MCX-6100 DNAN/NTO/RDX (32/53/15), MCX-8001 TNT/NTO/HMX (36/52/12), and MCX-8100 DNAN/NTO/HMX (35/53/12).

To stop the fragments, eight witness aluminium plates of 2 mm thickness was set up in a stack with a 25 mm gap between each plate. The plate width was1000 mm and the height was 2000 mm. 50 mm along all edges was not used in the fragment counting. The effective target area was therefore 900 mm x1900 mm. The witness plates were during evaluation divided into 100 mm high evaluation zones in the vertical direction. This gave 19 evaluation zones. We counted both fragment hits and penetrations.

The number of fragments penetrating the first witness plate was lowest for the MCX-6100 composition with 55 for both shells. The highest number of fragments was obtained for the HMX/GA/BAMO compositions, with 103 fragments for Sats 400/13 and 114 fragments for Sats 432/13. All compositions gave fragments penetrating 5 witness plates. Only one shell, filled with the MCX-6100 composition, had fragments penetrating all eight witness plates. Shells producing the lowest number of fragments have the highest penetration abilities. Both DNAN containing compositions, MCX-6100 and MCX-8100, gave fewer fragments than the corresponding TNT compositions, MCX-6002 and MCX-8001. The melt cast compositions with RDX gave on average fewer fragments than the corresponding HMX compositions.

Sammendrag

I EDA-prosjektet B-0585-GEM2-GC "Formulation and Production of New Energetic Materials" har ulike nitropyrazol-baserte smeltestøpte komposisjoner blitt studert, i tillegg til GA/BAMO-polymerer for bruk i krutt og pressefylte ladninger. Norges hovedaktivitet var syntese av GA/BAMO-polymerer for belegging av nitraminkrystaller, belagte krystaller eller granulat for pressefylling av ammunisjon eller produksjon av retta ladninger.

Norge var det eneste landet som benyttet energirike bindemiddel i sprengstoffkomposisjoner. Italia og Tyskland benyttet sine energirike bindemiddel i kruttkomposisjoner. Norge har studert komposisjoner med høyt innhold av HMX med primær anvendelse som booster eller hovedfylling i retta ladninger. Den andre delen av prosjektgruppen studerte smeltestøpte komposisjoner basert på pyrazoler til erstatning av TNT. For studie av virkning var det påkrevet med generisk testing. For krutt ble 2-toms rakettmotorer, og for smeltestøpte komposisjoner 40 mm granater, valgt som testobjekter for å studere brennhastighet og fragmenteringsegenskaper. Med våre pressa fyllinger valgte Norge å delta i gruppen som utførte fragmenteringstesting.

Ti 40 mm granater fylt med seks forskjellige komposisjoner ble fylt og omsatt for studier av fragmenteringsevnen. Fire smeltestøpte komposisjoner, hvorav to inneholdt DNAN og to inneholdt TNT, ble testet. De to siste komposisjonene inneholdt HMX og energirikt bindemiddel, GA/BAMO, og ble fylt ved pressing. HMX-innholdet i Sats 400/13 var 94,7 vektprosent, og i Sats 432/13 94,3 vektprosent HMX. Disse to komposisjonene inneholdt energirikt bindemiddel syntetisert ved FFI. De fire smeltestøpte komposisjonene var utviklet og fylt i granatene av Chemring Nobel. Betegnelse for disse samt nominell sammensetning er MCX-6002 TNT/NTO/RDX (34/51/15), MCX-6100 DNAN/NTO/RDX (32/53/15), MCX-8001 TNT/NTO/HMX 36/52/12) og MCX-8100 DNAN/NTO/HMX (35/53/12).

For å stanse fragmentene ble det benyttet en stabel på åtte 2 mm tykke aluminiumsplater med en avstand på 25 mm mellom hver plate. Platene hadde en bredde på 1000 mm og en høyde på 2000 mm. 50 mm rundt alle kanter var ikke med i arealet for opptelling av antall fragmenter. Vitneplatene ble under evalueringen delt inn i 100 mm høye soner i vertikal retning. Dette ga totalt 19 soner. Både fragmenttreff og gjennomslag ble registrert.

Antall penetrerende fragmenter for den første vitneplaten var lavest for granatene fylt med MCX-6100-komposisjon. Begge granatene med MCX-6100 ga 55 fragmenter som penetrerte plate nr. 1. Flest fragmenter ble oppnådd for granatene fylt med HMX/GA/BAMO-komposisjonene. Granaten med Sats 400/13 ga 103 penetrerende fragmenter, mens granaten fylt med Sats 432/13 ga 114 penetrerende fragmenter, i den nærmeste platen.

Alle granatene uavhengig av sprengstoffylling ga fragmenter som penetrerte fem vitneplater. Kun en granat, fylt med MCX-6100, ga fragmenter som penetrerte alle åtte vitneplatene. De granatene som ga færrest fragmenter, har den største penetrasjonsevnen. Komposisjonene med DNAN, MCX-6100 og MCX-8100 gir færre fragmenter enn tilsvarende TNT-komposisjoner, MCX-6002 og MCX-8001. Granater fylt med smeltestøpte komposisjoner med RDX gir noe færre fragmenter enn tilsvarende komposisjoner med HMX.

Contents

Abbreviations

BAMO	3,3-Bis-azidomethyl oxetane
DNAN	2,4-dinitroanisole
GA	Glycidyl azide
GA/BAMO	Glycidyl azide- (3,3-bis(azidomethyl)oxetane) copolymers
HMX	Octahydro-1,3,5,7-tetranitro-1,3,5,7-tetraazacyclooctane
IM	**I**nsensitive **M**unitions
IMX-104	**I**nsensitive **M**elt cast **E**xplosive No 104
IPDI	Isophorone di-isocyanate
MCX	**M**elt **C**ast **E**xplosive
MCX-6002	TNT/NTO/RDX (34/51/15)
MCX-6100	DNAN/NTO/RDX (32/53/15)
MCX-8001	TNT/NTO/HMX (36/52/12)
MCX-8100	DNAN/NTO/HMX (35/53/12)
NTO	3-Nitro-1,2,4 Triazol 5-one
PAX-48	**P**icatinny **A**rsenal e**X**plosive No 48
PETN	Pentaerythritol tetranitrate
RDX	Hexogen/1,3,5 -trinitro-1,3,5-triazacyclohexane
TMD	**T**heoretical **M**aximum **D**ensity
TNT	2,4,6-trinitrotoluene
WP	**W**ork Package

1 Introduction

In the EDA project B-0585-GEM2-GC “Formulation and Production of New Energetic Materials”, different melt cast compositions based on different nitropyrazoles and GA/BAMO polymers for use as binder in propellants and pressed explosives charges have been studied (1). Norway’s main activity has been in synthesis of GA/BAMO polymers suitable for coating nitramine crystals, coated crystals or granules applied for press filling of munition units or production of pressed charges.

Norway was the only country that used their energetic binders for explosive compositions. Italy and Germany used their polymers in propellant formulations (2-4). The compositions we have produced, with high content of HMX will have their primary applications as boosters or as main fillings for shaped charges. France, Sweden and Czech Republic studied melt cast compositions based on pyrazoles to replace TNT. To evaluate the performance of these compositions a generic fragmentation test of 40 mm shells was selected.

To broaden the number of compositions in the generic fragmentation testing in WP 4000, Norway included 4 melt cast compositions. These compositions, two with TNT and two with DNAN as binder and a filler of NTO/RDX or NTO/HMX mixtures, are all of interest for Norway as main filling preferentially for large calibre munitions. These compositions have in addition to fragmentation performance been characterized for important properties as detonation velocity, detonation pressure and critical diameter (5-8). In addition, for the two RDX containing compositions the shock sensitivity has been determined in Intermediate Scale GAP-test (9-10).

In this report we will report on the fragmentation ability in 40 mm shells of two GA/BAMO/HMX press filled compositions and 4 melt cast compositions. The two GA/BAMO/HMX compositions were: Sats 400/13: 5.3 % 40/60 GA/BAMO/IPDI (2) + 94.7 % HMX, and Sats 432/13: 5.7 % 50/50 GA/BAMO/IPDI + 94.3% HMX. These compositions were selected mainly due to the pressing properties (8). Both compositions have high detonation velocity and detonation pressure. The 4 included melt cast compositions were produced by Chemring Nobel; MCX-6002, MCX-6100, MCX-8001 and MCX-8100. We had access to 10 shells only and decided to use two on each of the melt cast compositions and one on each of the two selected press filled compositions. The difference in energy for the two press filled compositions is small.

The test arrangement used for fragmentation was design by BAE System and the firings were supported by them. In addition, except for the witness plates, all hardware was supported by BAE system to avoid test differences been the different test facilities. Testing was performed in France, Sweden and Czech Republic in addition to Norway. A stack of 8 Al-plates (2000 mm x 1000 mm x 2 mm) was used to stop the fragments. Analysis of penetrations and hits of fragments in each plate was performed with a predetermined method. All 4 countries participating in the fragmentation study used the same setup and analysis method to avoid interpretation variations.

2 Experimentally

2.1 Hardware

The shells used in the fragmentation tests were procured from BAE Systems in Karlskoga Sweden. These were old shells taken from stock for which the original explosive filling was melted out by Nammo Liab. The design and properties of the shell is given in Figure 2.1.

BAE Systems Bofors AB article no 01 168 527 (gen. drwg. 05 196 795).

Shell material designation

Bofors AB:	W3-1970-60.
Germany:	DIN 1651, 45S20.
GB:	BS 970:Part 1:1972 212M44.

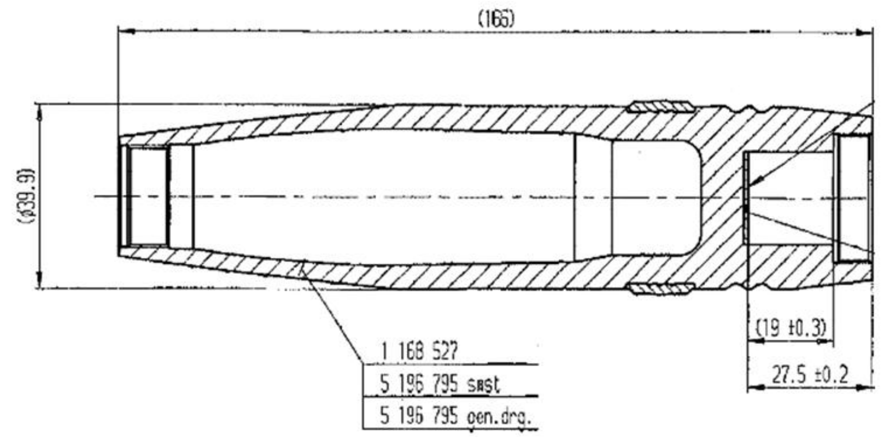

Figure 2.1 Drawing of the 40 mm shell used in the fragmentation testing.

The material properties for the shell are given in Appendix A. Figure 2.2 shows the test arrangement for detonating the shell. The shell was placed on a polycarbonate plate with a central hole for a plug going into the tracer well. This plug fixed the position of the shell both in horizontal and vertical direction. To position the detonator in the centre of the shell a polycarbonate plug was used. This plug had a hole with diameter equal to the diameter of the detonator and an outer diameter equal to the opening of the shell.

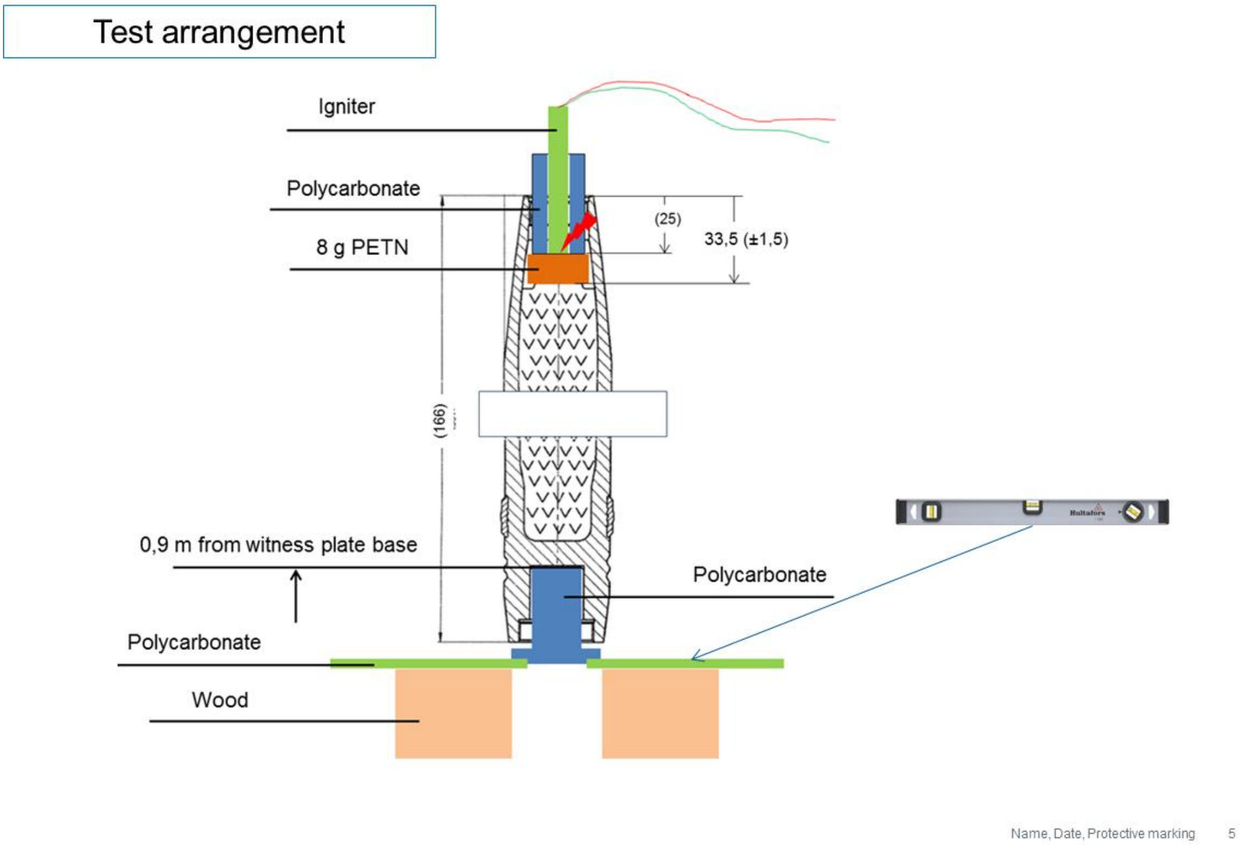

Figure 2.2 Test setup of the 40 mm shell for fragmentation testing.

2.2 Filling of shells

The shells containing melt cast compositions were filled by Chemring Nobel. After the compositions were melted and heated to 100-102 ^{o}C they were filled into the shells. Before filling, the shells had been stored in an incubator at the same temperature over the night. The filled shells were stored in the incubator for 2 hours. The solidification - cooling process of the casted items took then place at room temperature.

Figure 2.3 shows shells No 1 to No 4, filled with MCX-6100 and MCX-8100, as received from Chemring. Figure 2.4 shows the shells filled with TNT based compositions MCX-6002 and MCX-8001. The shells filled with Sats-400/13 and Sats-432/13 was pressed filled at FFI by use of the press shown in Figure 2.11. The filling process was done in several steps by addition of 20 g between each press cycle.

Figure 2.3 DNAN filled shells, with MCX-6100 number 1 and 2 from left and with MCX-8100 composition number 3 and 4 from left.

Figure 2.4 TNT filled shells, left with MCX-6002 and right with MCX-8001composition.

2.3 X-ray

All shells filled with melt-cast compositions were X-rayed to see what quality the cast had with regard to density. Figure 2.5 shows a picture of the x-ray film at 0^o. The shells are from left to right No 1 to No 8.

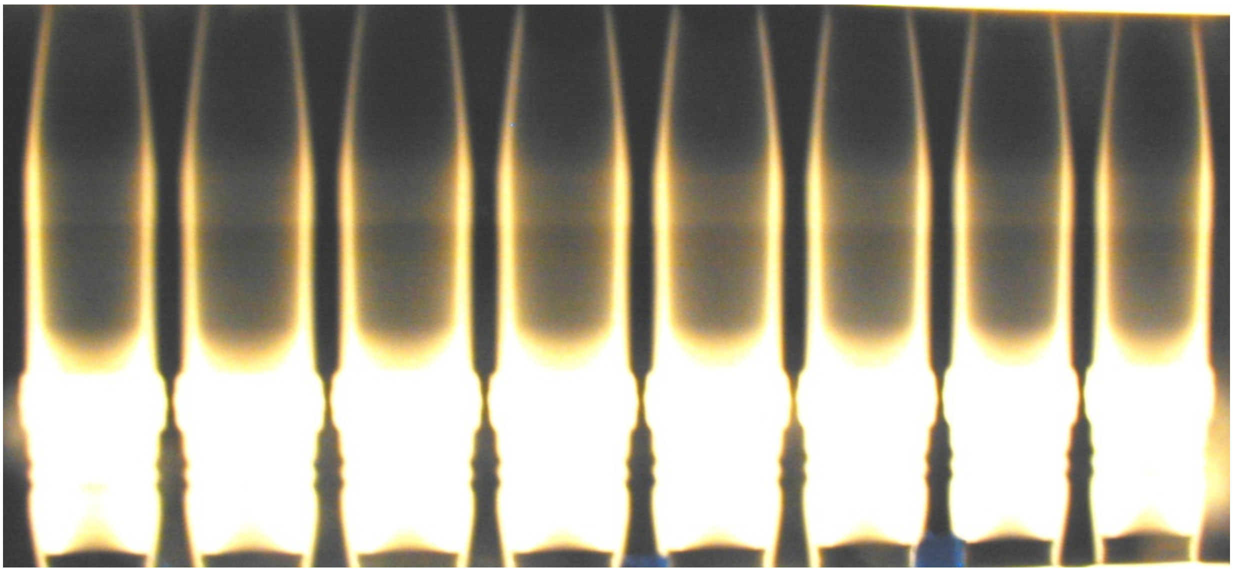

Figure 2.5 X-ray image of the 8 melt cast filled shells at 0°.

Figure 2.6 shows a picture of the X-ray image after the shells were turned 90°. Finally, Figure 2.7 shows a magnified picture of shells No 3 to No 5. Shell No 3 and shell No 4 were both filled with MCX-8100 composition while shell No 5 was filled with the MCX-6002 composition. All fillings seem to be homogeneous with some bubbles. There are no significant differences between DNAN and TNT based fillings with respect to filling quality. The observed bubbles are randomly distributed.

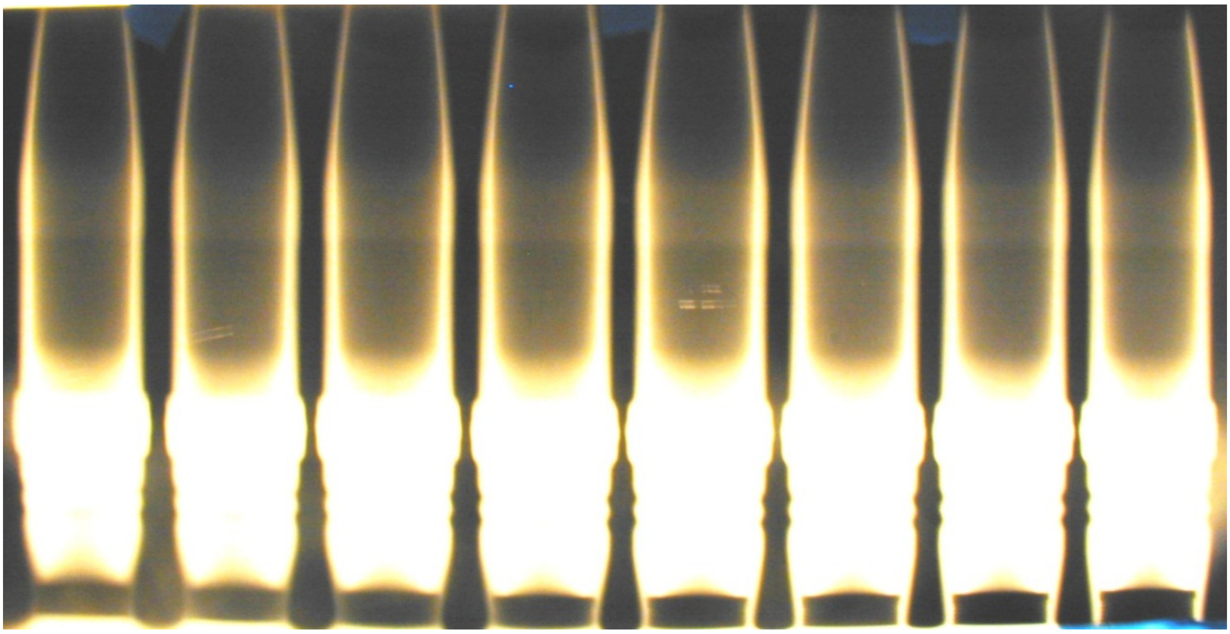

Figure 2.6 X-ray image of the 8 melt cast filled shells at 90°.

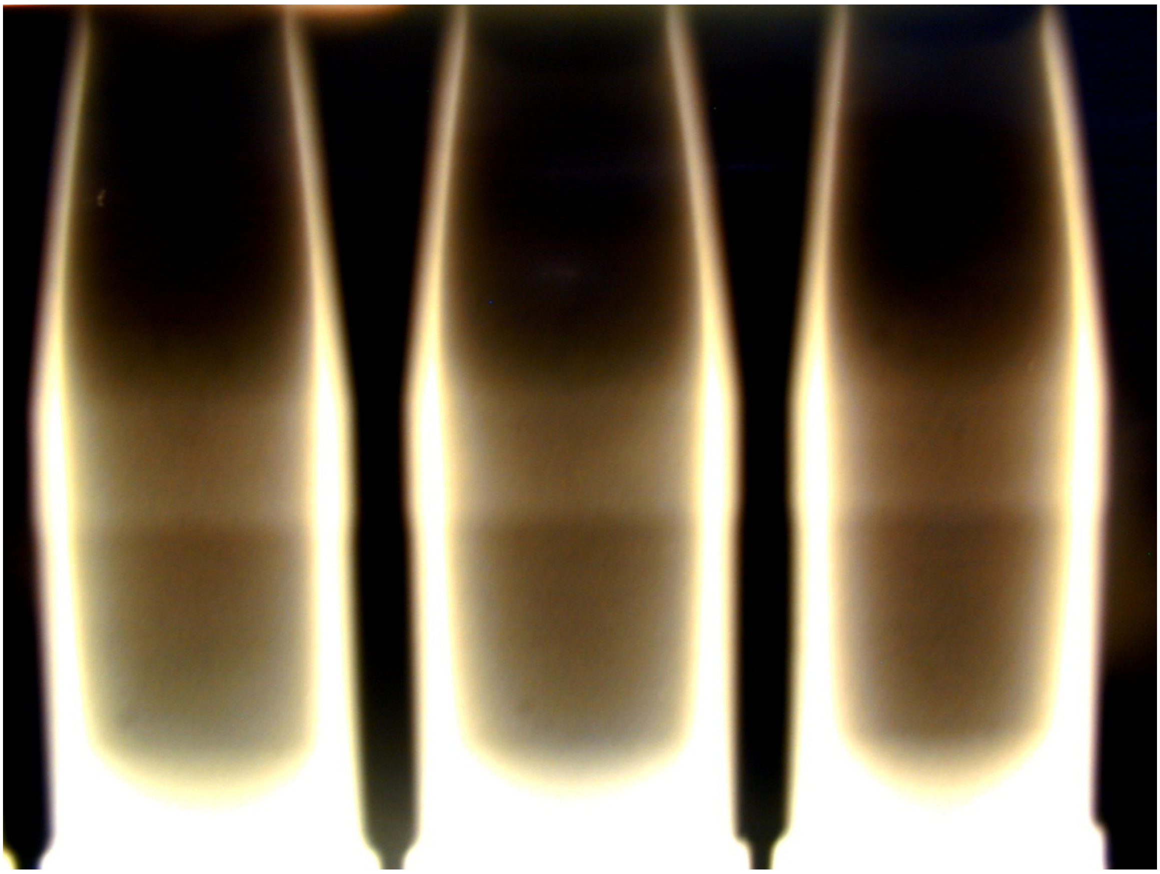

Figure 2.7 Magnified picture showing from left, shell No 3 to shell No 5.

2.4 Machining

After being X-rayed the filling in each shell was reduced to give space for the booster with a height of 33 $\pm$ 0.3 mm, Figures 2.9 and 2.10. Figure 2.8 shows a picture of the lathe we used for this operation. The machining was performed by manual turning.

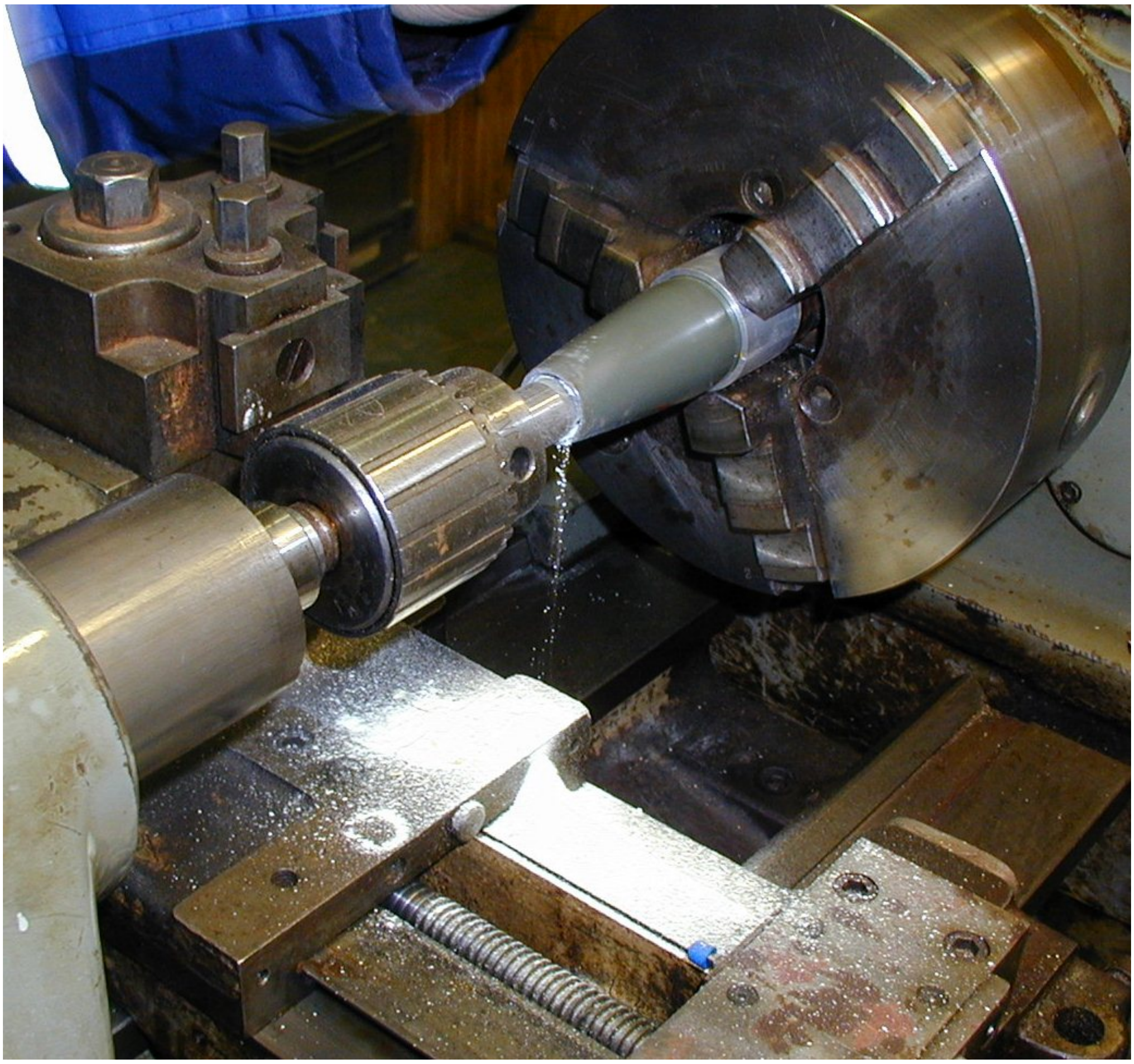

Figure 2.8 Picture of the lathe used for producing the fuze well.

Figure 2.9 The DNAN filled shells after modification: from left No 1 and No 2 containing MCX-6100 composition, No 3 and No 4 containing MCX-8100 composition.

Figure 2.10 The TNT filled shells after modification: from left shell No 5 and No 6 containing MCX-6002, No 7 and No 8 containing MCX-8001 composition.

Figure 2.11 The pictures show the press used for filling, and the shells after being filled with Sats 400/13 and Sats 432/13 compositions.

2.5 Density of fillings

The received empty shells were weighted. Volume was measured by weighing of water filled shells. The density of the fillings was calculated from the difference in mass between empty and filled shells and the measured volume. Table 2.1 summarizes the results. There is some variation in the filling quality. Shell No 1, No 2 and No 5 have the lowest % of TMD (Theoretical Maximum Density). Table 2.2 gives TMD for all tested compositions in addition to theoretical detonation velocities and pressures calculated by Cheetah (11) and the BKWC product library. Appendix D gives the summary printouts for Sats 400/13 and Sats 432/13 at different densities. Experimentally detonation velocities and pressures have been determined for all compositions and are summarized in Table 2.2 (5-8). The experimentally results are obtained at densities different from TMD.

Shell No	Composition	Empty weight (g)	Weight with filling (g)	Weight of filling (g)	Density (V=57 cm^3) (g/cm^3)	Density (V=57.3 cm^3) (g/cm^3)
1	6100	764.90	863.55	98.65	1.731	1.722
2	6100	763.57	862.52	98.95	1.736	1.727
3	8100	763.34	863.41	100.07	1.756	1.746
4	8100	763.30	863.94	100.64	1.766	1.756
5	6002	764.32	864.12	99.80	1.751	1.742
6	6002	758.00	860.27	102.27	1.794	1.785
7	8001	760.01	864.27	104.26	1.829	1.820
8	8001	764.76	868.4	103.64	1.818	1.809
9	S 400/13*	762.44	867.44	105.00	1.842	1.832
10	S 432/13*	765.74	870.14	104.40	1.832	1.822

**BAMO/GA/IPDI-HMX: Sats 400/13:5.3 % 40/60 GA/BAMO/IPDI (2) + 94.7 % HMX,*
Sats 432/13: 5.7 % 50/50 GA/BAMO/IPDI + 94.3% HMX

Table 2.1 The table gives the fillings and densities for tested shells.

Properties	MCX-6002	MCX-6100	MCX-8001	MCX-8100	Sats 400/13	Sats 432/13
Theoretical density (g/cm^3)	1.7997	1.7629	1.8087	1.7650	1.8571	1.8530
Filling density Shell (1) (g/cm^3)	1.742	1.722	1.820	1.746	1.832	1.822
Shell (2) (g/cm^3)	1.785	1.727	1.809	1.756		
Det. Pressure Calculated*(GPa)	26.53	24.54	26.59	24.19	36.43	36.16
Det. Pressure Measured (GPa)	24.72	19.0±0.7	24.58	20.82	28.2±0.2	28.4±0.6
Velocity Calculated* (m/s)	8001	7671	7998	7610	9001	8974
Velocity Measured (m/s)	7877±130	7199±81	7792±66	7106±148	8669±14	8583±47

*BKWC product library

Table 2.2 Properties of applied compositions.

2.6 Test conditions

2.6.1 Initiation

To initiate the shell 8.0 g of PETN was pressed by hand into the fuze well. The holder for the detonator was then put in. Finally, when the position of the shell had been fixed, a detonator No 8 was placed into the polycarbonate holder as shown in Figure 2.12.

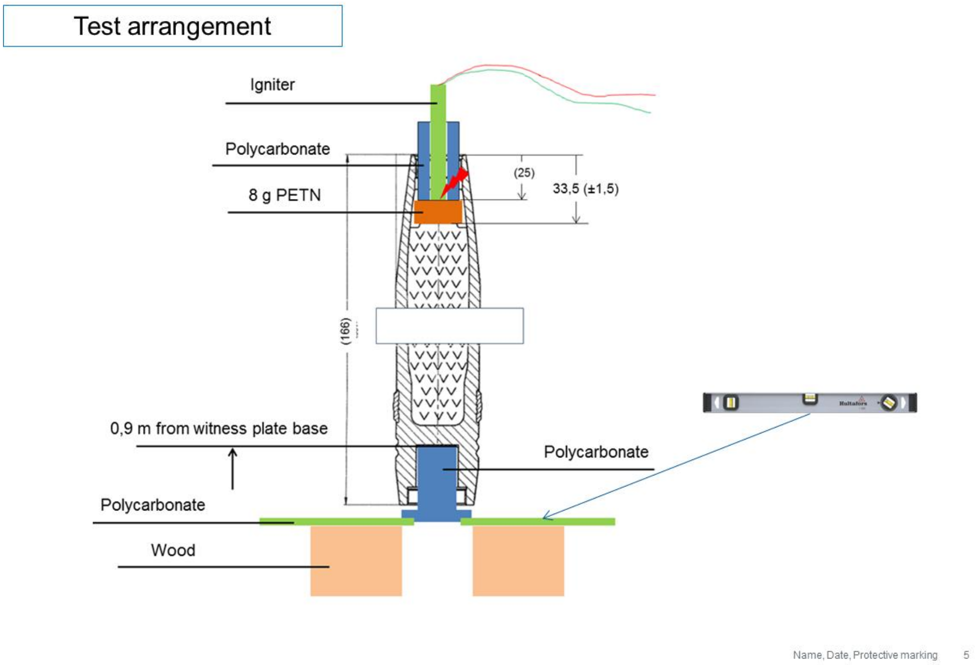

Figure 2.12 Test setup for the fragmentation of the 40 mm shells.

2.6.2 Witness plates

The witness plates were originally specified to be EN AW 2014 T6 AlCu4 SiMg. However, this quality is not produced anymore. Therefore they were replaced by EN AW-2017A-T4 quality. Appendix A gives the certificate of the used plates.

2.6.3 Test place and setup

The test setup was as outlined in Figure 2.13. The tests were performed in protection of an old explosive store as shown by Figure 2.14. The concrete walls were covered by different wood type plates to avoid ricochets. Figure 2.15 shows the test place after all firings had been performed.

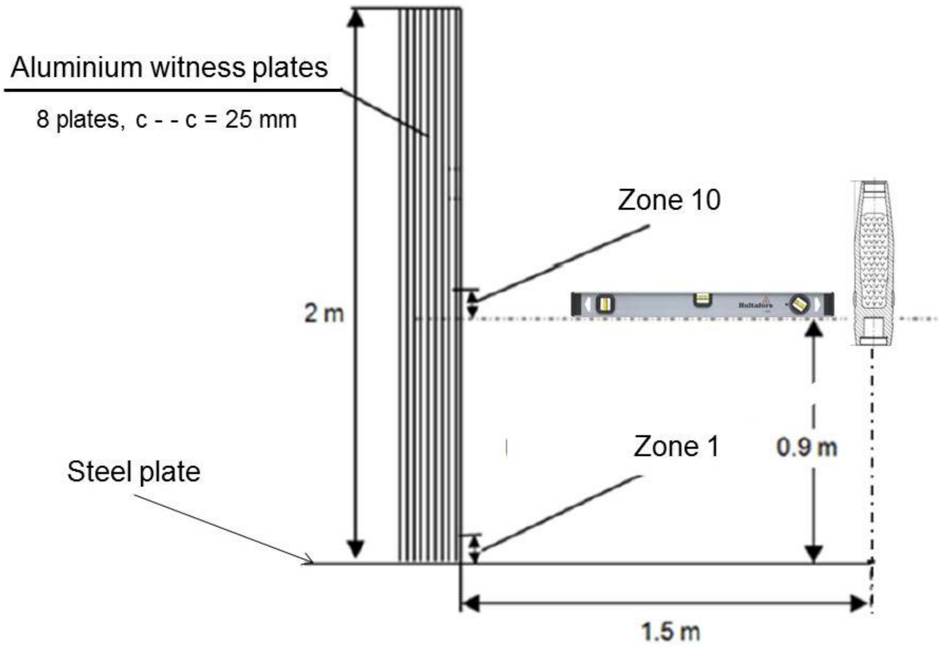

Figure 2.13 Position of the witness plate and shell for the fragmentation testing.

Figure 2.14 The test place before testing.

Figure 2.15 The test place after 10 40 mm shells had been tested.

3 Results

3.1 Fragmentation firings

3.1.1 Firing No 1 with MCX-8001 composition

The first firing was performed with shell No 8 containing MCX-8001 NTO/TNT/HMX (52/36/12). 8 g PETN pressed by hand into the fuze well with a 20 mm cylindrical piston was used as booster. Initiation was performed with a detonator No 8. Figure 3.1 shows the stack of witness plates after the firing was performed.

Figure 3.1 The witness plate stack after detonation of shell No 8 filled with MCX-8001 composition.

To analyse the fragmentation pattern all witness plates were marked vertically in 10 cm zones starting 50 mm from the bottom of the plate. In horizontal direction also 50 mm from the edge was excluded on both sides so that the total width of the plate was 90 cm. Figure App C.1 shows how the witness plate was divided into 19 measuring zones. The number of fragment hits and penetrations in each zone was counted. The same process was performed for all 8 witness plates in the stack. Table 3.1 gives the complete results both with regards to fragment hits and fragment penetrations. Pictures of all witness plates are given in Appendix C C.1.

Zone	Plate No 1		Plate No 2		Plate No 3		Plate No 4		Plate No 5		Plate No 6	
	Number of fragments		Number of fragments		Number of fragments		Number of fragments		Number of fragments		Number of fragments	
	Hit	Through	Hit	Through	Hit	Through	Hit	Through	Hit	Through	Hit	Through
19	1	1	1									
18	2											
17	2	1	1									
16	2	2	2									
15	1											
14	4											
13	12	3	4	3	3	2	1	1	1			
12	10	3	2	2	2	2	2					
11	7	4	5	2	2	1						
10	20	12	11	6	5	3	2					
9	27	17	12	10	9	4	4	2	3	2	1	
8	28	19	21	13	11	7	6	3	3			
7	10	7	7	4	2	3	2	2	2			
6	8	5	2									
5	10	2	2	1	1							
4	11	3	1	1	1	1	1					
3	14	3	3	1								
2	6	2	2	1	1	1	1					
1	4	2	1									
Sum	**179**	**86**	**77**	**44**	**37**	**24**	**19**	**8**	**9**	**2**	**1**	

Table 3.1 Fragment distribution for shell No 8 filled with MCX-8001 composition.

Figure 3.2 shows a diagram of the data from Table 3.1 with regard to hit of fragments in each 10 cm zone in each of the 6 witness plates. Figure 3.3 shows a diagram of the data in Table 3.1for fragments penetration in each 10 cm zone in all 5 different witness plates. As expected both the number of fragment hits and penetrations are highest in zones 8-10. For this firing we got penetrations through 5 plates or 10 mm of aluminium.

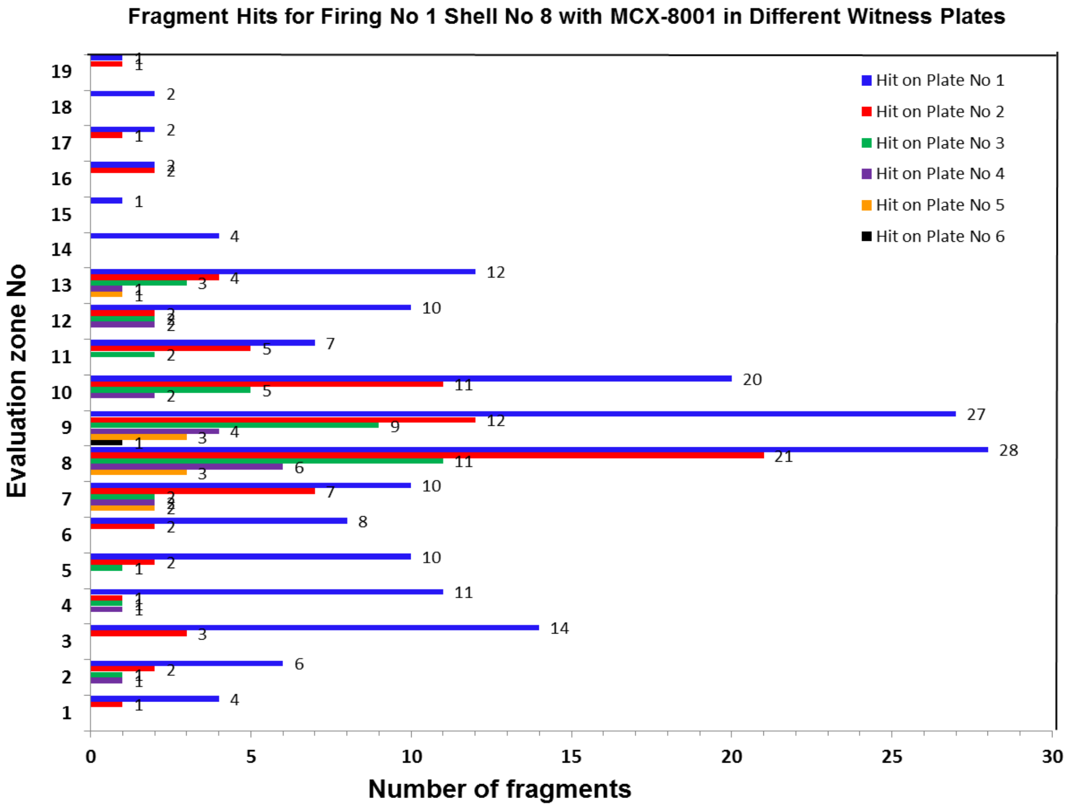

Figure 3.2 Number of fragment hits in each evaluation zone for all witness plates from firing of shell No 8 filled with MCX-8001 composition.

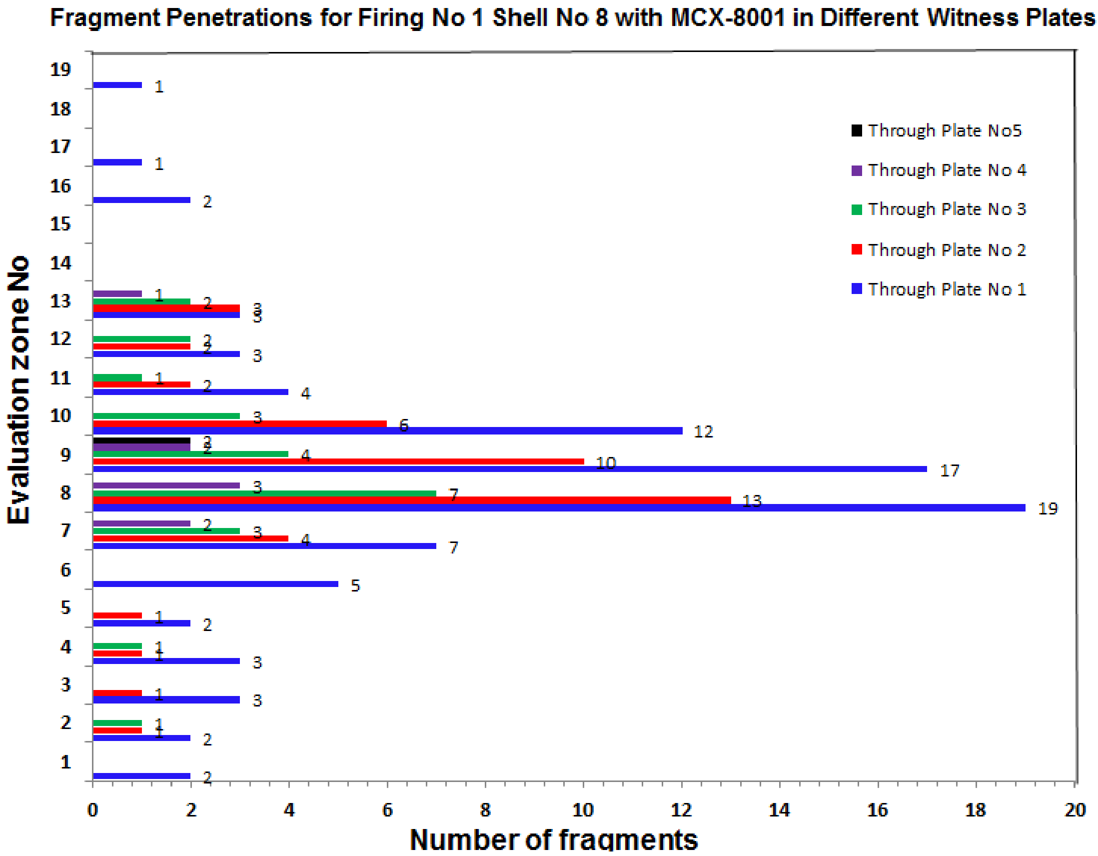

Figure 3.3 Number of fragment penetrations in each evaluation zone for all witness plates from firing of shell No 8 filled with MCX-8001 composition.

3.1.2 Firing No 2 with MCX-6002 composition

The second firing was performed with shell No 6 filled with MCX-6002 containing NTO/TNT/RDX (51/34/15). In addition to the main filling 8 g PETN was hand pressed into the fuze well as booster. Initiation was performed with a detonator No 8. Figure 3.4 shows the setup and the witness plate stack after firing. Pictures of all witness plates are given in Appendix C C.2.

Figure 3.4 Pictures from different angles of shell No 6 before firing, and of the stack of witness plates after firing.

Zone	Plate No 1		Plate No 2		Plate No 3		Plate No 4		Plate No 5		Plate No 6	
	Number of fragments		Number of fragments		Number of fragments		Number of fragments		Number of fragments		Number of fragments	
	Hit	Through	Hit	Through	Hit	Through	Hit	Through	Hit	Through	Hit	Through
19	1											
18	2		1	1								
17	5	3	3	1	1							
16	1											
15	3	1										
14	8	1					1					
13	16	8	8	4	5	5	3	1				
12	19	5	5	3	2							
11	11	4	4	3	3	3	2					
10	22	12	11	7	6	3	4	1				
9	39	20	18	12	11	9	5	1				
8	36	17	16	13	10	7	6	2	1	1	1	
7	2	1			1	1						
6	5	2	1	1	1	1	1					
5	4	3	1									
4	7	2	1									
3	11	4	2	1	1	1	1					
2	7	3	3	1								
1	5	1	1	1	1							
Sum	**204**	**87**	**75**	**48**	**42**	**30**	**23**	**5**	**1**	**1**	**1**	

Table 3.2 Fragment distribution for firing No 2 with shell No 6 containing MCX-6002.

Figure 3.5 shows a diagram of the data from Table 3.2 with regard to fragment hits in each 10 cm zone in all 6 witness plates. Figure 3.6 shows a diagram of the data in Table 3.2 with regard to fragment penetrations in each 10 cm zone in all 5 different witness plates. As expected both the number of hits and penetrations are highest in zones 8-10.

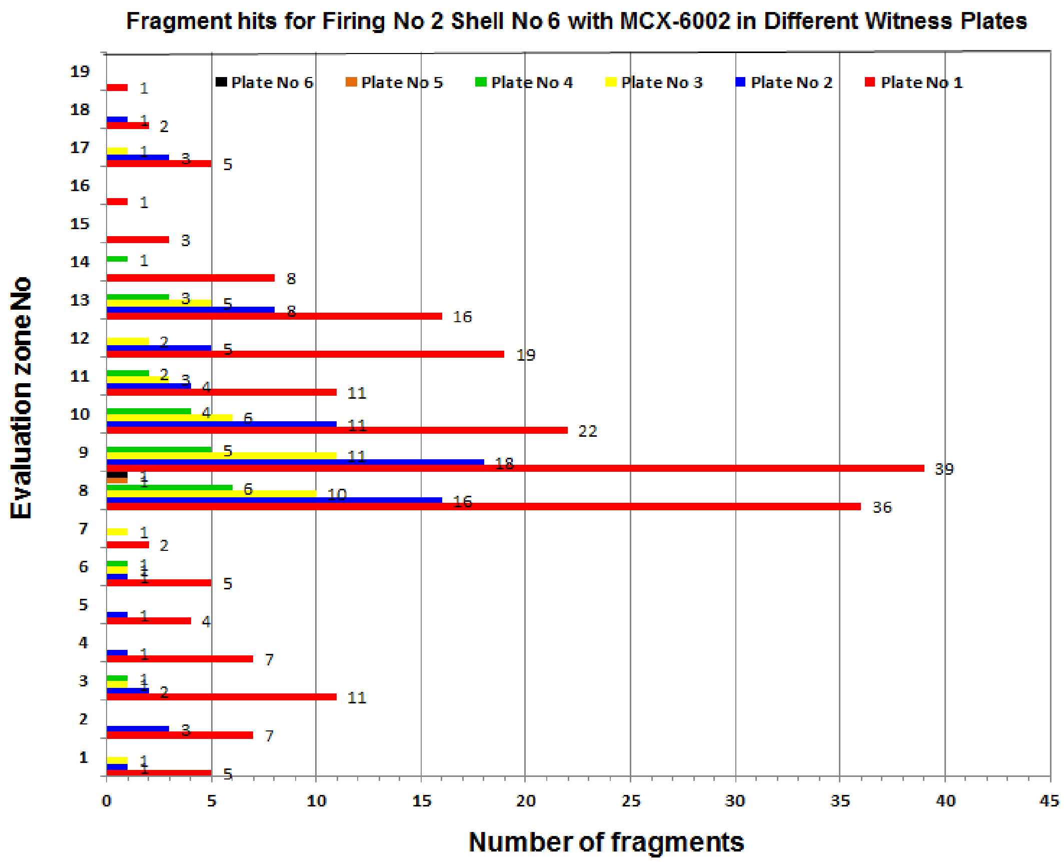

Figure 3.5 Fragment hits in different witness plates and evaluation zones for shell No 6 filled with MCX-6002 composition.

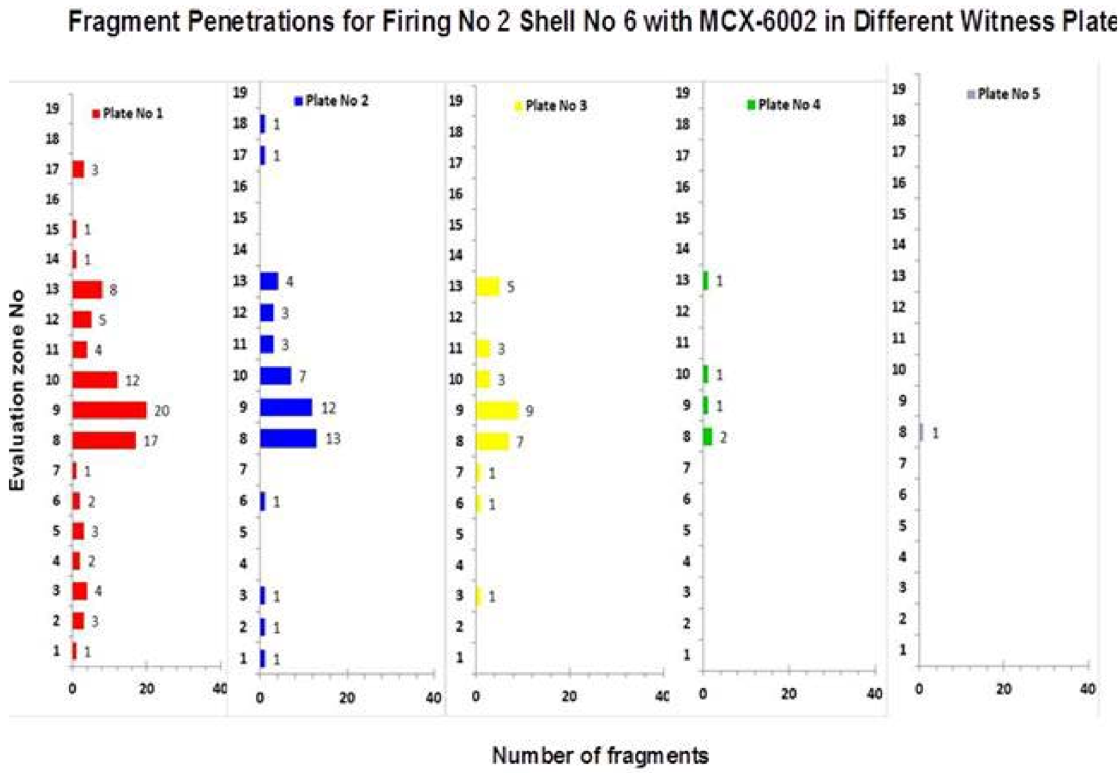

Figure 3.6 Fragment penetrations of all witness plates and evaluation zones for shell No 6.

3.1.3 Firing No 3 with MCX-8100 composition

The third firing was performed with shell No 4 filled with MCX-8100 composition consisting of DNAN/NTO/HMX (53/35/12) or a composition close to PAX-48. In addition to the main filling 8 g PETN was hand pressed as booster into the fuze well. Initiation was performed with a detonator No 8. Figure 3.7 shows the setup and the stack of witness plates after firing. Pictures of each witness plate after firing are given in Appendix C C.3.

Figure 3.7 The figure shows a picture of shell No 4 before firing and a picture of the stack of witness plates after the firing.

Zone	Plate No 1		Plate No 2		Plate No 3		Plate No 4		Plate No 5		Plate No 6		Plate No 7		Plate No 8	
	Number of fragments		Number of fragments		Number of fragments		Number of fragments		Number of fragments		Number of fragments		Number of fragments		Number of fragments	
	Hit	Through	Hit	Through	Hit	Through	Hit	Through	Hit	Through	Hit	Through	Hit	Through	Hit	Through
19	1															
18	2															
17	2	1	2													
16	2	2	1	1	1											
15	4	1														
14	1															
13	14	2														
12	17	5	5	4	4	2	2	2	1	1	1	1				
11	7	3	3	3	2	1	1									
10	18	12	11	8	4	3	3	2								
9	20	14	12	6	7	6	3	1	1	1	1	1	1	1	1	
8	17	9	8	7	7		3	3	2							
7	11	3	3	2	2	2	2	2	2	2	2					
6	2	1	1	1	1	1	1									
5	3	1	1													
4	5	3	1	1												
3	3	3	2													
2	7	3	2	1												
1	4	2														
Sum	**140**	**65**	**52**	**34**	**28**	**15**	**15**	**10**	**6**	**4**	**4**	**2**	**1**	**1**	**1**	

Table 3.3 Fragment distributions for shell No 4 filled with MCX-8100 composition.

Table 3.3 gives distribution of fragment hits and penetrations in each evaluation zone for all witness plates. Figure 3.8 shows a diagram of the results in Table 3.3 with regard to fragment hits in each 10 cm evaluation zone for all 8 witness plates. Figure 3.9 shows a similar diagram of the results in Table 3.3 with regard to fragments penetrations in each 10 cm evaluation zone for the 7 witness plates penetrated. As expected both the number of hits and penetrations are highest in zones 7-12. Fragments from this shell penetrate seven plates and stop in the eight plate. This composition gives relatively few fragments but they have high penetration ability.

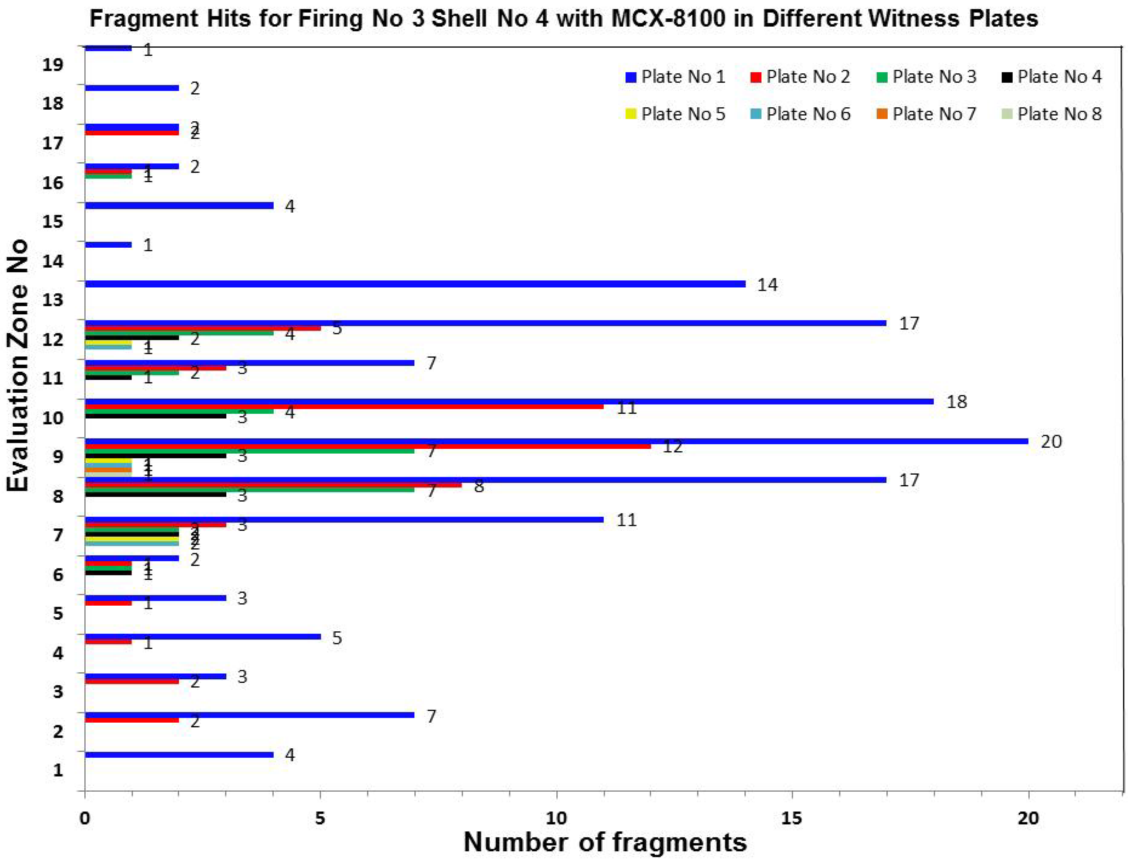

Figure 3.8 Fragment hits in the different witness plates and evaluation zones for shell No 4 filled with MCX-8100 composition.

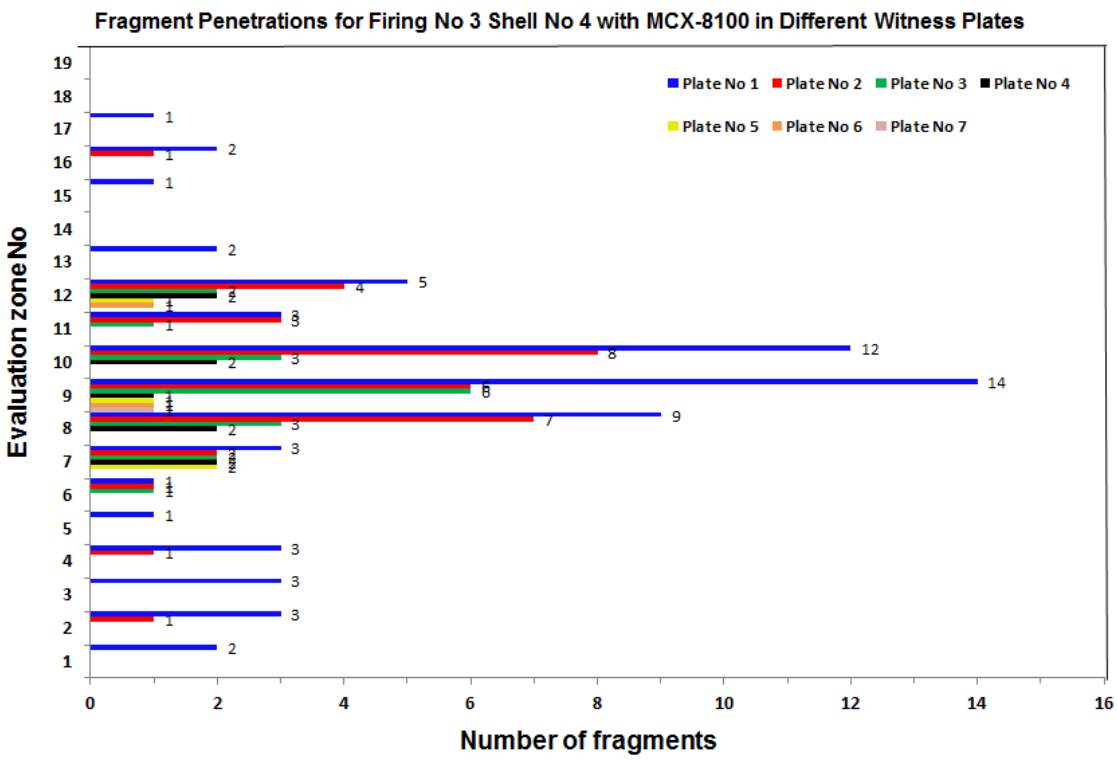

Figure 3.9 Fragment penetrations in the different witness plates and evaluation zones for shell No 4 filled with MCX-8100 composition.

3.1.4 Firing No 4 with MCX-6100 composition

The fourth firing was performed with shell No 2 filled with MCX-6100 composition consisting of DNAN/NTO/RDX (52/53/15), a composition close to IMX-104. In addition to the main filling 8 g PETN was hand pressed into the fuze well as booster. The initiation was performed with a detonator No 8. Figure 3.10 shows pictures of the setup and the stack of witness plates after firing. Pictures of all witness plates for this firing are given in Appendix C C.4.

Figure 3.10 The Figure shows pictures of shell No 2 before firing and the stack of witness plates after firing.

Zone	Plate No 1		Plate No 2		Plate No 3		Plate No 4		Plate No 5		Plate No 6		Plate No 7	
	Number of fragments		Number of fragments		Number of fragments		Number of fragments		Number of fragments		Number of fragments		Number of fragments	
	Hit	Through	Hit	Through	Hit	Through	Hit	Through	Hit	Through	Hit	Through	Hit	Through
19														
18														
17			1											
16	2	2												
15	3	1	1											
14	1		1											
13	3	1	1	1										
12	13	4	4	2	2									
11	7													
10	18	9	6	5	5	4	4	3	3					
9	19	9	5	2	3	2	1							
8	25	14	15	9	7	7	7	5	4	1	1	1	1	1
7	9	3	2	2	2									
6	8	3	3	2	1	1	1							
5	4	2	1											
4	5	2	3											
3	13	2	2	1	1	1	1							
2	6	1												
1	4	2	1											
Sum	**140**	**55**	**46**	**24**	**21**	**15**	**14**	**8**	**7**	**1**	**1**	**1**	**1**	**1**

Table 3.4 Fragment distributions for firing No 4 with shell No 2 with MCX-6100.

Table 3.4 gives distribution of fragment hits and penetrations in each evaluation zone for all witness plates. Figure 3.11 shows a diagram of the results in Table 3.4 with regard to fragment hits in each 10 cm evaluation zone in all 7 witness plates. Figure 3.12 shows a diagram of the results in Table 3.4 with regard to fragment penetrations in each 10 cm evaluation zone for 7 different penetrated witness plates. As expected both the number of hits and penetrations are highest in zones 8-10. Composition MCX-6100 gives relatively few fragments, but the fragment with highest energy penetrates 7 aluminium plates or 14 mm aluminium.

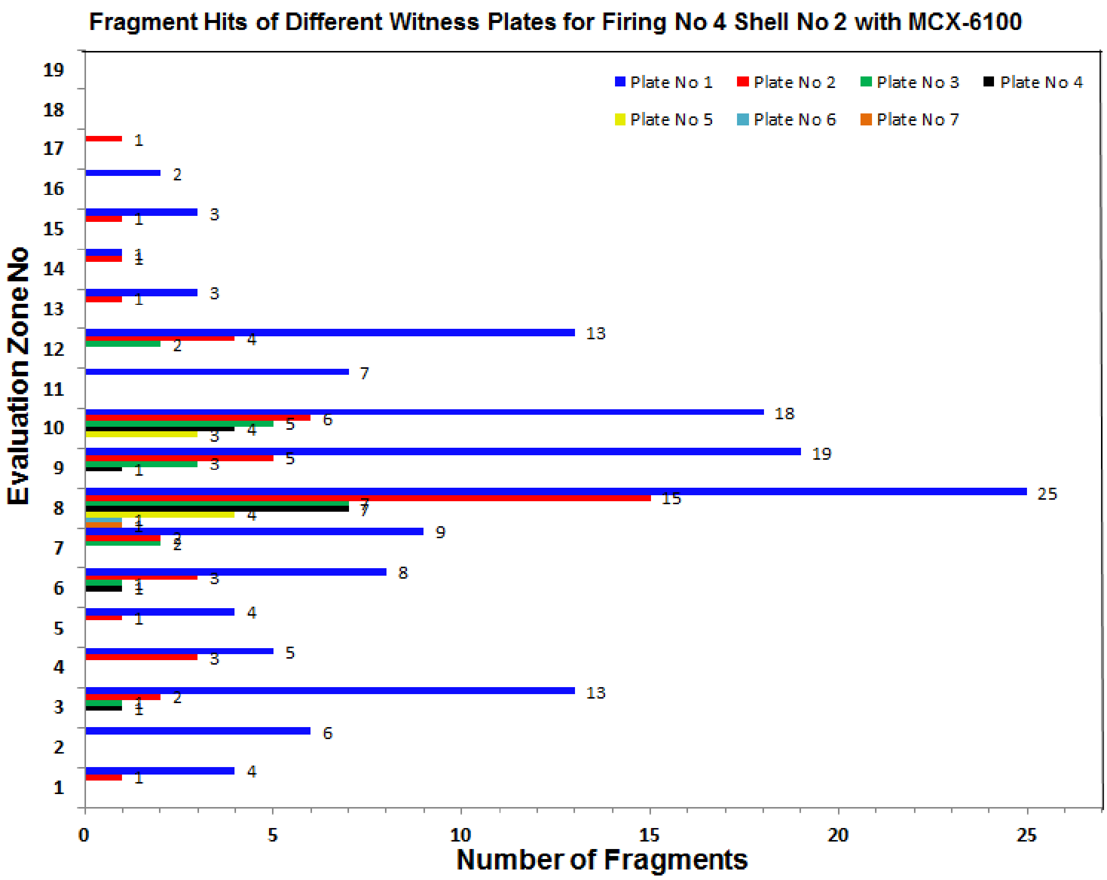

Figure 3.11 Fragment hits in different witness plates and evaluation zones for shell No 2 filled with MCX-6100 composition.

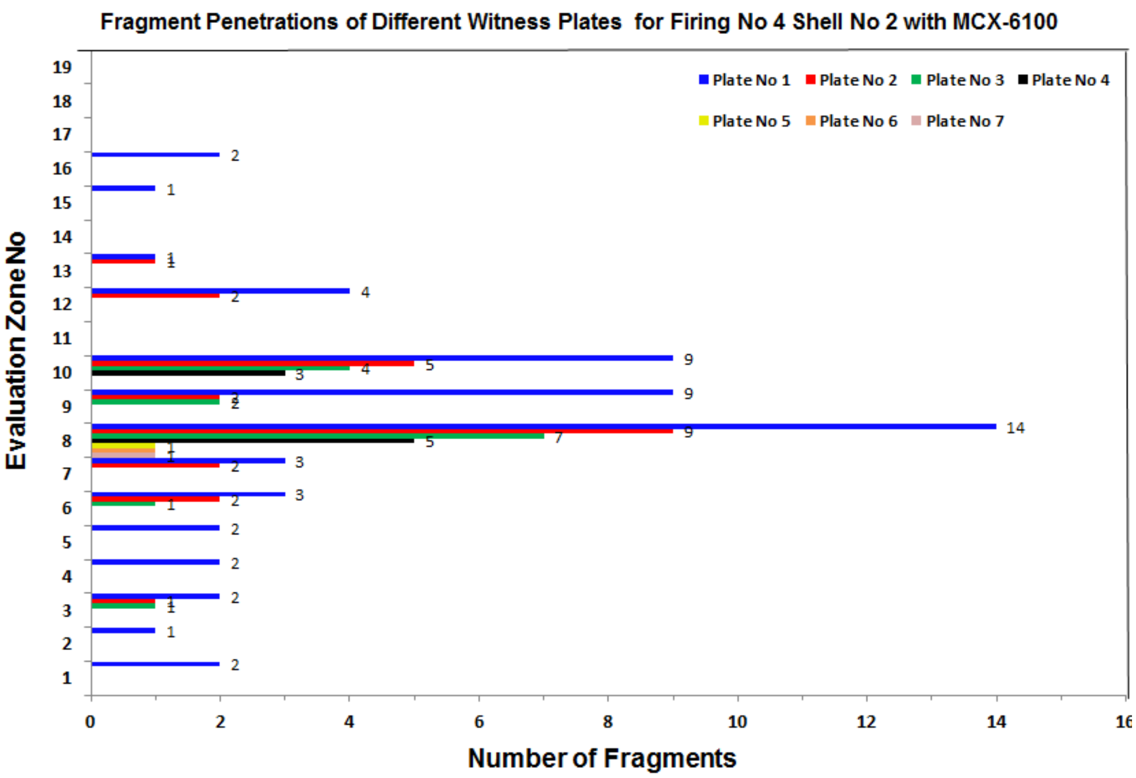

Figure 3.12 Fragment penetrations of different witness plates and evaluation zones for shell No 2 filled with MCX-6100 composition.

3.1.5 Firing No 5 with Sats 432/13

The fifth firing was performed with shell No 10 press filled with 50-GA/50-BAMO/IPDI-HMX (5.7/94.3) composition. In addition to the main filling 8 g PETN was hand pressed into the fuze well as booster. Initiation was performed with a detonator No 8. Pictures of the witness plates are given in Appendix C C.5. Table 3.5 summarizes all fragment hits and penetrations in all witness plates and evaluation zones for this firing with composition Sats 432/13.

Zone	Plate No 1		Plate No 2		Plate No 3		Plate No 4		Plate No 5		Plate No 6	
	Number of fragments		Number of fragments		Number of fragments		Number of fragments		Number of fragments		Number of fragments	
	Hit	Through	Hit	Through	Hit	Through	Hit	Through	Hit	Through	Hit	Through
19												
18												
17	3	2	2	1								
16	6	3	3	2	2							
15	8	3	2	2	2	2	1					
14	10	4	4	2	2	2	2					
13	17	9	9	5	5	3	2					
12	11	6	5	5	6	4	3					
11	9	2	2	1	1							
10	21	16	14	10	12	2	2	1	1			
9	48	26	23	18	20	10	6	3	2	1	1	
8	41	27	26	21	14	10	9	1	1			
7	11	3	2	1	1	1	1	1	1			
6	6	2	2	1	1							
5	13	1	1									
4	4	3	3	1	1							
3	9	2	2	1	1							
2	5	2	2	2	2							
1	6	3	2	1	1							
Sum	**228**	**114**	**104**	**74**	**71**	**34**	**26**	**6**	**5**	**1**	**1**	

Table 3.5 Fragment hits and penetrations for shell No10 with GA/BAMO/IPDI Sats 432/13 composition.

Figure 3.13 shows a diagram of the results in Table 3.5 with regard to fragment hits in each 10 cm evaluation zone for all witness plates. Figure 3.14 shows a diagram of the results in Table 3.5 with regard to fragment penetrations in each 10 cm evaluation zone for all penetrated witness plates. As expected both the number of hits and penetrations are highest in zones 8-10. For this composition the number of fragments is higher than for the tested melt cast compositions. The fragment with the highest penetration ability stops in plate No 6. This is after having penetrated 10 mm aluminium. The number of fragments penetrating 3 plates is high. This indicates that the velocity of the fragments is higher for this composition than for the melt cast compositions.

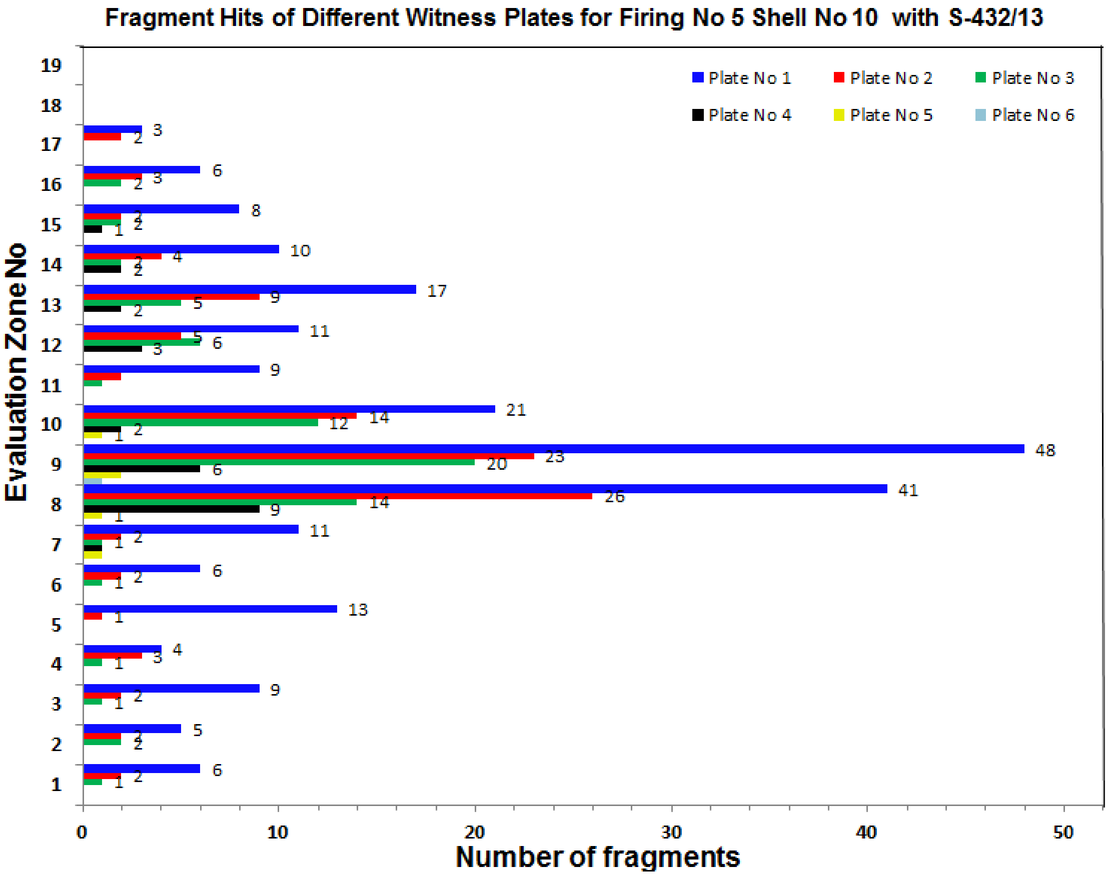

Figure 3.13 Fragment hits of different witness plates and evaluation zones for shell No 10 press filled with Sats-432/13 composition.

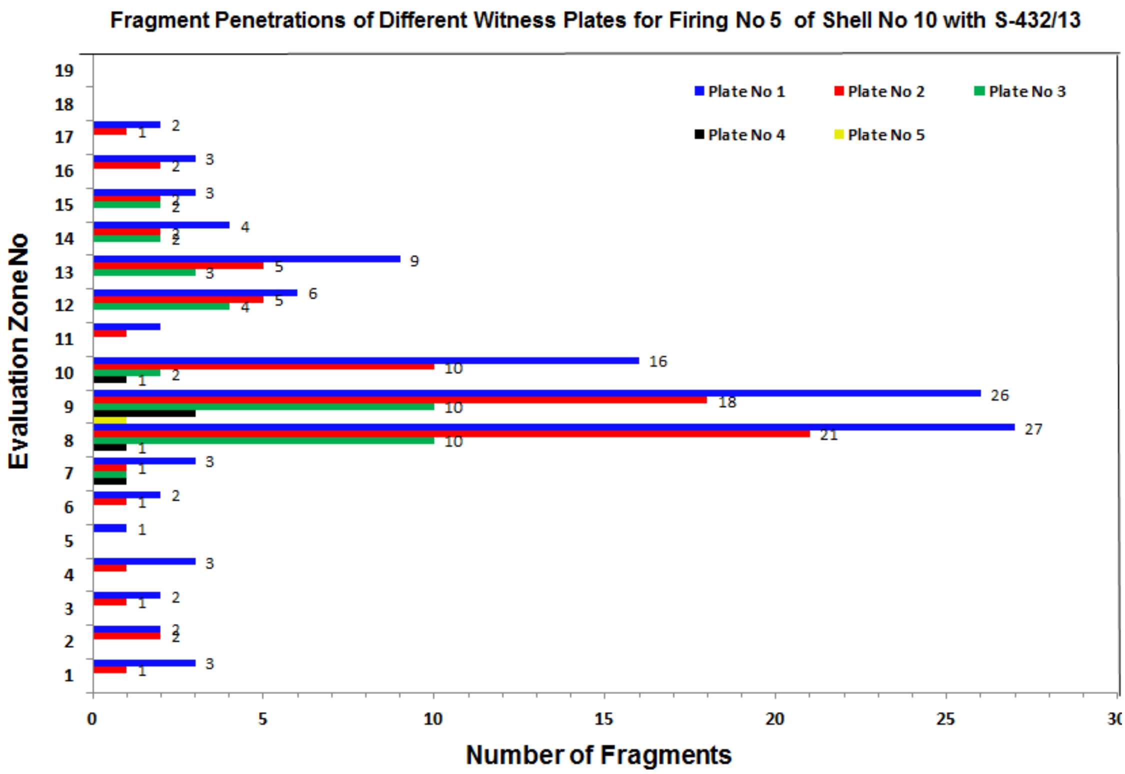

Figure 3.14 Fragment penetrations of different witness plates and evaluation zones for shell No 10 press filled with Sats-432/13 composition.

3.1.6 Firing No 6 with MCX-8001 composition

The sixth firing was performed with shell No 7 containing MCX-8001 NTO/TNT/HMX (52/36/12) composition. An 8 g PETN booster was hand pressed into the fuze well with a 20 mm cylindrical piston. Initiation was performed with a detonator No 8. Pictures of all witness plates are given in Appendix C C.6. This firing was a duplicate of firing No 1. Table 3.6 gives distribution of fragment hits and penetrations in each evaluation zone for all witness plates.

Zone	Plate No 1		Plate No 2		Plate No 3		Plate No 4		Plate No 5		Plate No 6	
	Number of fragments		Number of fragments		Number of fragments		Number of fragments		Number of fragments		Number of fragments	
	Hit	Through	Hit	Through	Hit	Through	Hit	Through	Hit	Through	Hit	Through
19	1											
18	2	2	1									
17	2	1	1									
16	3	1	1	1	1							
15	4											
14	8	2	2	1								
13	16	6	4	2	2	2	1	1				
12	18	9	8	5	3	2	2	1				
11	9	4	2	2	2	1	1	1				
10	19	7	6	5	5	1	1					
9	40	20	16	11	10	7	5	2	2			
8	23	17	15	12	11	9	7	4	3	1	1	
7	6	4	3	3	2		1					
6	6	1										
5	5	2										
4	10	1										
3	13	5	2	1	1							
2	7	2	3	1								
1	3	1	1	1								
Sum	195	85	65	45	37	22	18	9	5	1	1	

Table 3.6 Fragment distributions for firing No 6 with shell No 7 with MCX-8001 composition.

Figure 3.15 shows a diagram of the results in Table 3.6 with regard to hit of fragments in each 10 cm evaluation zone for all 6 witness plates that were hit. Figure 3.16 shows a diagram of the results in Table 3.6 with regard to fragment penetrations in each 10 cm evaluation zone for all 5 witness plates that were penetrated. As expected both the number of hits and penetrations are highest in evaluation zones 8-13. Compared with the number of fragments obtained in firing No 1 with shell No 8 having the same filling the results in Table 3.6 are very similar.

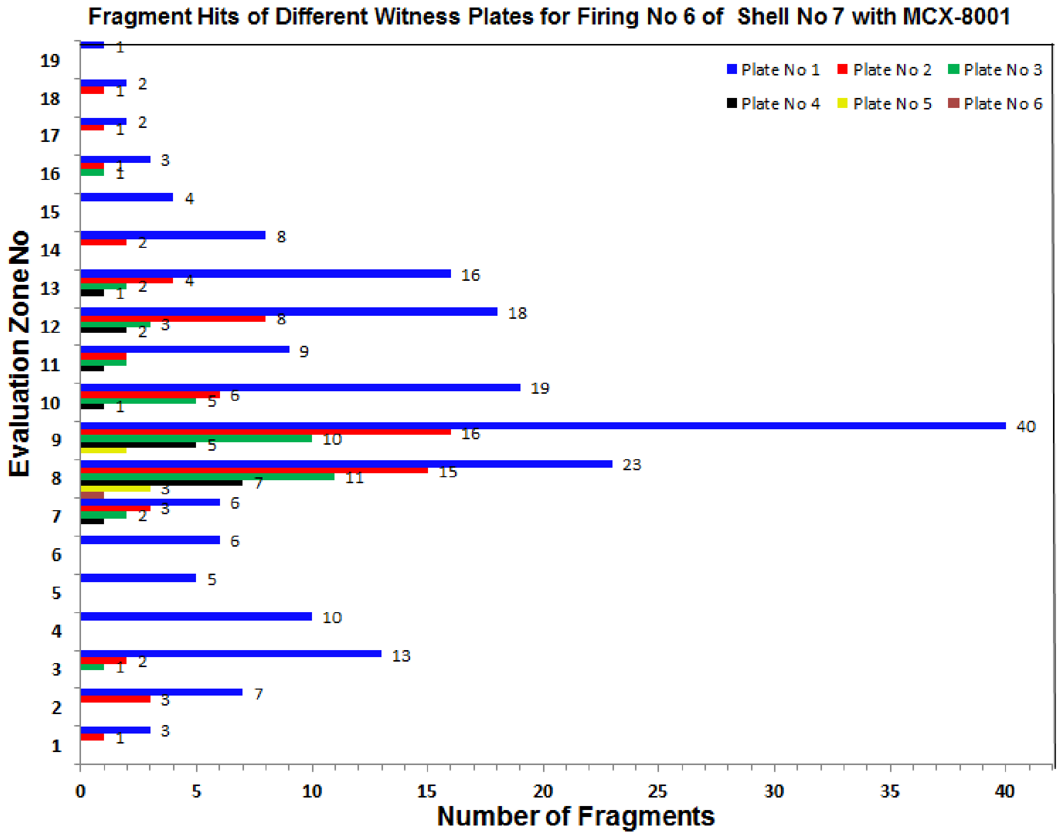

Figure 3.15 Fragment hits in different witness plates and evaluation zones for shell No 7 filled with MCX-8001 composition.

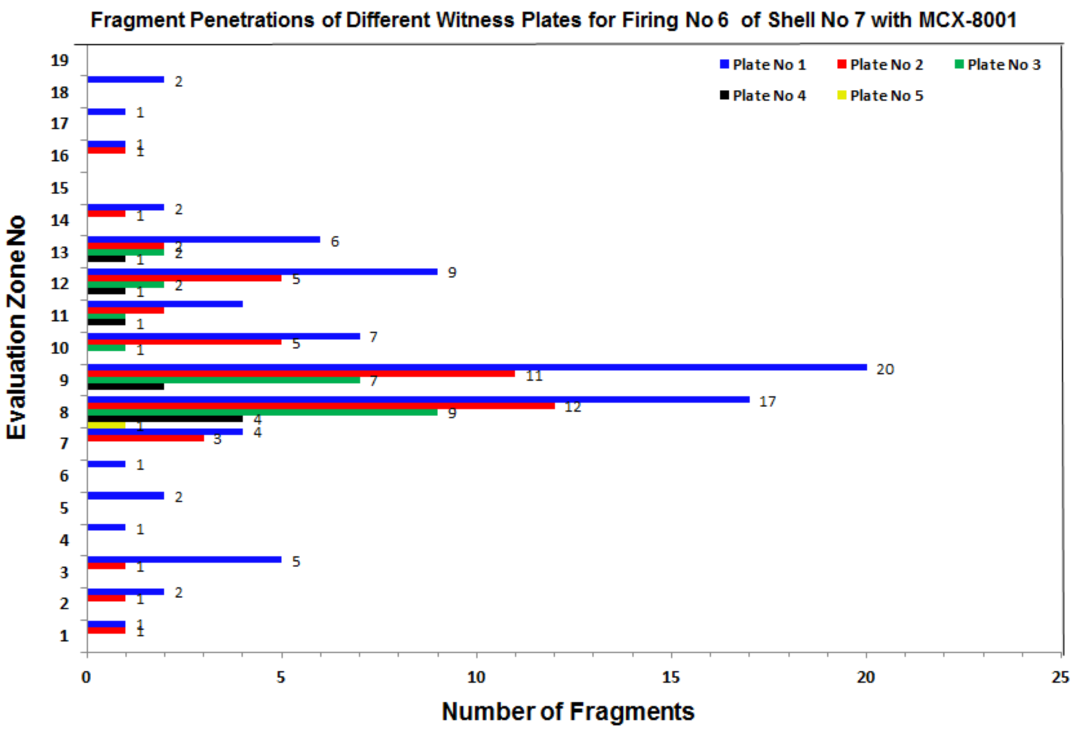

Figure 3.16 Fragment penetrations of different witness plates and evaluation zones for shell No 7 filled with MCX-8001 composition.

3.1.7 Firing No 7 with MCX-6002 composition

The seventh firing was performed with shell No 5 filled with MCX-6002 composition containing NTO/TNT/RDX (51/34/15). 8 g PETN was hand pressed as booster into the fuze well with a 20 mm piston. Initiation was performed with a detonator No 8. Figure 3.17 shows pictures of the setup and the stack of witness plates after firing. Pictures of all witness plates after firing are given in Appendix C C.7.

Figure 3.17 Pictures from firing No 7 of shell No 5 filled with MCX-6002 composition.

Zone	Plate No 1		Plate No 2		Plate No 3		Plate No 4		Plate No 5		Plate No 6		Plate No 7		Plate No 8	
	Number of fragments		Number of fragments		Number of fragments		Number of fragments		Number of fragments		Number of fragments		Number of fragments		Number of fragments	
	Hit	Through	Hit	Through	Hit	Through	Hit	Through	Hit	Through	Hit	Through	Hit	Through	Hit	Through
19																
18																
17																
16	5	2	2	2	1											
15																
14	4	1	1													
13	9	2	2	2	2	1										
12	15	7	6	4	3	3	2	2	2	2	2	1				
11	8	5	5	4	1	1	1									
10	14	9	9	5	4	1	1	1	1							
9	28	16	14	11	9	8	5	2	2	2	2	1	1	1	1	
8	32	19	20	16	14	10	7	3	2	1	1					
7	8	3	3	3	3	1	1	1	1	1	1					
6	7	3	3													
5	6	3	3	1												
4	9	2	2													
3	9															
2	8	3	2	2	1											
1	3	1	1	1												
Sum	**165**	**76**	**73**	**51**	**38**	**25**	**17**	**9**	**8**	**6**	**6**	**2**	**1**	**1**	**1**	

Table 3.7 Fragment distributions for shell No 5 filled with MCX-6002 composition.

Table 3.7 gives distribution of fragment hits and penetrations in each evaluation zone for all witness plates. Figure 3.18 shows a diagram of the results in Table 3.7 with regard to hit of fragments in each 10 cm evaluation zone for all 8 witness plates. Figure 3.19 shows a diagram of the results in Table 3.7 with regard to fragment penetrations in each 10 cm evaluation zone for all 7 penetrated witness plates. As expected both the number of hits and penetrations are highest in evaluation zones 8-10. Compared with shell No 6 with the same composition shell No 5 has fewer fragments that penetrate the first plate. The number of fragments that penetrate plate No 2 is however higher for shell No 5 than for shell No 6. Shell No 5 has more fragments penetrating 4 or more plates compared with shell No 6. For shell No 5 the fragments with highest energy penetrated 7 plates, while for shell No 6 they penetrated 5 plates.

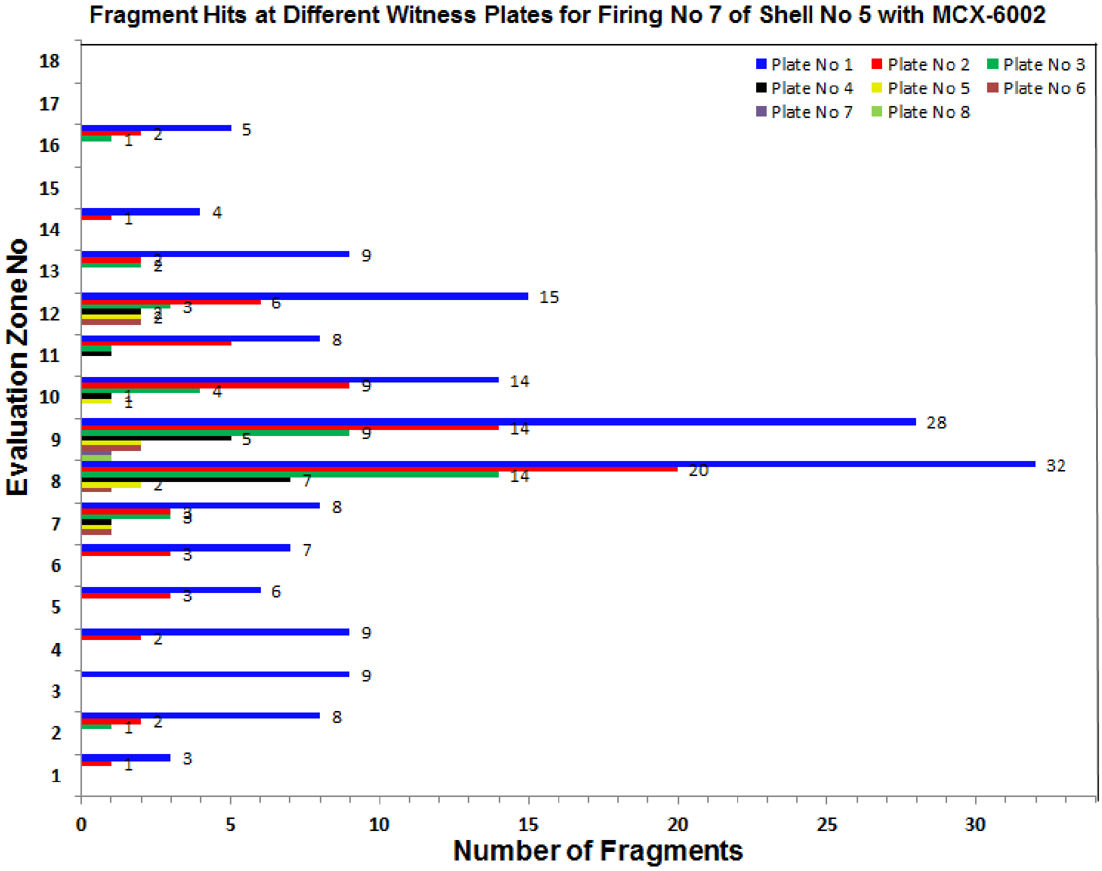

Figure 3.18 Fragment hits at different witness plates and evaluation zones for shell No 5 filled with MCX-6002 composition.

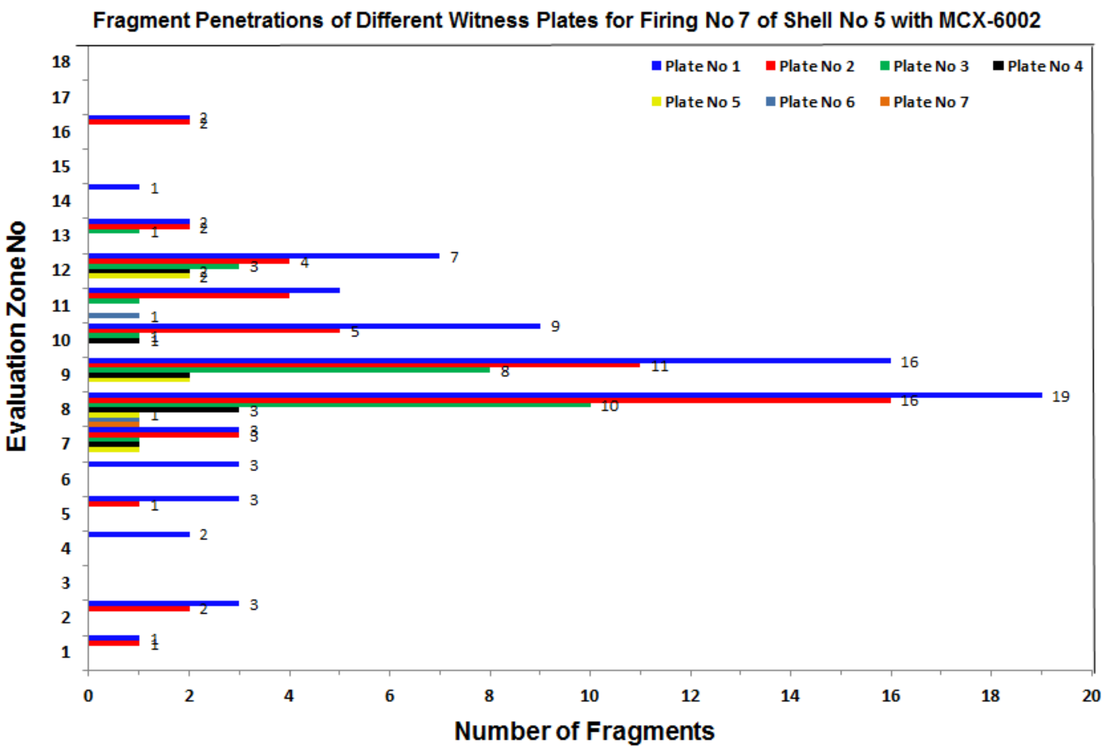

Figure 3.19 Fragment penetrations of different witness plates and evaluation zones for shell No 5 filled with MCX-6002 composition.

3.1.8 Firing No 8 with MCX-8100 composition

Firing No 8 was carried out with shell No 3 containing MCX-8100 composition with relatively high density of the filling. MCX-8100 consists of DNAN/NTO/HMX (35/53/12), a composition close to PAX-48. In addition to the main filling 8 g PETNwas hand pressed as booster into the fuze well. Initiation was performed with a detonator No 8. Figure 3.20 shows the setup and the stack of witness plates after firing. Pictures of each witness plate for this firing are given in Appendix C C.8. This firing was a replicate of firing No 3 with shell No 4.

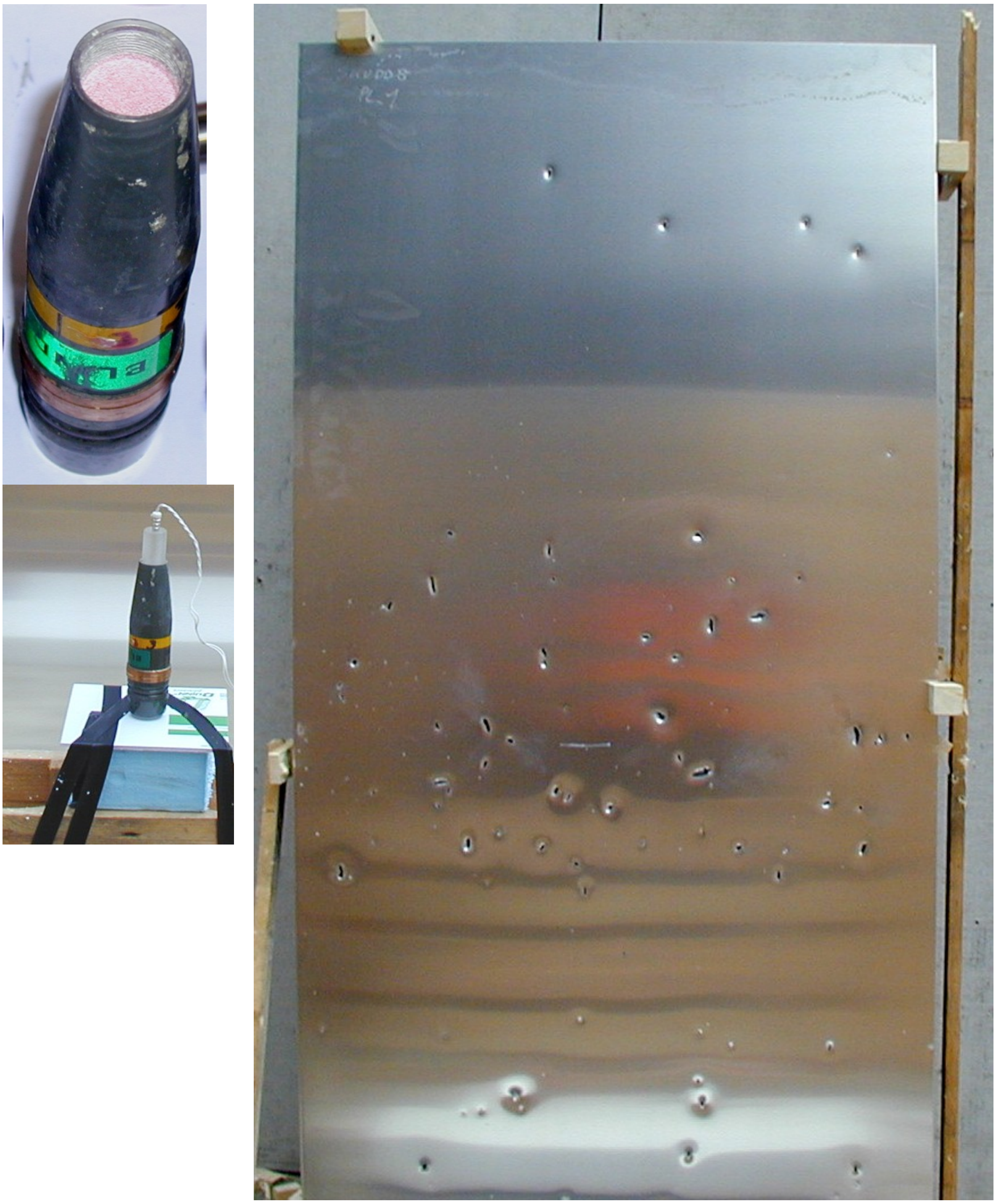

Figure 3.20 Pictures from firing No 8 with shell No 3 filled with MCX-8100 composition.

Zone	Plate No 1 Number of fragments		Plate No 2 Number of fragments		Plate No 3 Number of fragments		Plate No 4 Number of fragments		Plate No 5 Number of fragments		Plate No 6 Number of fragments	
	Hit	Through	Hit	Through	Hit	Through	Hit	Through	Hit	Through	Hit	Through
19												
18	1	1	1									
17	3	3	3									
16												
15												
14	4	1										
13	8											
12	11	6	6	2	2	2	2	1				
11	15	8	7	4	4	3	3	1				
10	25	9	8	6	4	1						
9	23	11	11	7	7	6	6	2	1			
8	21	12	11	7	6	3	2	2	2	1	1	
7	16	11	11	6	5	4	4	1				
6	2	1	1									
5	2											
4	6	3	1									
3	6	1										
2	11	4	3	2	2	2	1					
1	**4**		**1**	**1**	**1**	**1**						
Sum	**158**	**71**	**64**	**35**	**31**	**22**	**18**	**7**	**3**	**1**	**1**	

Table 3.8 Fragments distribution for shell No 3 filled with MCX-8100 composition.

Table 3.8 gives distribution of fragment hits and penetrations in each evaluation zone for all witness plates. Figure 3.21 shows a diagram of the results in Table 3.8 with regard to hit of fragments in each 10 cm evaluation zone for each of the 6 witness plates that was hit. Figure 3.22 shows a diagram of the results in Table 3.8 with regard to fragment penetrations in each 10 cm evaluation zone for the 5 witness plates with fragment penetrations. As expected both the number of hits and penetrations are highest in zones 8-10. Compared with shell No 4 the number of fragment penetrations in the first 3 plates is higher for shell No 3 (71/65, 35/34, 22/15). For shell No 4 fragments penetrated 7 plates, while for shell No 3 only 5 plates were penetrated.

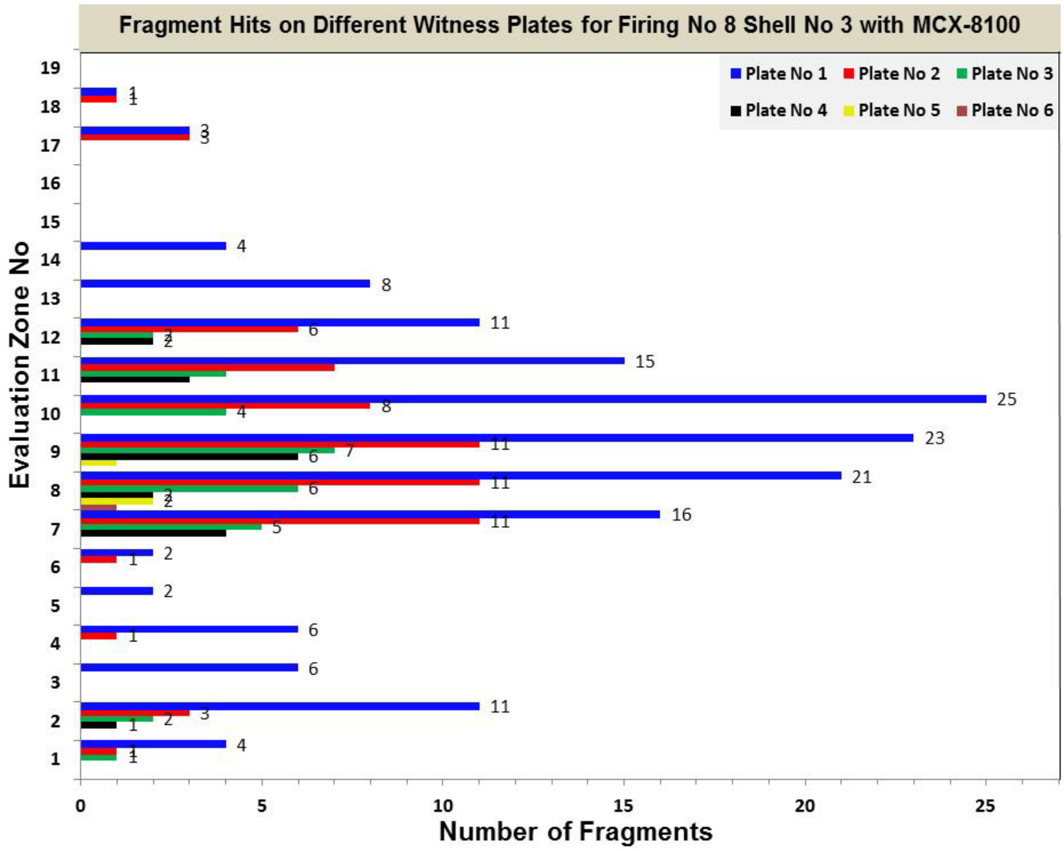

Figure 3.21 Fragment hits on different witness plates and evaluation zones for shell No 3 filled with MCX-8100 composition.

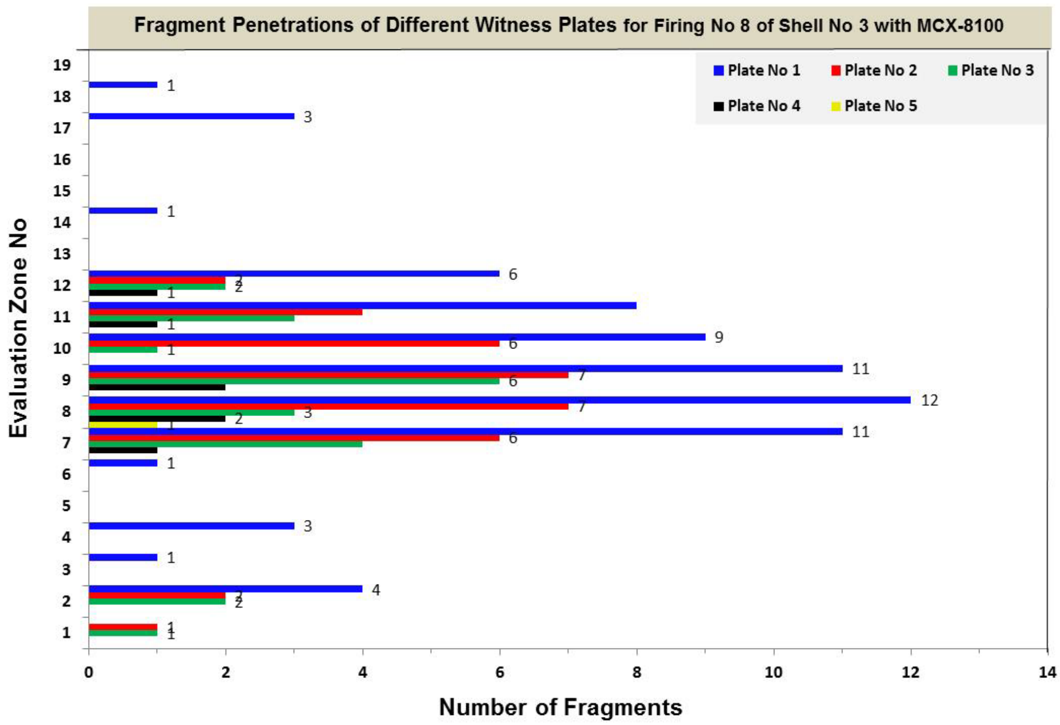

Figure 3.22 Fragment penetrations of different witness plates and evaluation zones for shell No 3 filled with MCX-8100 composition.

3.1.9 Firing No 9 with MCX-6100 composition

The ninth firing was performed with shell No 1 filled with MCX-6100 composition consisting of DNAN/NTO/RDX (32/53/15), a composition close to IMX-104. 8 g PETN hand pressed into the fuze well was used as booster. Initiation was performed with a detonator No 8. Figure 3.23 shows pictures of the setup and the stack of witness plates after firing. Pictures of each witness plate are given in Appendix C C.9. This firing was a replicate of firing No 4 with shell No 2.

Figure 3.23 Pictures from firing No 9 with 40 mm shell No 1 containing MCX-6100 composition.

Zone	Plate No 1		Plate No 2		Plate No 3		Plate No 4		Plate No 5		Plate No 6		Plate No 7		Plate No 8	
	Number of fragments		Number of fragments		Number of fragments		Number of fragments		Number of fragments		Number of fragments		Number of fragments		Number of fragments	
	Hit	Through	Hit	Through	Hit	Through	Hit	Through	Hit	Through	Hit	Through	Hit	Through	Hit	Through
19																
18	1															
17	2	2	2													
16	2	1	1	1	1											
15																
14	7															
13	2															
12	10	3	1	1												
11	20	10	10	7	5	4	3	1							1	
10	22	8	5	2	3	3	2	2	2	2	2	2	2	2		
9	25	10	10	2	2	2	2	2	2	1	1	1			1	1
8	23	12	11	8	7	6	5	1	1	1						
7	8	4	4	2												
6	3															
5	5	1														
4	10	1														
3	9		1													
2	6	3	3	3	2	1										
1	1															
Sum	**156**	**55**	**48**	**26**	**20**	**16**	**12**	**6**	**5**	**4**	**3**	**3**	**2**	**2**	**2**	**1**

Table 3.9 Fragment distribution for shell No 1 containing MCX-6100 composition.

Table 3.9 gives distribution of fragment hits and penetrations in each evaluation zone for all witness plates. Figure 3.24 shows a diagram of the results in Table 3.9 with regard to hit of fragments in each 10 cm evaluation zone in all 8 witness plates with hits. Figure 3.25 shows a diagram of the results in Table 3.9 with regard to fragment penetrations in each 10 cm evaluation zone for the 7 witness plates with fragment penetrations. As expected both the number of hits and penetrations are highest in zones 8-10. Fragments from firing of shell No 1 penetrate 8 witness plates. This is the same number as for shell No 2. For these two shells with identical filling (MCX-6100), the differences in the numbers of penetrating fragments in the different witness plates are small: 55 (55), 26 (24), 16 (15), 6 (8), 4 (1), 3 (1), 2 (1) for the first 7 plates.

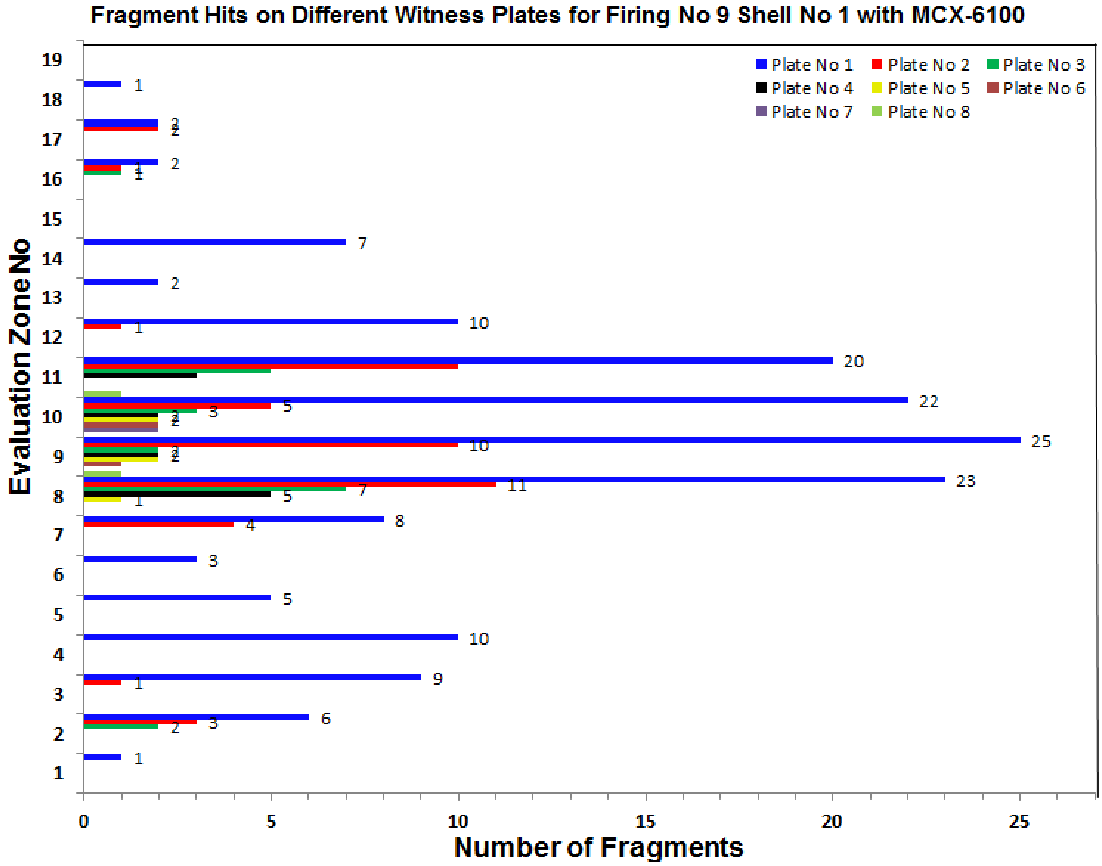

Figure 3.24 Fragment hits on the different witness plates and evaluation zones for shell No 1 filled with MCX-6100 composition.

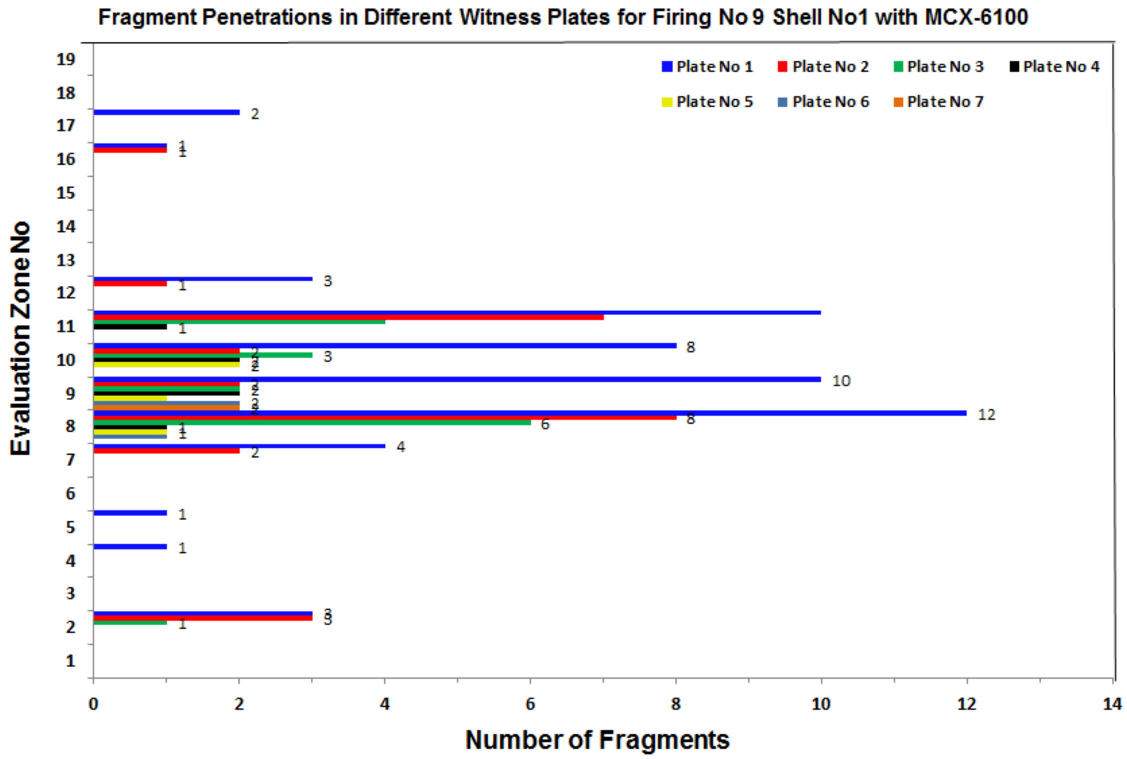

Figure 3.25 Fragment penetrations in different witness plates and evaluation zones for shell No1filled with MCX-6100 composition.

3.1.10 Firing No 10 with Sats 400/13

The tenth firing was performed with shell No 9 filled with 40-GA/60-BAMO/IPDI (2)-HMX (5.3/94.7) or Sats 400/13 composition. This composition was filled by pressing. 8 g PETN was hand pressed into the fuze well as booster. Initiation was performed with a detonator No 8. Pictures of each witness plate are given in Appendix C C.10. Figure 3.26 shows pictures of the shell before firing and of the stack of witness plates after firing. This firing contained a composition not equal to the one in firing No 5 (shell No 10) but very similar.

Figure 3.26 Pictures of the shell before firing and of the stack of witness plates after firing for shell No 9

Zone	Plate No 1		Plate No 2		Plate No 3		Plate No 4		Plate No 5		Plate No 6		Plate No 7	
	Number of fragments		Number of fragments		Number of fragments		Number of fragments		Number of fragments		Number of fragments		Number of fragments	
	Hit	Through	Hit	Through	Hit	Through	Hit	Through	Hit	Through	Hit	Through	Hit	Through
19	1													
18	1	1	1											
17	2	1	1	1										
16	4	1	1	1	1									
15	6	3												
14	9	1	1	1	1	1	1							
13	15	8	7	4	4	2	1	1	1					
12	7	4	5	3	2	1	1	1	1	1	1			
11	10	5	5	3	4	3	3							
10	21	11	6	2	2	1	1	1	1					
9	38	22	17	12	12	6	5	3	3	2	2	1	1	
8	32	18	20	14	11	6	5	3	2	1	1	1	1	
7	23	13	10	7	7	4	4	2	1	1				
6	10	4	3											
5	6	3	1											
4	4	2	1											
3	16	1												
2	9	4	2	1										
1	12	1	4	2	2									
Sum	**226**	**103**	**85**	**51**	**46**	**24**	**21**	**11**	**9**	**5**	**4**	**2**	**2**	

Table 3.10 Fragment distribution for shell No 9 press filled with Sats-400/13 composition.

Table 3.10 gives distribution of fragment hits and penetrations in each evaluation zone for all witness plates. Figure 3.27 shows a diagram of the results in Table 3.10 with regard to hit of fragments in each 10 cm evaluation zone for the 7 witness plates with hits. The fragments penetrated 6 witness plates and hit No 7. Figure 3.28 shows a diagram of the results in Table 3.10 with regard to fragment penetrations in each 10 cm evaluation zone for all witness plates. As expected both the number of hits and penetrations are highest in evaluation zones 8-10. Compared with shell No 10 the fragmentation of shell No 9 has some differences: penetrations 114 (104 shell No 9) through plate No 1, 74 (51) through plate No 2, 34 (24) through plate No 3 and 6 (11) through plate No 4. Shell No 10 has more fragments in plates No 1 to No 3 than shell No 9. For plate No 4 the order is opposite. Shell No 9 has fragments penetrating 6 witness plates compared with only 5 plates for shell No 10. The fragments with highest energy are produced by shell No 10.

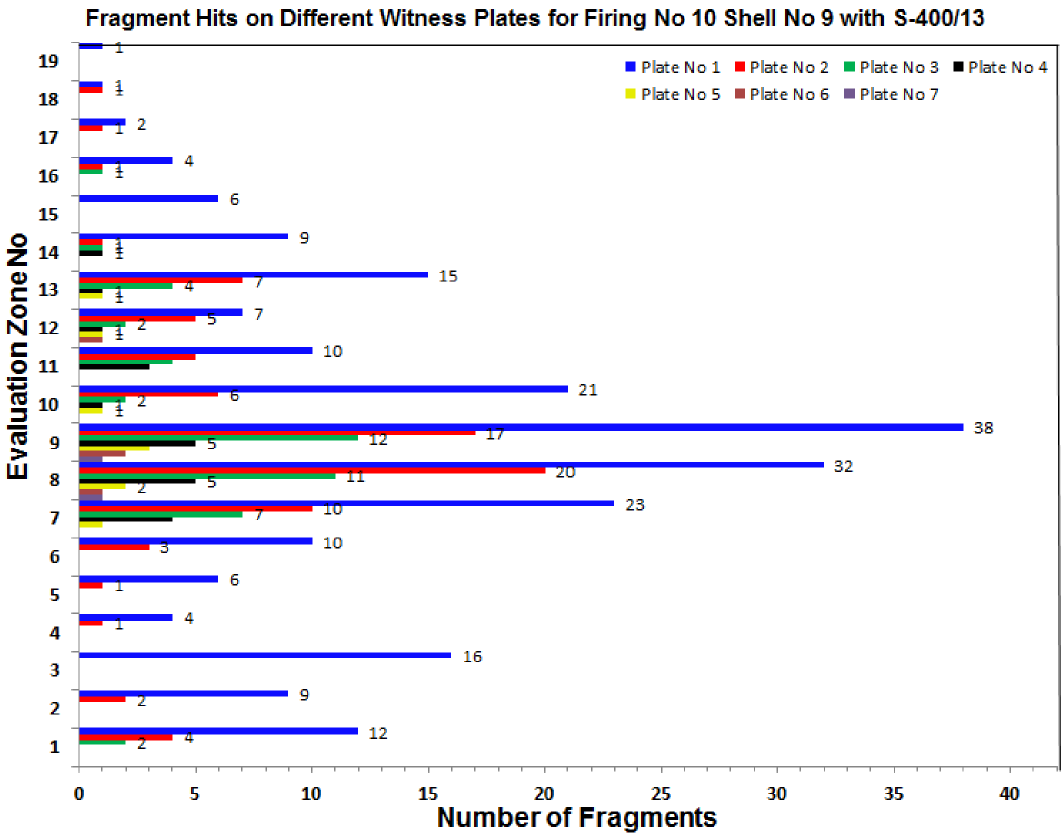

Figure 3.27 Fragment hits in different witness plates and evaluation zones for shell No 9 press filled with Sats-400/13 composition.

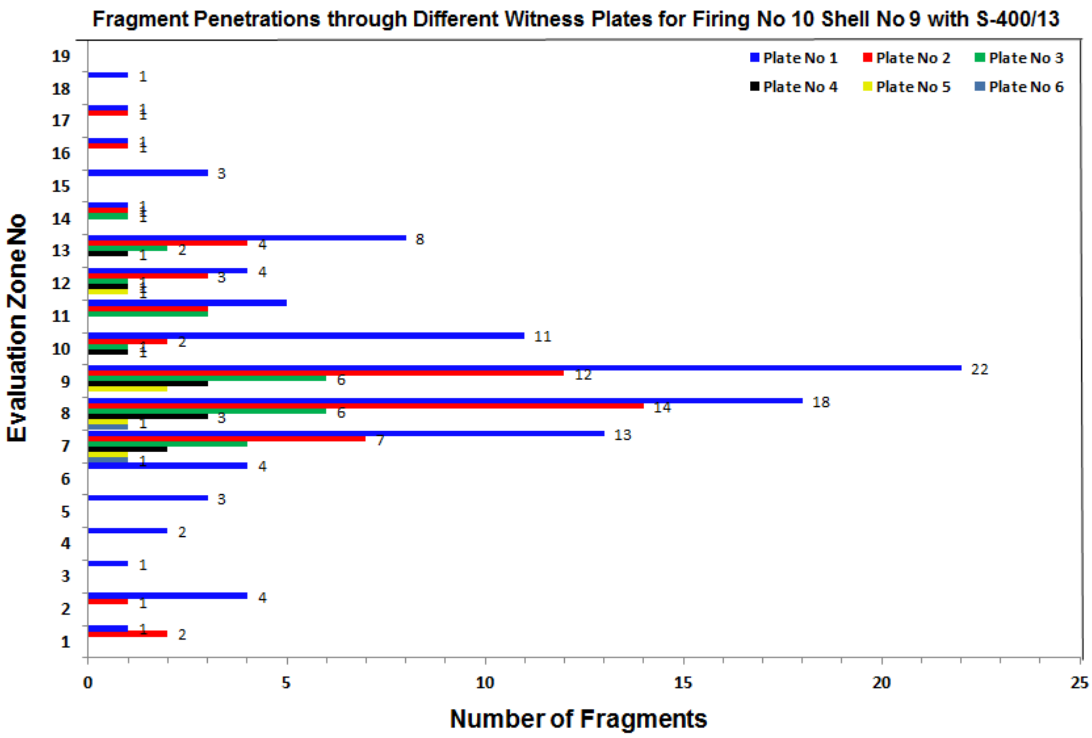

Figure 3.28 Fragment penetrations in different witness plates and evaluation zones for shell No 9 press filled with Sats-400/13 composition.

3.2 Summary – comparison

3.2.1 Hits and penetrations in each witness plate

For firings No 1 to firing No 10 all fragment hits and penetrations of the witness plates in the area 90 cm width and 190 cm height are summarized in Table 3.11. Firings with the same composition are grouped together in Table 3.12 to make it easier to compare the results.

Firing No	Plate No 1 Number of fragments		Plate No 2 Number of fragments		Plate No 3 Number of fragments		Plate No 4 Number of fragments		Plate No 5 Number of fragments		Plate No 6 Number of fragments		Plate No 7 Number of fragments		Plate No 8 Number of fragments	
	Hit	Through	Hit	Through	Hit	Through	Hit	Through	Hit	Through	Hit	Through	Hit	Through	Hit	Through
1	179	86	77	44	37	24	19	8	9	2	1					
2	204	87	75	48	42	30	23	5	1	1	1					
3	140	65	52	34	28	15	15	10	6	4	4	2	1	1	1	
4	140	55	46	24	21	15	14	8	7	1	1	1	1	1		
5	228	114	104	74	71	34	26	6	5	1	1					
6	195	**85**	65	**45**	37	**22**	18	**9**	5	**1**	1					
7	165	76	73	51	38	25	17	9	8	6	6	2	1	1	1	
8	158	71	64	35	31	22	18	7	3	1	1					
9	156	55	48	26	20	16	12	6	5	4	3	3	2	2	2	1
10	226	103	85	51	46	24	21	11	9	5	4	2	2			

Table 3.11 Fragment hits and penetrations summary.

MCX	Plate No 1 Number of fragments		Plate No 2 Number of fragments		Plate No 3 Number of fragments		Plate No 4 Number of fragments		Plate No 5 Number of fragments		Plate No 6 Number of fragments		Plate No 7 Number of fragments		Plate No 8 Number of fragments	
	Hit	Through	Hit	Through	Hit	Through	Hit	Through	Hit	Through	Hit	Through	Hit	Through	Hit	Through
6100	156	**55**	48	**26**	20	**16**	12	**6**	5	**4**	3	**3**	2	**2**	2	**1**
6100	140	**55**	46	**24**	21	**15**	14	**8**	7	**1**	1	**1**	1	**1**		
8100	158	**71**	64	**35**	31	**22**	18	**7**	3	**1**	1					
8100	140	**65**	52	**34**	28	**15**	15	**10**	6	**4**	4	**2**	1	**1**	1	
6002	165	**76**	73	**51**	38	**25**	17	**9**	8	**6**	6	**2**	1	**1**	1	
6002	204	**87**	75	**48**	42	**30**	23	**5**	1	**1**	1					
8001	195	**85**	65	**45**	37	**22**	18	**9**	5	**1**	1					
8001	179	**86**	77	**44**	37	**24**	19	**8**	9	**2**	1					
Sats 400/13	226	**103**	85	**51**	46	**24**	21	**11**	9	**5**	4	**2**	2			
Sats 432/13	228	**114**	104	**74**	71	**34**	26	**6**	5	**1**	1					

Table 3.12 Fragment hits and penetrations summary. Firings of equal compositions are grouped together.

The number of fragments for the different compositions can be looked on in different ways. Compositions with DNAN (MCX-6100 and MCX-8100) have fewer fragments than the compositions containing TNT (MCX-6002 and MCX-8001). Compositions with RDX (MCX-6002 and MCX-6100) have on average fewer fragments than compositions with HMX (MCX-8001 and MCX-8100). The compositions with HMX and energetic binder (Sats 400/13 and Sats 432/13) produce the highest number of fragments.

3.2.2 Total number of fragments

To obtain the total number of fragments for 360^o the number of fragments in each witness plate in the stack had to be corrected. Table 3.13 gives agreed conversion factors that BAE System recommended to use to obtain a 360^o distribution.

Witness Plate No	Distance (m)	Conversion Factor (k)
1	1.500	10.7789
2	1.527	10.9622
3	1.554	11.1457
4	1.581	11.3293
5	1.608	11.5131
6	1.635	11.6971
7	1.662	11.8811
8	1.689	12.0654

Table 3.13 Conversion factors used to calculate the total number of fragments.

3.2.3 Total number of fragment hits

By using the conversion factors in Table 3.13 on the results in Table 3.12 the total number of fragment hits in the different plates covering 360^o is obtained. These results are given in Table 3.14. Figure 3.29 shows the same information as a plot. Shells with the same filling have the same colour. The total number of fragments for firings with the same composition is approximately the same.

Composition	Number of fragment hits in							
	Plate No 1 (1.500 m)	Plate No 2 (1.527 m)	Plate No 3 (1.554 m)	Plate No 4 (1.581 m)	Plate No 5 (1.608 m)	Plate No 6 (1.635 m)	Plate No 7 (1.662 m)	Plate No 8 (1.689 m)
MCX-6100	1682	526	223	136	58	35	24	24
MCX-6100	1509	504	234	159	81	12	12	
MCX-8100	1703	702	346	204	35	12		
MCX-8100	1509	570	312	170	69	47	12	12
MCX-6002	1779	800	424	193	92	70	12	12
MCX-6002	2199	822	468	261	12	12		
MCX-8001	2102	713	412	204	58	12		
MCX-8001	1929	844	412	215	104	12		
Sats-400/13	2436	932	513	238	104	47	24	
Sats-432/13	2458	1140	791	295	58	12		

Table 3.14 Total number of fragment hits in different witness plates for all firings.

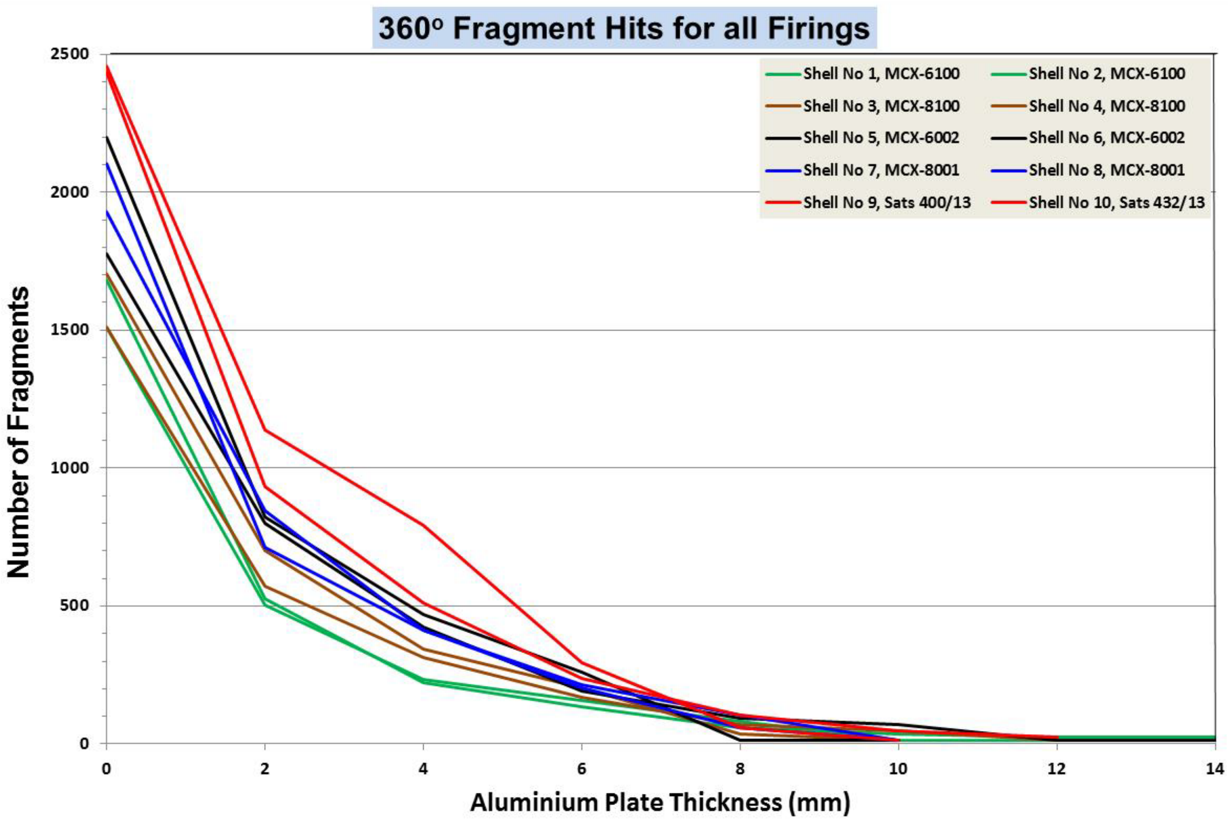

Figure 3.29 Total number of fragment hits on different witness plate for all firings.

3.2.4 Total number of fragment penetrations

By using the conversion factors given in Table 3.13 on the results in Table 3.12 we obtain Table 3.15 showing the total number of fragment penetrations for 360°. Figure 3.30 shows the same information as a plot. Shells with the same filling have the same colour. For firings with the same composition the total number of fragments is approximately equal.

Composition	Number of fragment penetrations in							
	Plate No 1	Plate No 2	Plate No 3	Plate No 4	Plate No 5	Plate No 6	Plate No 7	Plate No 8
MCX-6100	593	285	178	68	46	35	24	12
MCX-6100	593	263	167	91	12	12	12	
MCX-8100	765	384	245	79	12			
MCX-8100	701	373	167	113	46	23	12	
MCX-6002	819	559	279	102	69	23	12	
MCX-6002	938	526	334	57	12			
MCX-8001	916	493	245	102	12			
MCX-8001	927	482	267	91	23			
Sats 400/13	1110	559	267	125	58	23		
Sats 432/13	1229	811	379	68	12			

Table 3.15 Fragment penetrations through different witness plates for all firings.

For the shells filled with MCX-6002 there are some differences. Shell No 5, as shown in Table 2.1, has lower filling density (1.742 g/cm^3) than shell No 6 (1.785 g/cm^3). The shell (No 5) with lowest filling density gives fewer fragments, but the fragments have better penetration ability. Also for the two press filled shells some difference in fragmentation pattern is observed.

The highest number of fragments is obtained with the pressed fillings. For the melt-cast fillings TNT based fillings give more fragments than the DNAN based fillings, Figure 3.31.

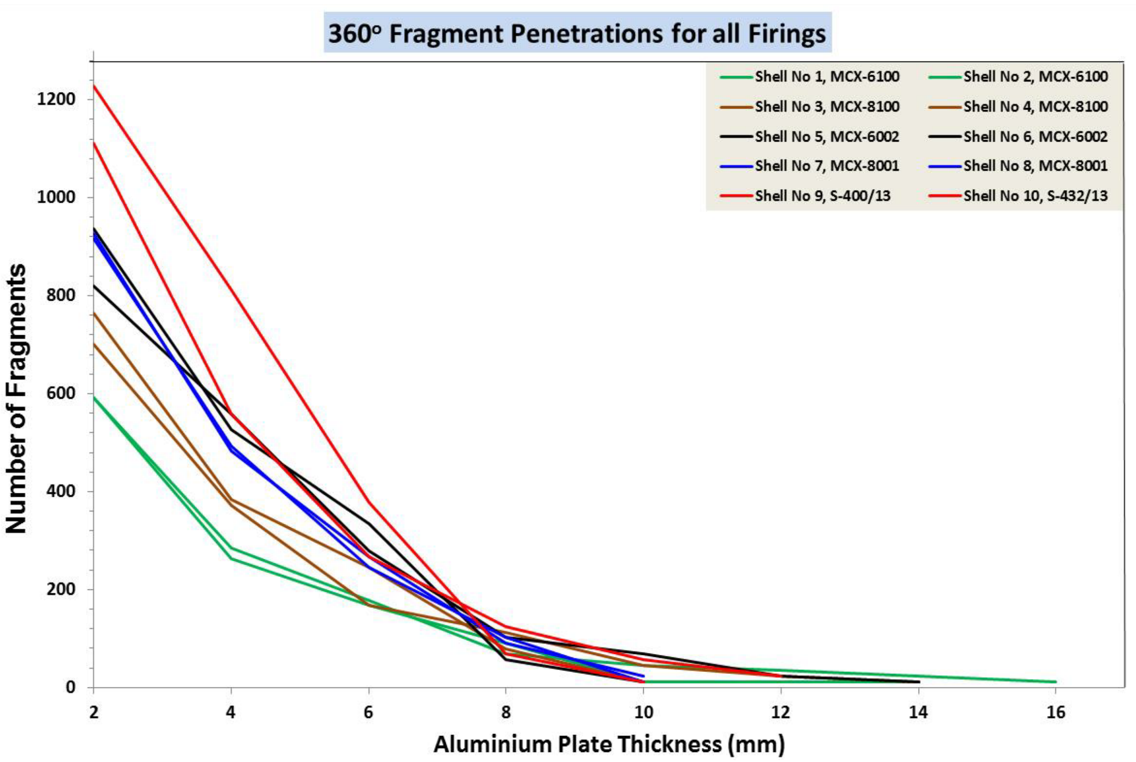

Figure 3.30 The figure shows the 360^o fragment penetrations in the different witness plates for all firings.

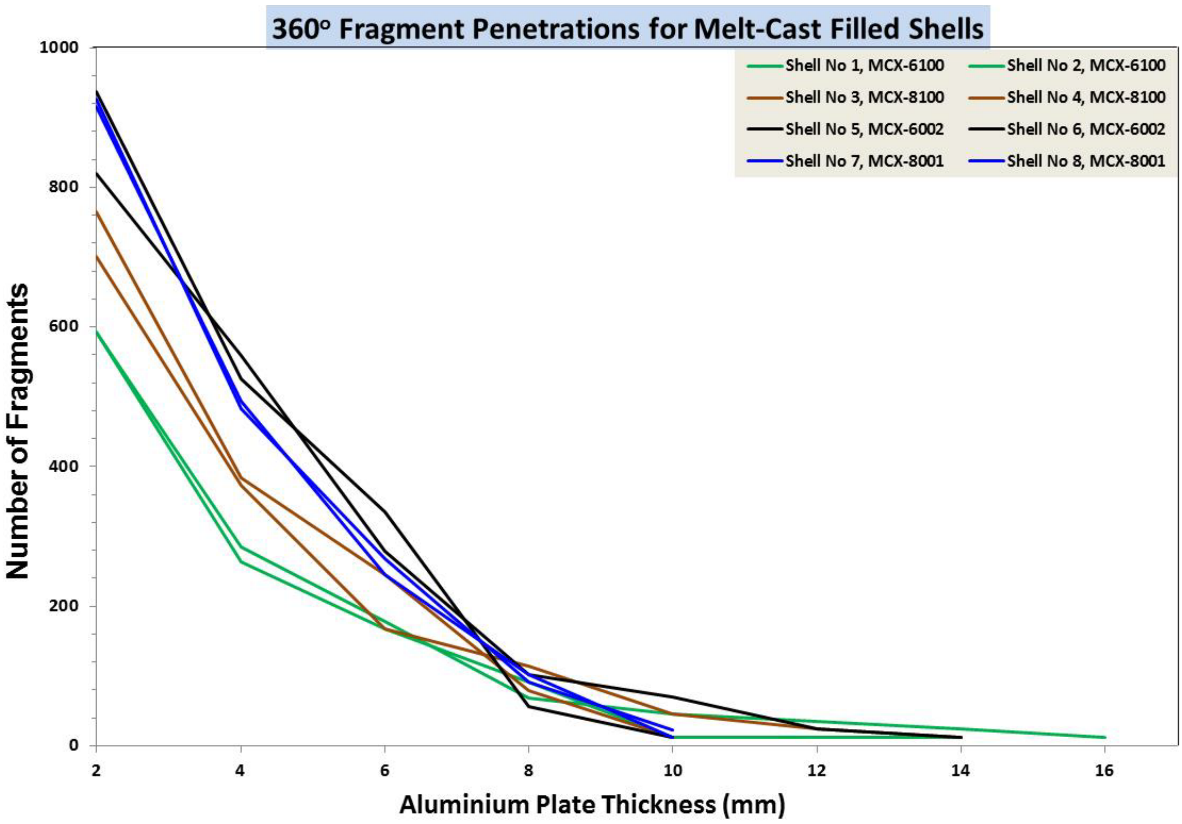

Figure 3.31 The 360° fragmentation distributions in the different witness plates for firings with melt-cast compositions.

3.2.5 DNAN based compositions

Figure 3.32 shows the number of fragment hits for DNAN-based compositions, while Figure 3.33 shows the fragment penetrations. Generally MCX-8100 gives more fragments than MCX-6100. However, the fragments from shells filled with MCX-6100 have higher energy and penetrate more plates than the fragment from shell filled with MCX-8100 compositions. The lower number of fragments for MCX-6100 gives larger fragments that penetrate more aluminium.

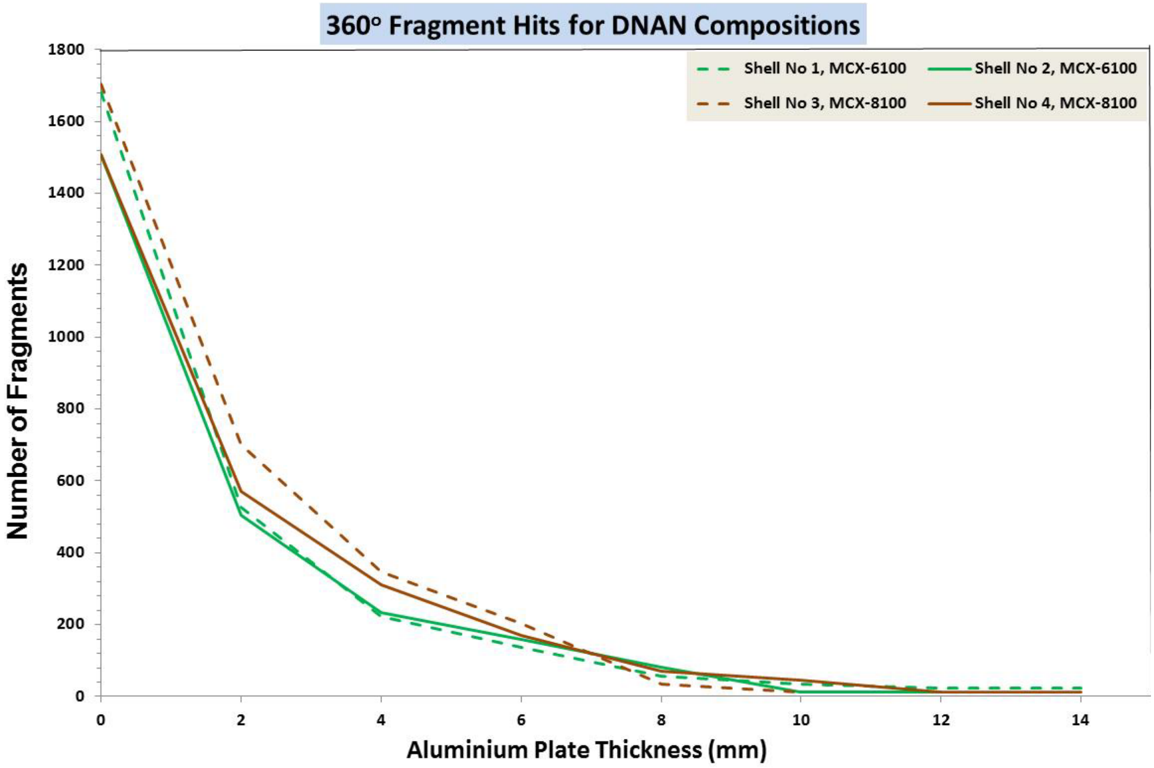

Figure 3.32 The total number of fragment hits in different thicknesses of aluminium for 40 mm shells filled with DNAN-based compositions.

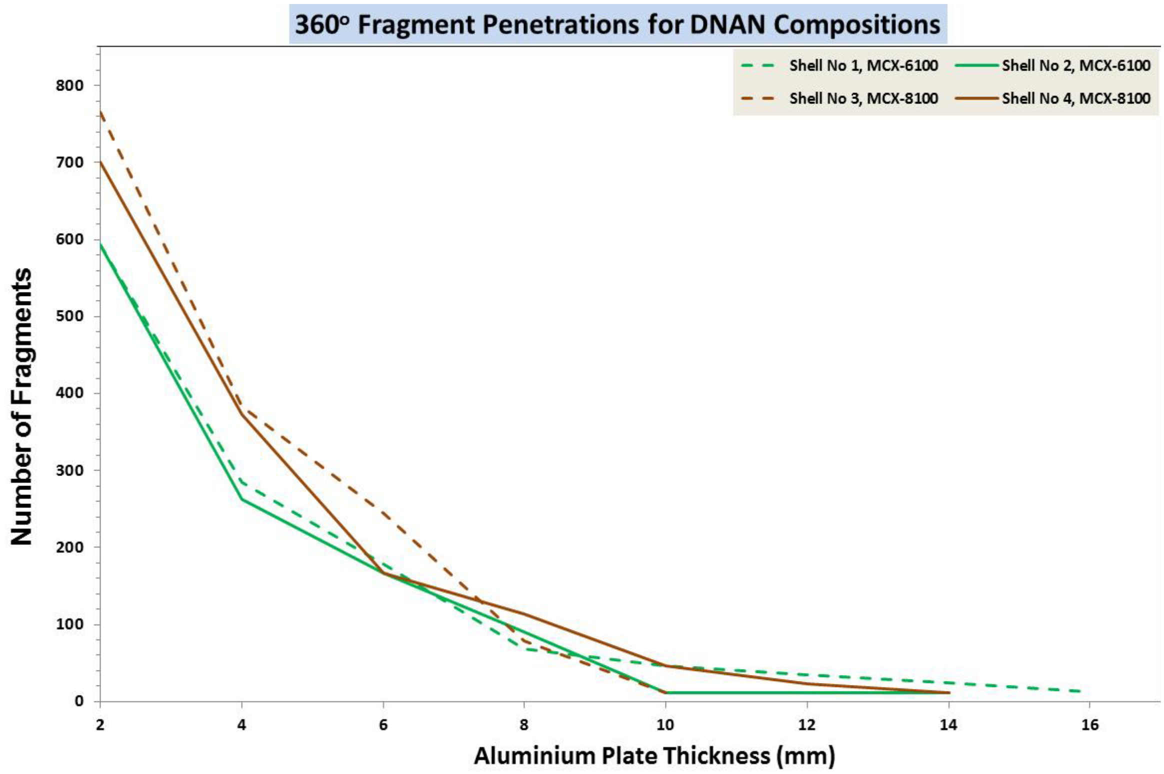

Figure 3.33 The figure shows the total number of fragment penetrations in different thicknesses of aluminium for 40 mm shells filled with DNAN-based compositions.

3.2.6 TNT-based compositions

Figure 3.34 shows the number of fragment hits for TNT-based compositions, while Figure 3.35 shows the fragment penetrations. There are only minor differences in both number of fragment hits and fragment penetrations between shells filled with MCX-6002 and MCX-8001 compositions. Shell No 5 filled with MCX-6002 composition has the lowest filling density. This shell produces the lowest number of fragments. Since the shell mass is constant this must result in larger fragments. The penetration ability for fragments from shell No 5 is two aluminium plates (4 mm) higher than for fragments from the three other TNT containing shells.

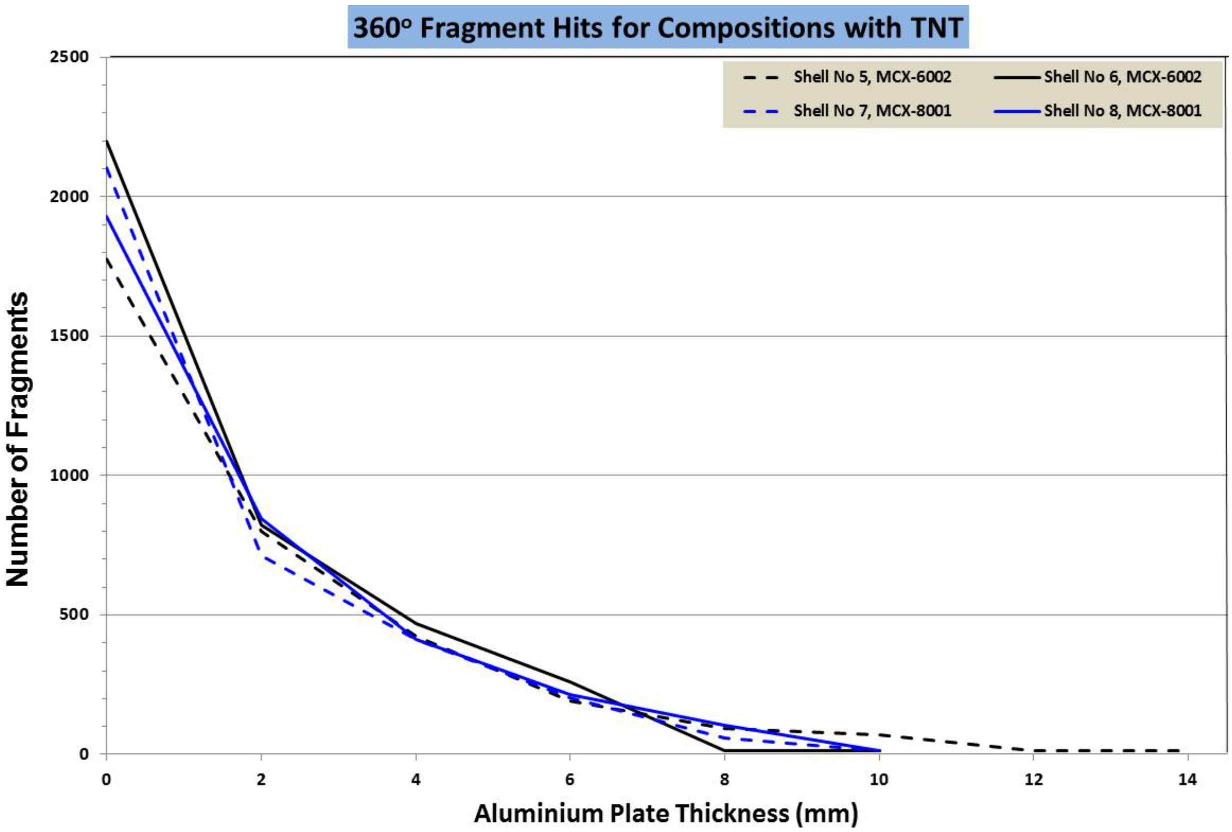

Figure 3.34 The total number of fragment hits in different thicknesses of aluminium for 40 mm shells filled with TNT-based compositions.

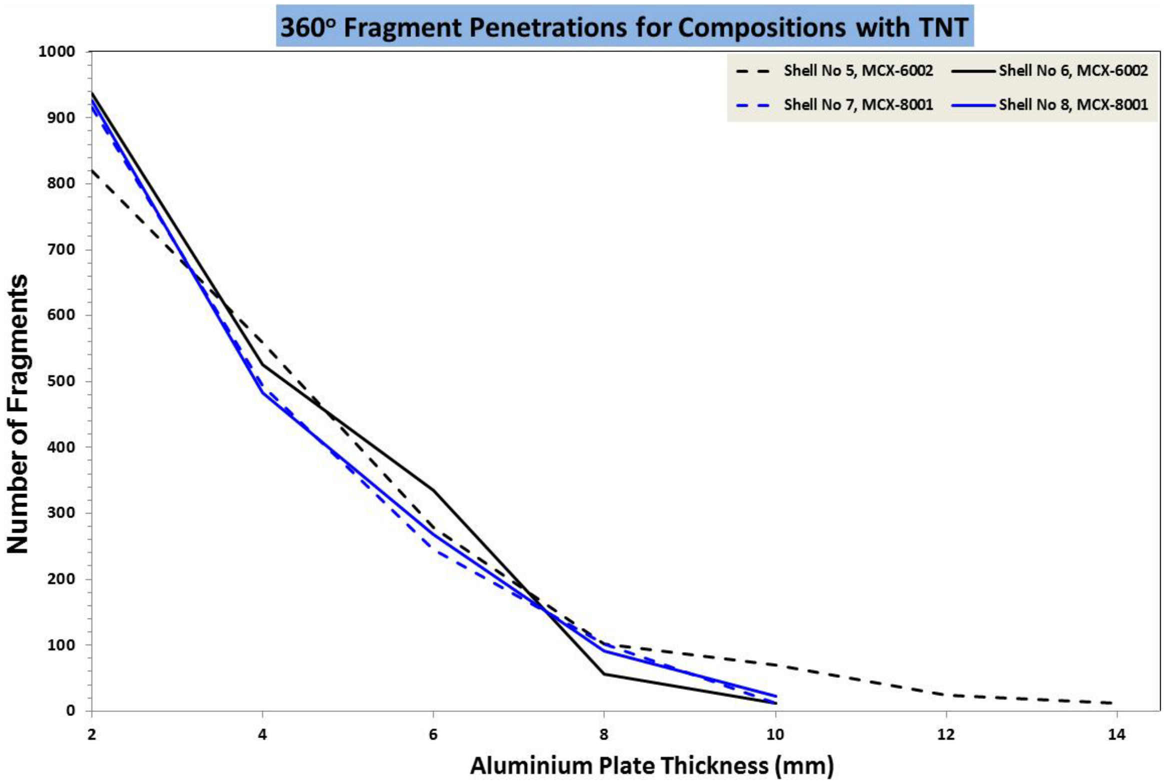

Figure 3.35 The total number of fragment penetrations in different thickness of aluminium for 40 mm shells filled with TNT-based compositions.

3.2.7 Pressed fillings

Both Sats 400/13 and Sats 432/13 give a higher number of fragment hits and penetrations than the melt cast compositions. The difference is most marked for an aluminium thickness up to 8 mm. Figure 3.36 gives a plot of the fragment hits for these two shells. Figure 3.37 shows a plot of penetrating fragments.

From the same shell mass a higher number of fragments on average give smaller fragments. Fragments from shell No 9 therefore penetrate one more plate than the fragments from shell No 10.

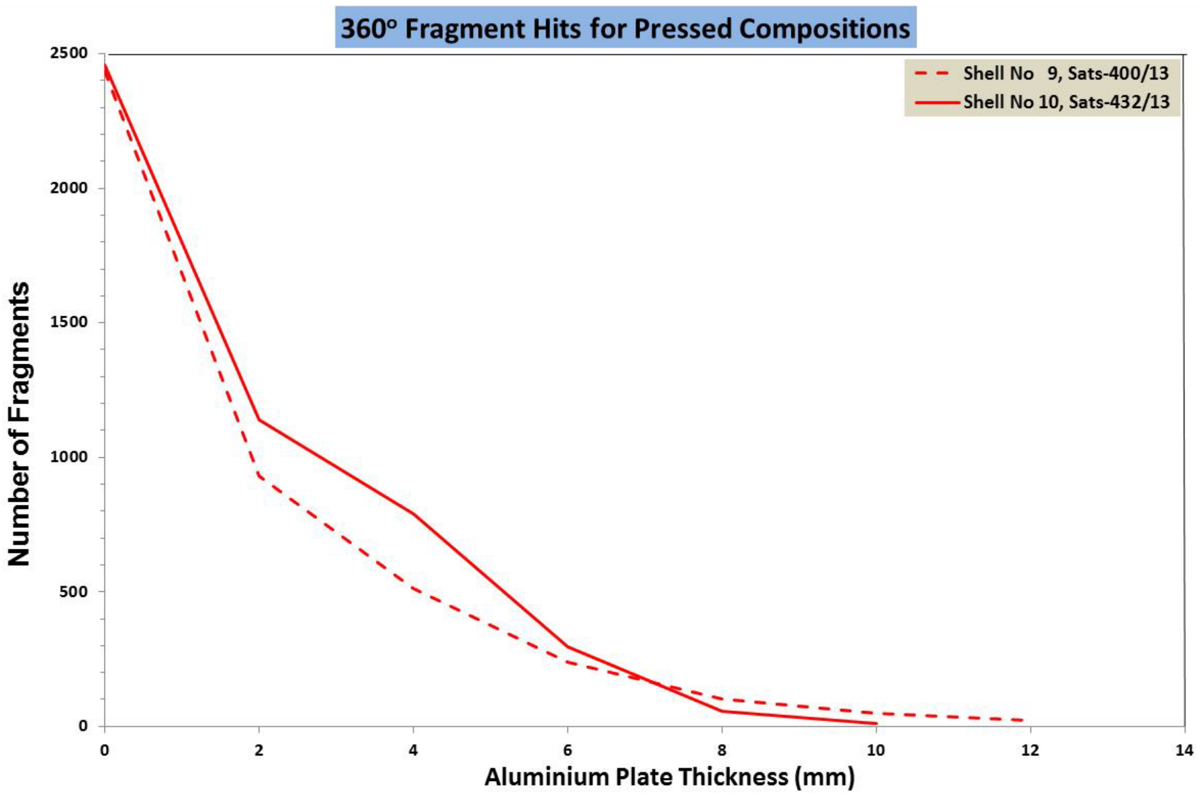

Figure 3.36 The figure shows the total number of fragment hits in different thickness of aluminium for 40 mm shells filled with GA/BAMO/HMX compositions.

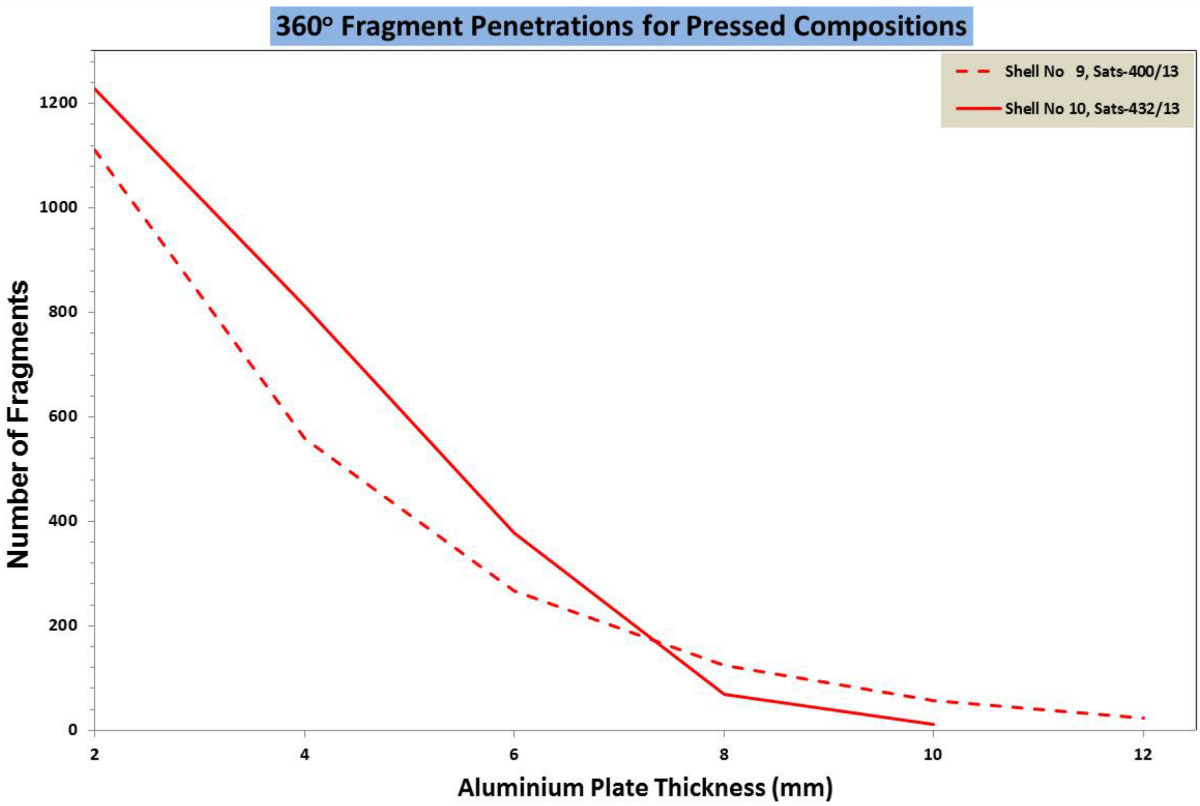

Figure 3.37 The figure shows the total number of fragment penetrations of different thicknesses of aluminium for 40 mm shells filled with GA/BAMO/HMX compositions.

4 Summary

10 40 mm shells filled with 6 different compositions have been detonated for study of the fragmentation ability. 4 melt cast compositions, two containing DNAN and two containing TNT have been tested in duplicate. The last two compositions were press filled HMX compositions with energetic GA/BAMO binder. The HMX content for Sats 400/13 was 94.7 wt. % and for Sats 432/13 94.3 wt. %. These two compositions contained an energetic binder synthesised at FFI. The four melt cast compositions were developed and filled by Chemring Nobel. Their names and nominal content was: MCX-6002 TNT/NTO/RDX (34/51/15), MCX-6100 DNAN/NTO/RDX (32/53/15), MCX-8001 TNT/NTO/HMX 36/52/12, MCX-8100 DNAN/NTO/HMX (35/53/12).

To stop the fragments 8 witness plates of aluminium with 2 mm thickness were set up in a stack with a gap of 25 mm between each plate. The plate width was1000 mm and the height 2000 mm. 50 mm along the edges was not used when counting fragments. The effective area was therefore 900 mm x1900 mm. During evaluation the witness plates were divided into 100 mm high evaluation zones in the vertical direction. This gave 19 evaluation zones for each plate. Both fragment hits and penetrations were counted.

The number of fragments penetrating the first witness plate was lowest for the MCX-6100 compositions with 55 for both shells. The highest number of penetrating fragments was obtained for the HMX/GA/BAMO compositions. For Sats 400/13 103 fragments and for Sats 432/13 114 fragments penetrated the first plate. All compositions gave fragments penetrating 5 witness plates. Only one shell, filled with MCX-6100 composition had fragments penetrating all 8 witness plates. Shells giving the lowest number of fragments have highest penetration abilities. Both DNAN compositions gave fewer fragments than the corresponding TNT compositions. The melt cast compositions with RDX gave on average fewer fragments than the corresponding HMX compositions.

References

(1) Patrick Goede, Ugo Barbieri, Sebastién Comte, J. Quaresma, Kamil Dudek,Genevieve Eck, Gino Fundarò, Thomas Keicher, Lise Liljeroth Løken, Gunnar Ove Nevstad and Helen Stenmark: Formulation and Production of New Energetic Materials", 44th International Annual Conference of the Fraunhofer ICT, June 25-28, 2013. P47-1 –P47-18.

(2) Ugo Barbieri, Giovanni Polacco, Thomas Keicher, Roberto Massimi: Preliminary Characterization of Propellants Based on p(GA/BAMO) and pAMMO Binders, Propellants Explosives Pyrotechnic, 2009, 34, 427-435.

(3) Ugo Barbieri, Thomas Keicher, Roberto Massimi, Giovanni Polacco: Preliminary Characterization of Propellants Based on p(GA/BAMO) and pAMMO Binders, 39th International Annual Conference of ICT 2008, p-130.

(4) Asparecida M. Kawamoto, Ugo Barbieri, Giovanni Polacco, Horst Krause, J. A. Saboia Hollanda, Manfred Kaiser and Thomas Keicher: Synthesis and Characterization of glycidyl azide-r(3,3-bis(azidomethyl)oxetane copolymer, 38th International Annual Conference of ICT 2007, p-71

(5) Gunnar Ove Nevstad: Determination of Detonation Velocity and Pressure for MCX-6100, FFI-rapport 2015/02323, 2 December 2015.

(6) Gunnar Ove Nevstad: Characterization of MCX-8100, FFI-rapport 2015/02448, 15 December 2015.

(7) Gunnar Ove Nevstad: Characterization of MCX-6002 and MCX-8001, FFI-rapport 2015/02182, 18 November 2015.

(8) Gunnar Ove Nevstad: Characterization of GA/BAMO/HMX Compositions - Detonation Velocity and Pressure, FFI-rapport 2015/02326, 2 December 2015.

(9) Gunnar Ove Nevstad: Intermediate Scale Gap Test of MCX-6002, FFI-rapport 2015/02184, 18 November 2015.

(10) Gunnar Ove Nevstad: Intermediate Scale Gap Test of MCX-6100, FFI-rapport 2015/02183, 18 November 2015.

(11) Laurence E. Fried, W. Michael Howard, P. Clark Souers (1998): Cheetah 2.0 User's Manual, UCRL-MA-117541 Rev. 5; Energetic Materials Center Lawrence Livermore National Laboratory, 20 August.

Appendix A Certificate Al-plates

AMAG ROLLING

Abnahmeprüfzeugnis 3.1 (EN 10204)
Inspection certificate - mill certificate

Nr.: 85247460 01 / 1
Rev.: 0
Seite / page: 1 von / of 2
Datum / date: 2013 04 10

Zertifiziert nach / certified to ISO 9001, ISO/TS 16949, EN/AS 9100, ISO 14001, NADCAP

Auftraggeber / customer: ThyssenKrupp MetalServ GmbH PM NE-Metalle Westfaliastraße 185 44147 DORTMUND GERMANY **Warenempfänger / consignee:** ThyssenKrupp MetalServ GmbH LC Dortmund Heinrich-August-Schulte-Str. 6 44147 DORTMUND GERMANY	Bestell Nr. / order no.: S15M-5402840643 Datum / date: 2013 03 22 Auftragsbest. Nr. / order confirm no.: 655120 Datum / date: 2013 03 22 Lieferschein Nr. / delivery note: 85247460 Datum / date: 2013 04 11

Produkt / product	**Bedingungen / terms**
Form / form: Bleche Werkstoff / material: EN AW 2017A Zustand / temper: T4 Dim. / dim.: [mm]: 2,00x1000,0x2000,0 Kundenartikel Nr. / cust. article no.: S201700200A	Technische Lieferbedingungen / techn. spec.: EN 485-2 : 2008 EN 485-4 : 1993 EN 573-3 : 2003 Sondervorschrift / special terms:

AB-Pos. ord.-item	BNr/Los/Teillos Lot/No./Part	Guss Nr. cast no.	Werkstoff material	Kollo packno.	Gewicht netto weight net	Stk. pcs.
01	59453/01/00	01/0054240/2	EN AW 2017A	6551200004	1002 kg	89
01	59453/01/00	01/0054240/2	EN AW 2017A	6551200005	1001 kg	89

Chemische Zusammensetzung ([%] Gewichtsanteile) / Chemical composition ([%] weight proportion (OES))

Guss Nr. / cast no.	material										
01/0054240/2	EN AW 2017A	Ti	Si	Fe	Cu	Mn	Mg	Cr	Zn	Ti+Zr	Sonst Einzel
	spec. min.	-	0,20	-	3,5	0,40	0,40	-	-	-	-
	spec. max.	-	0,8	0,7	4,5	1,0	1,0	0,10	0,25	0,25	0,05
	actual	0,04	0,69	0,4	4,1	0,58	0,72	0,02	0,18	0,04	0,02
		Sonst Summe									
	spec. min.	-									
	spec. max.	0,15									
	actual	0,04									

AMAG rolling GmbH, Postfach 32, A-5282 Ranshofen, Österreich - www.amag.at
AMAG rolling GmbH, P.O. Box 32, A-5282 Ranshofen, Austria - www.amag.at

AMAG ROLLING

Abnahmeprüfzeugnis 3.1 (EN 10204)
Inspection certificate - mill certificate

Nr.: 85247460 **01 / 1**
Rev.: 0

Seite / page: 2 von / of 2

Zertifiziert nach / certified to ISO 9001, ISO/TS 16949, EN/AS 9100, ISO 14001, NADCAP

Datum / date: 2013 04 10

Zugprüfung LT / tensile test LT										
BNr/Los	**Zustand**	**Richtung**	**Tests**		**Rm**	**Rp0.2**	**A50**			
Lot/No.	**temper**	**direction**			**[MPa]**	**[MPa]**	**[%]**			
				spec.min.	390	245	15			
				spec.max.	-	-	-			
59453/01	T4	LT	2	from	411	276	17			
59453/01	T4	LT		to	416	298	19			

Sonstige Prüfungen / other tests
Maßkontrolle: OK. / Dimensional Check: OK.
Oberfläche: OK. / Surface inspection: OK.

Es wird bestätigt, dass die Lieferung geprüft wurde und den Vereinbarungen bei der Bestellung entspricht.
We hereby certify that the material described above has been tested and complies with the terms of the order contract.

Werksachverständiger / factory specialist	**E-Mail / e-mail**
Josef Klampfer	josef.klampfer@amag.at

Herstellerland: Österreich / goods origin: The goods are of Austrian origin.
Maschinell erstellt - Gültig ohne Unterschrift / Automated - valid without being signed.

AMAG rolling GmbH, Postfach 32, A-5282 Ranshofen, Österreich - www.amag.at
AMAG rolling GmbH, P.O. Box 32, A-5282 Ranshofen, Austria - www.amag.at

Appendix B Material properties of the shell

Bofors standard W3–1970

Datum/Date	Dok.nr/Doc. No.
1985-03-01	38 005 074
Utgåva/Issue	Sida/Page
3	1 (1)

AB BOFORS • STANDARD • BOX 500 • S-691 80 • BOFORS • SWEDEN • EFTERTRYCK UTAN SKRIFTLIGT MEDGIVANDE FÖRBJUDS • COPYRIGHT

STÅL BOFORS W3-1970 AUTOMAT OCH SPRÄNGGRANATSTÅL	STEEL BOFORS W3-1970 FREE CUTTING STEEL AND STEEL FOR EXPLOSIVE SHELLS

LEVERANSFORM

Stång

FORM OF SUPPLY

Bar

MATERIALFORDRINGAR

MATERIAL REQUIREMENTS

Sammansättning

Chemical composition

	C %	Si %	Mn %	P %	S %
Min	0,46	0,20	0,70	0,060	0,18
Max	0,51	0,35	0,90	0,080	0,22

Hållfasthet

Mechanical properties

Beteckning *Designation*	Tillstånd *Condition*	Form	Godstjocklek *Thickness* mm	Draghållfasthet *Tensile properties*			Hårdhet *Hardness*
				R_{eL} N/mm² min	R_m N/mm² min	A_{10} %	HB
W3-1970-50	Obehandlat *Untreated*	Stång *Bar*	≤ 90	330	640	8–18	180–220
W3-1970-60	Obehandlat *Untreated*	Stång *Bar*	≤ 90	370	690	8–18	200–240 V

KOMPLETTERANDE UPPLYSNINGAR

SUPPLEMENTARY INFORMATION

Tekniska data

Densitet .... 7,83 g/cm³

Elasticitetsmodul.............. 210000 N/mm²

Längdutvidgningskoefficient ... 13x10⁻⁶

Technical data

Density .... 7,83 g/cm³

Modulus of elasticity ... 210000 N/mm²

Coefficient of thermal expansion .... 13x10⁻⁶

Svetsning

Olämpligt att svetsa

Welding

Unsuitable for welding

Övriga upplysningar

Äldre beteckning B 9 UL

Jämförbara material

Storbritannien BS 970:Part 1:1972, 212M44
Västtyskland DIN 1651, 45S20
Werkstoffnummer 1.0727

Other information

Older designation B 9 UL

Comparable materials

Great Britain BS 970:Part 1:1972, 212M44
West Germany DIN 1651, 45S20
Werkstoffnummer 1.0727

Figure App B. 1 Material certificate for the shell body.

Appendix C Pictures of all witness plates

C.1 Witness plates for firing No 1 with MCX-8001

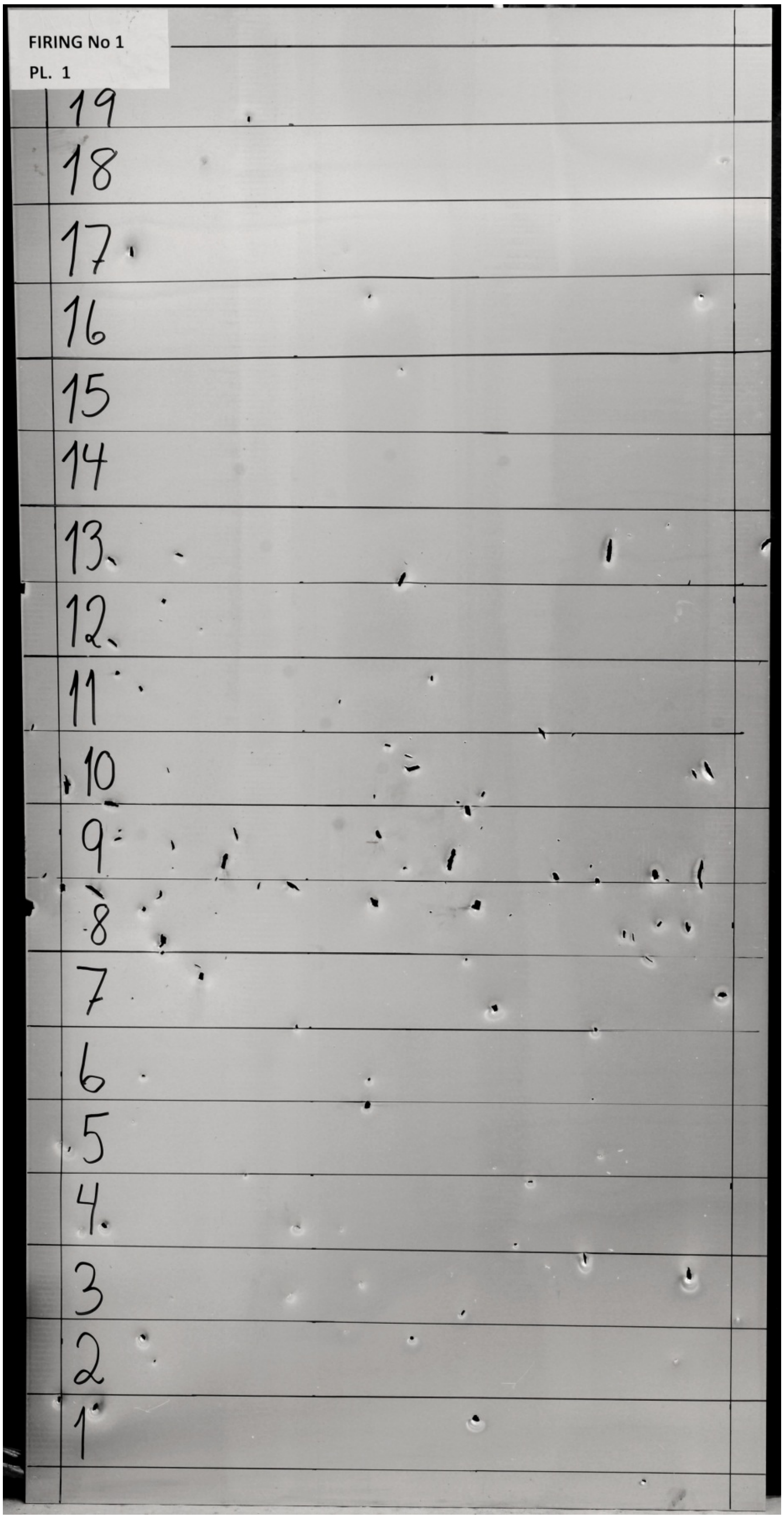

Figure App C. 1 The witness plate closest to the shell from firing of shell No 8 with MCX-8001 composition.

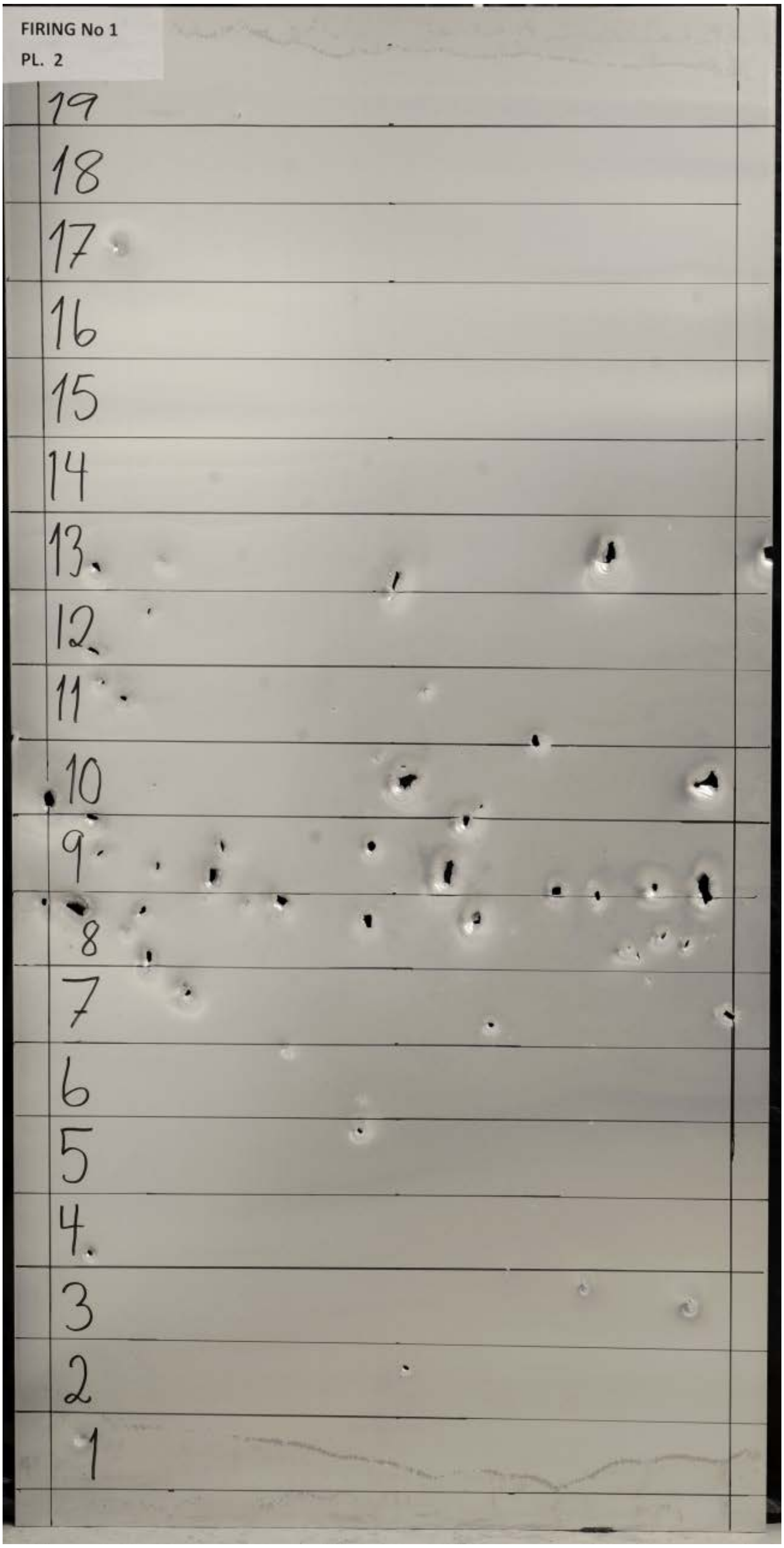

Figure App C. 2   Witness plate No 2 from firing of shell No 8 filled with MCX-8001 composition.

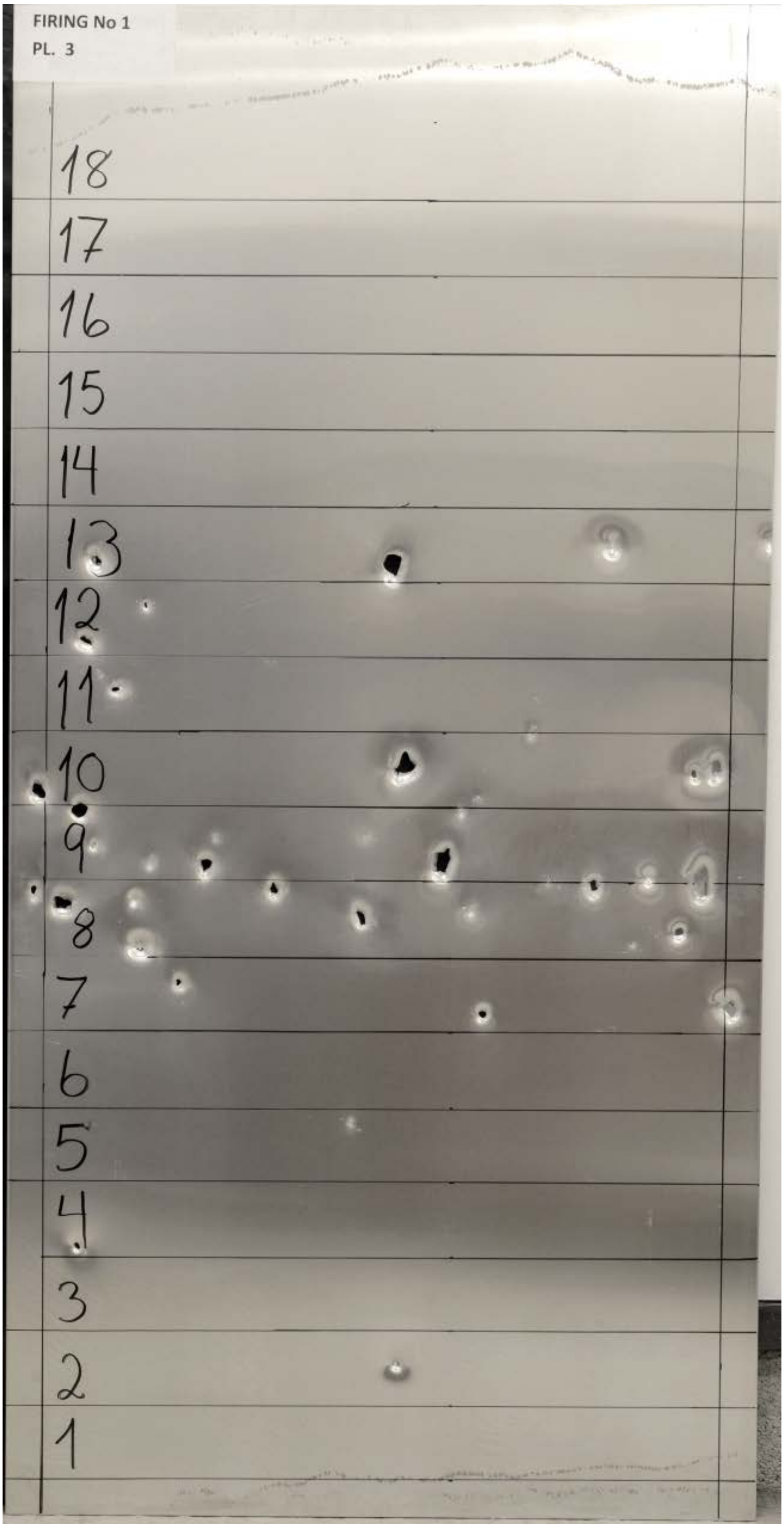

Figure App C. 3   Witness plate No 3 from firing of shell No 8 filled with MCX-8001 composition.

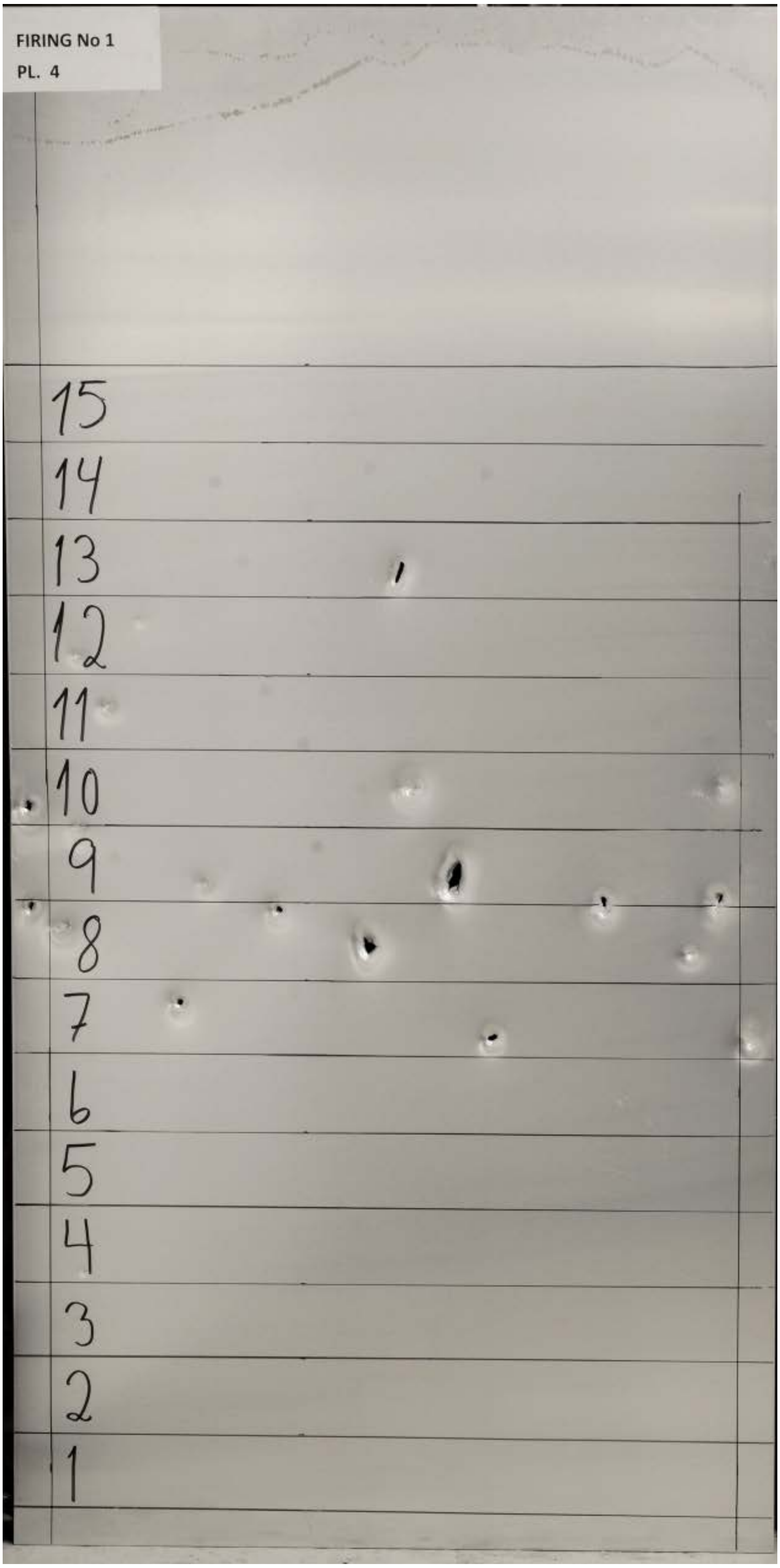

Figure App C. 4   Witness plate No 4 from firing of shell No 8 filled with MCX-8001 composition.

Figure App C. 5 Witness plates No 5 and 6 from firing of shell No 8 filled with MCX-8001 composition.

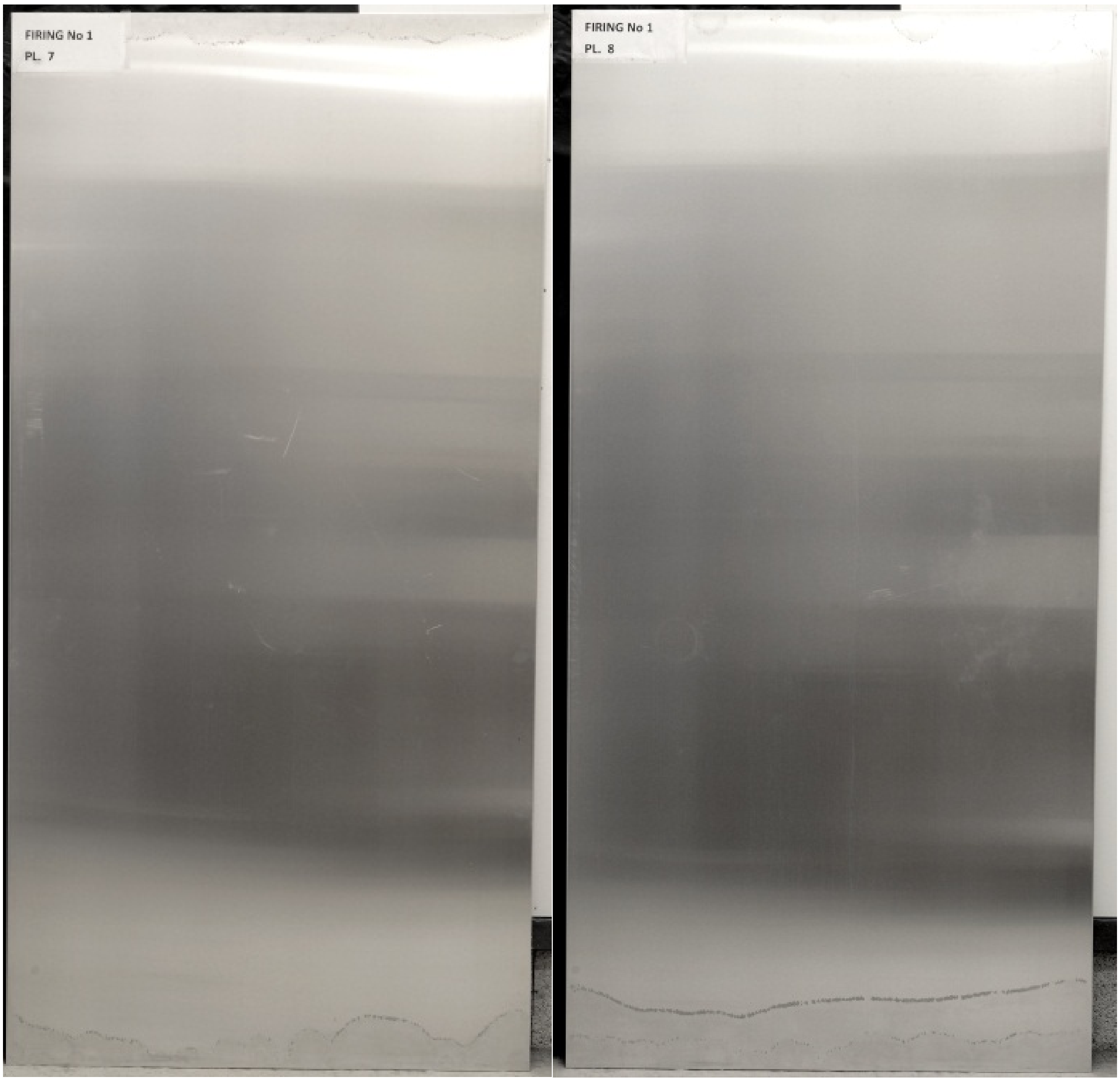

Figure App C. 6 Witness plates No 7 and No 8 for firing of shell No 8 filled with MCX- 8001 composition.

C.2 Witness plates for firing No 2 with MCX-6002 composition

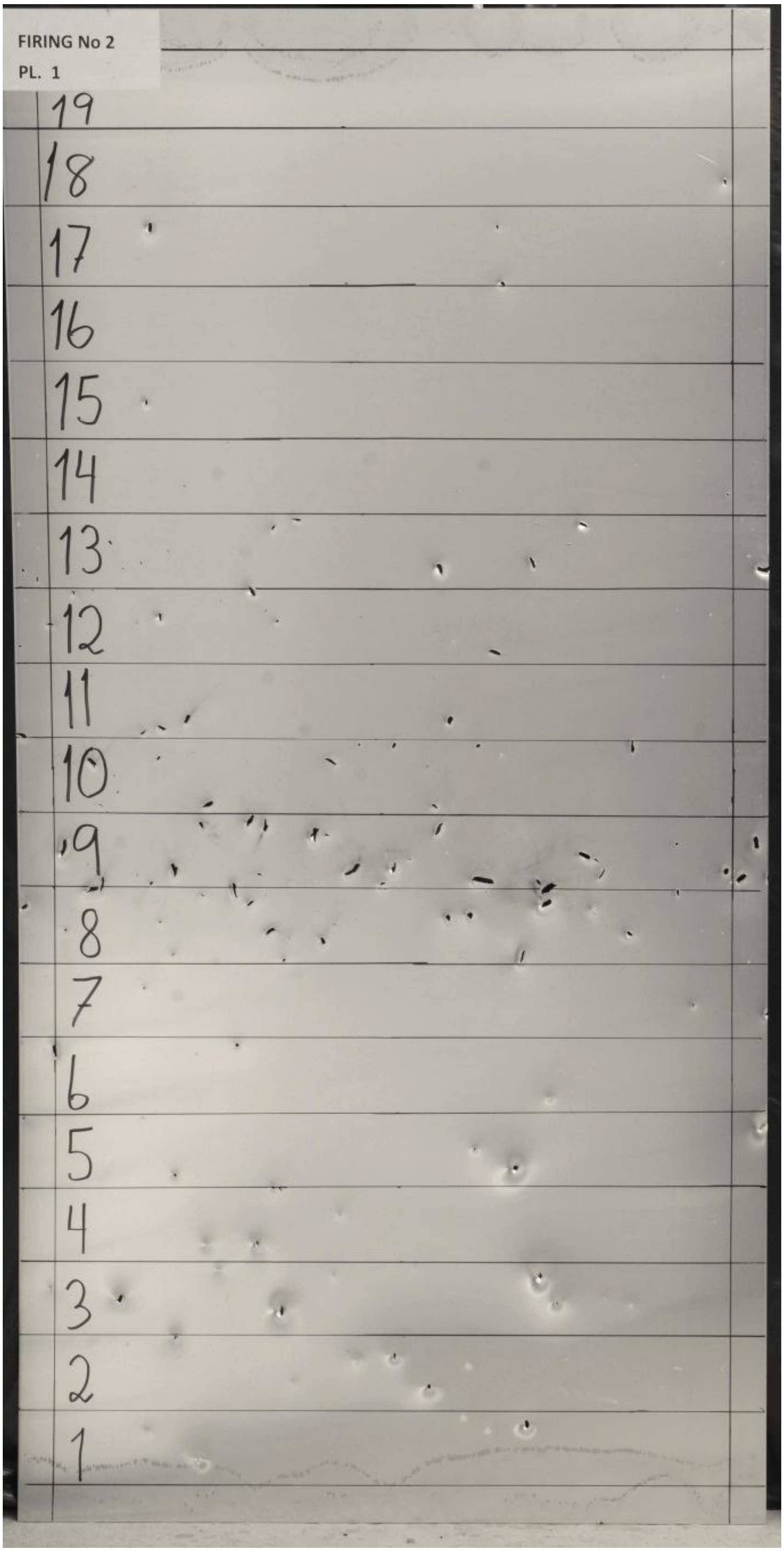

Figure App C. 7 The Figure shows a picture of the front witness plate for firing of shell No 6 filled with MCX-6002 composition.

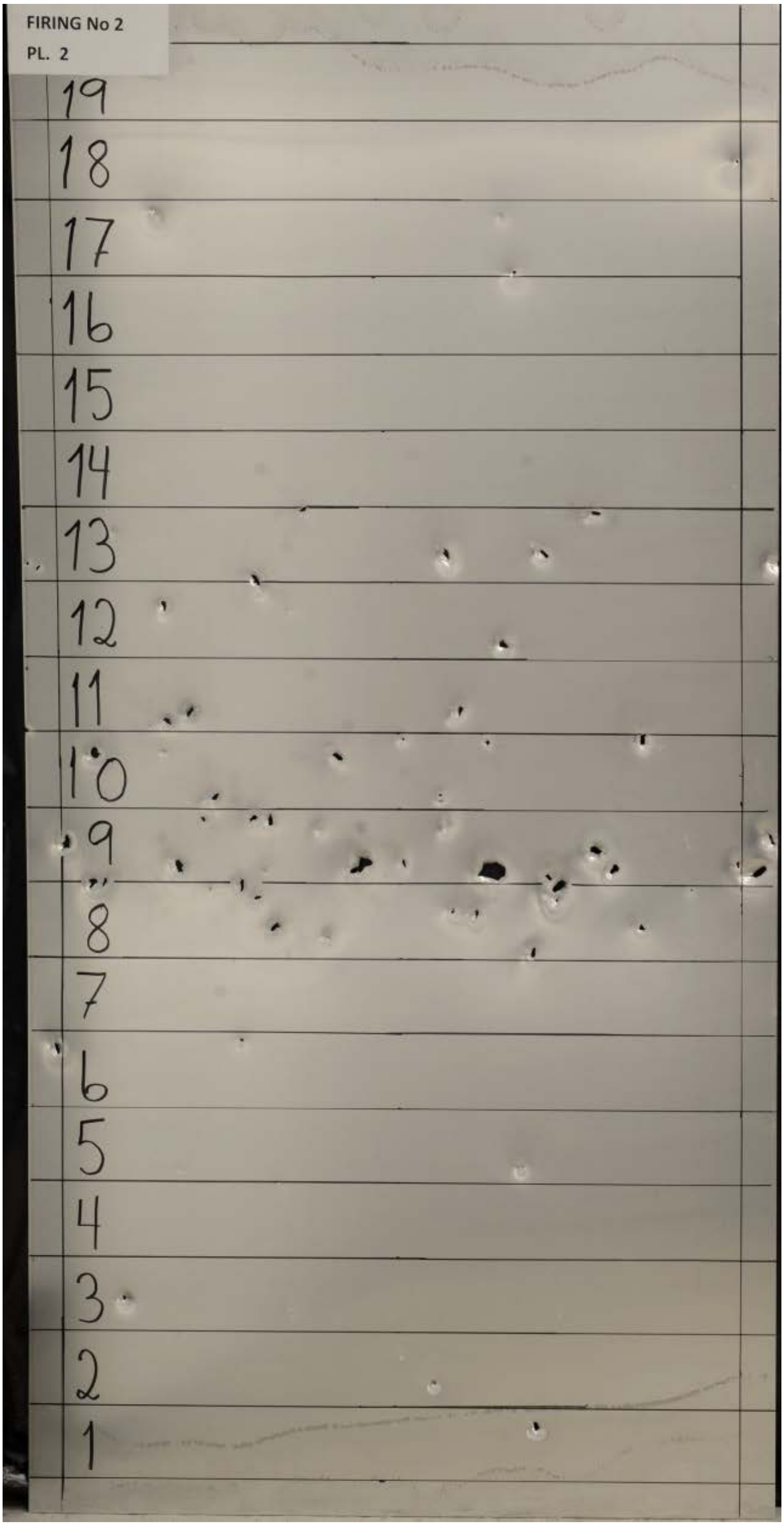

Figure App C. 8 Witness plate No 2 from firing of shell No 6 filled with MCX-6002 composition.

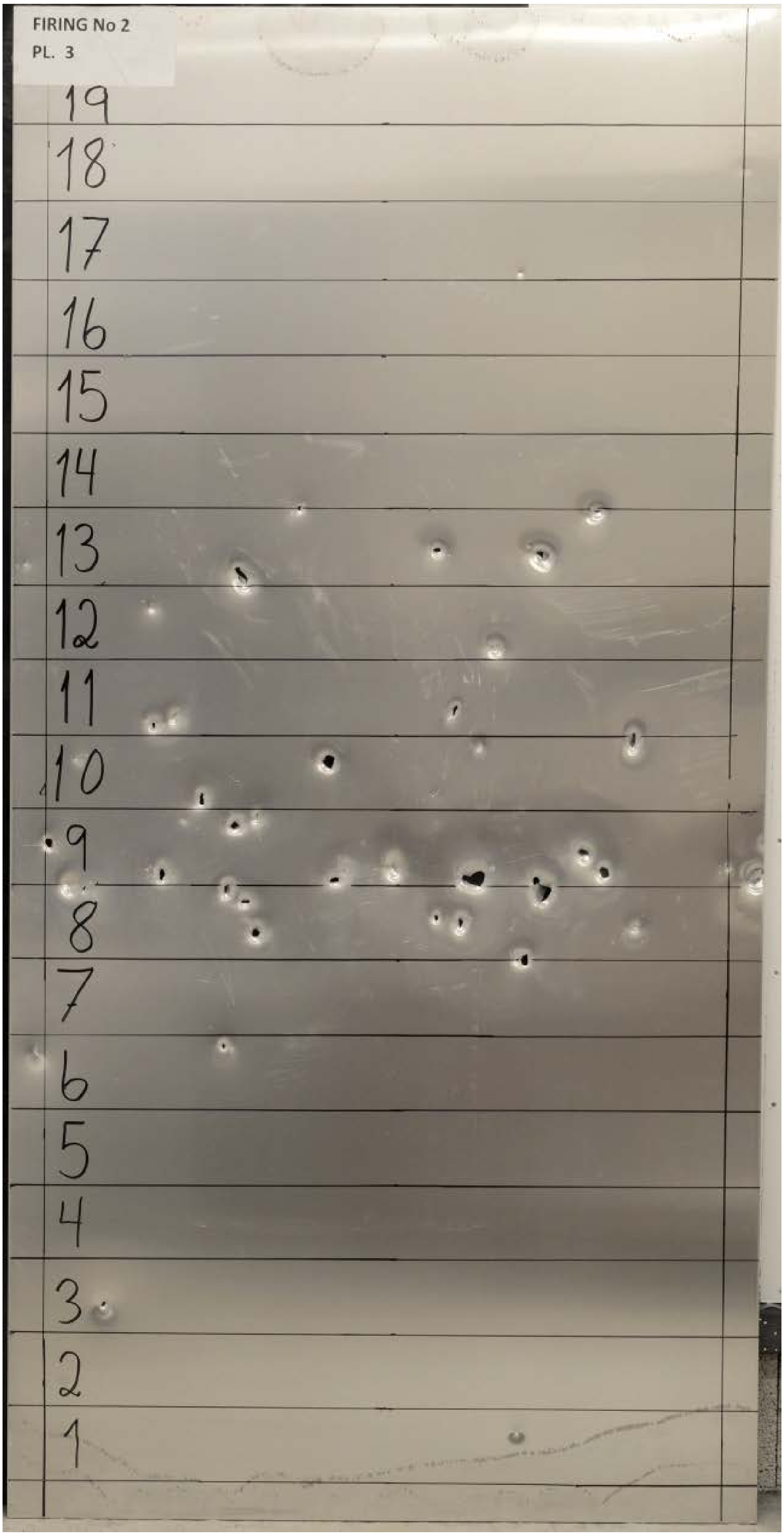

Figure App C. 9 Witness plate No 3 from firing of shell No 6 filled with MCX-6002 composition.

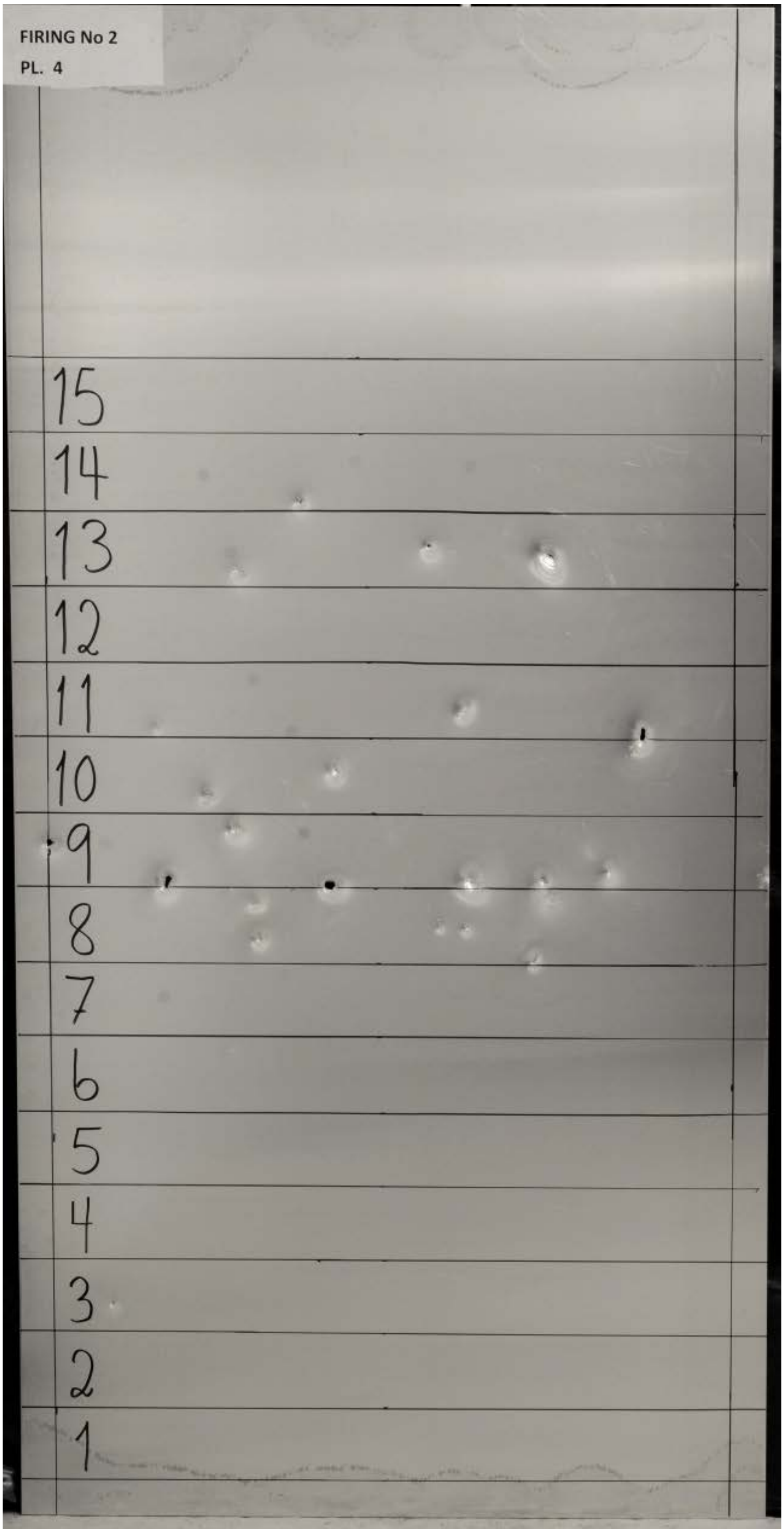

Figure App C. 10 Witness plate No 4 from firing of shell No 6 filled with MCX-6002 composition.

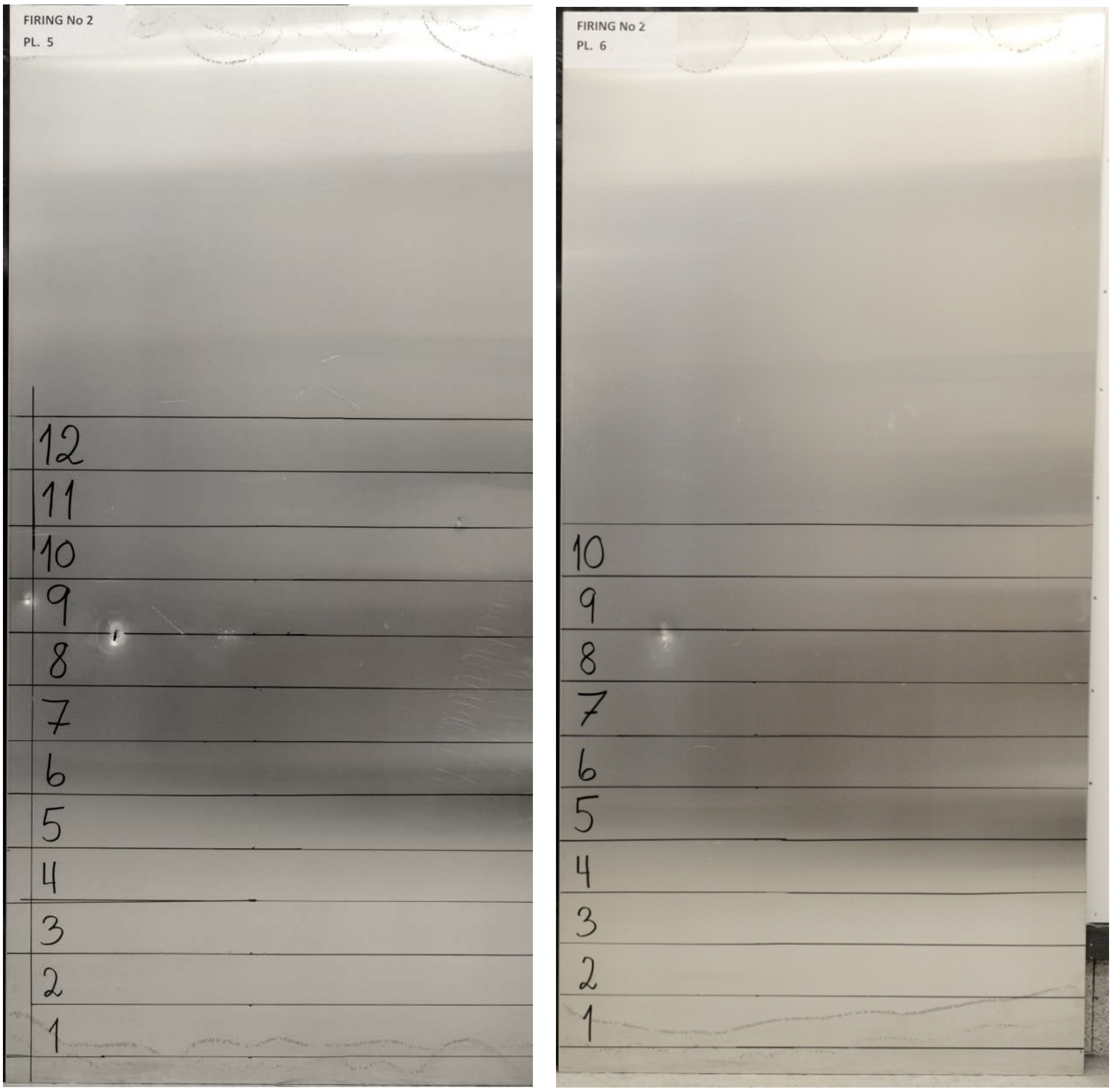

Figure App C. 11 Witness plates No 5 and No 6 from firing of shell No 6 filled with MCX-6002 composition.

Figure App C. 12 Witness plates No 7 and No 8 from firing of shell No 6 filled with MCX-6002 composition.

C.3 Witness plates for firing No 3 with MCX-8100 composition

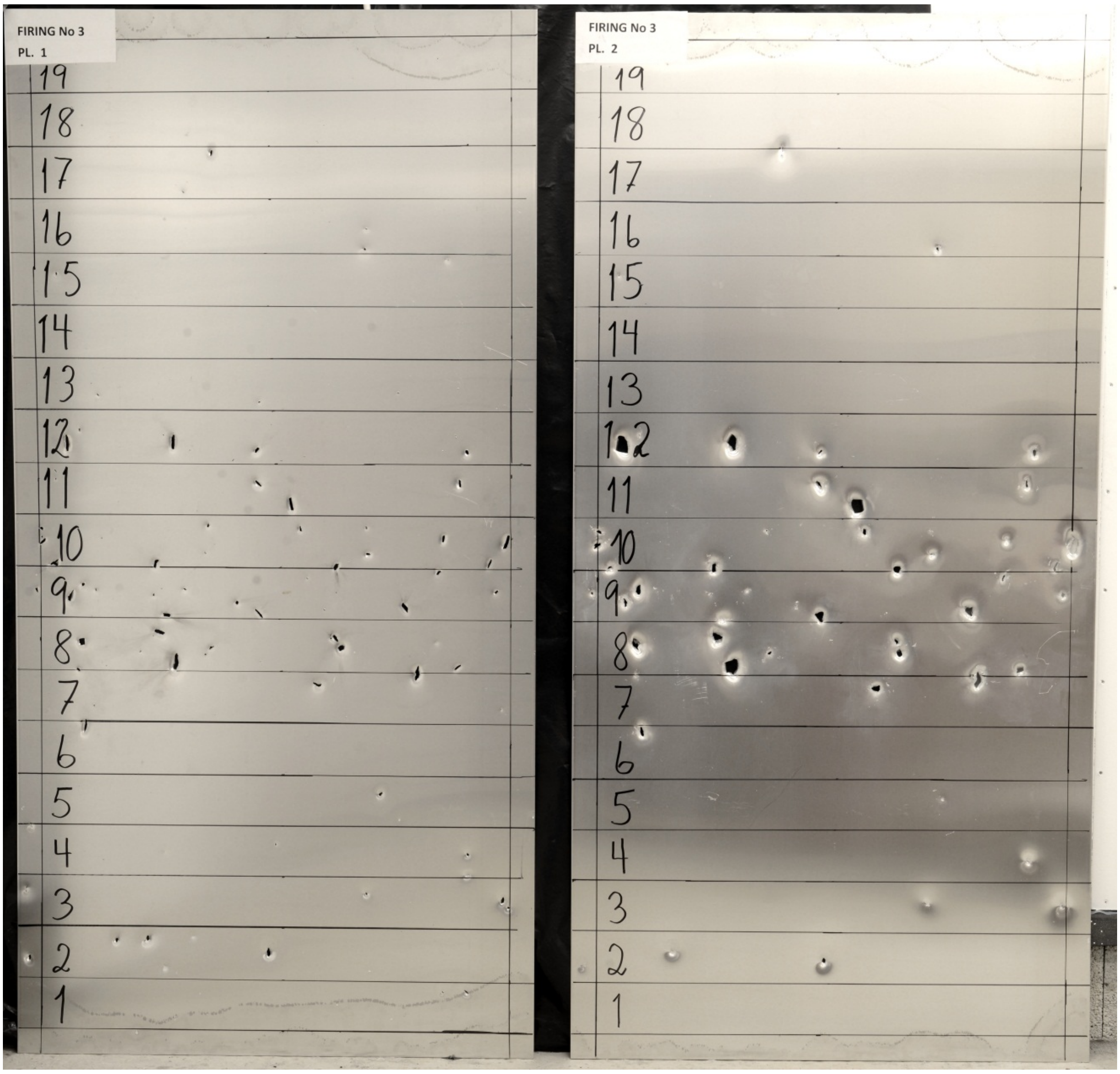

Figure App C. 13 Witness plates No 1 and No 2 from firing of shell No 4 filled with MCX-8100 composition

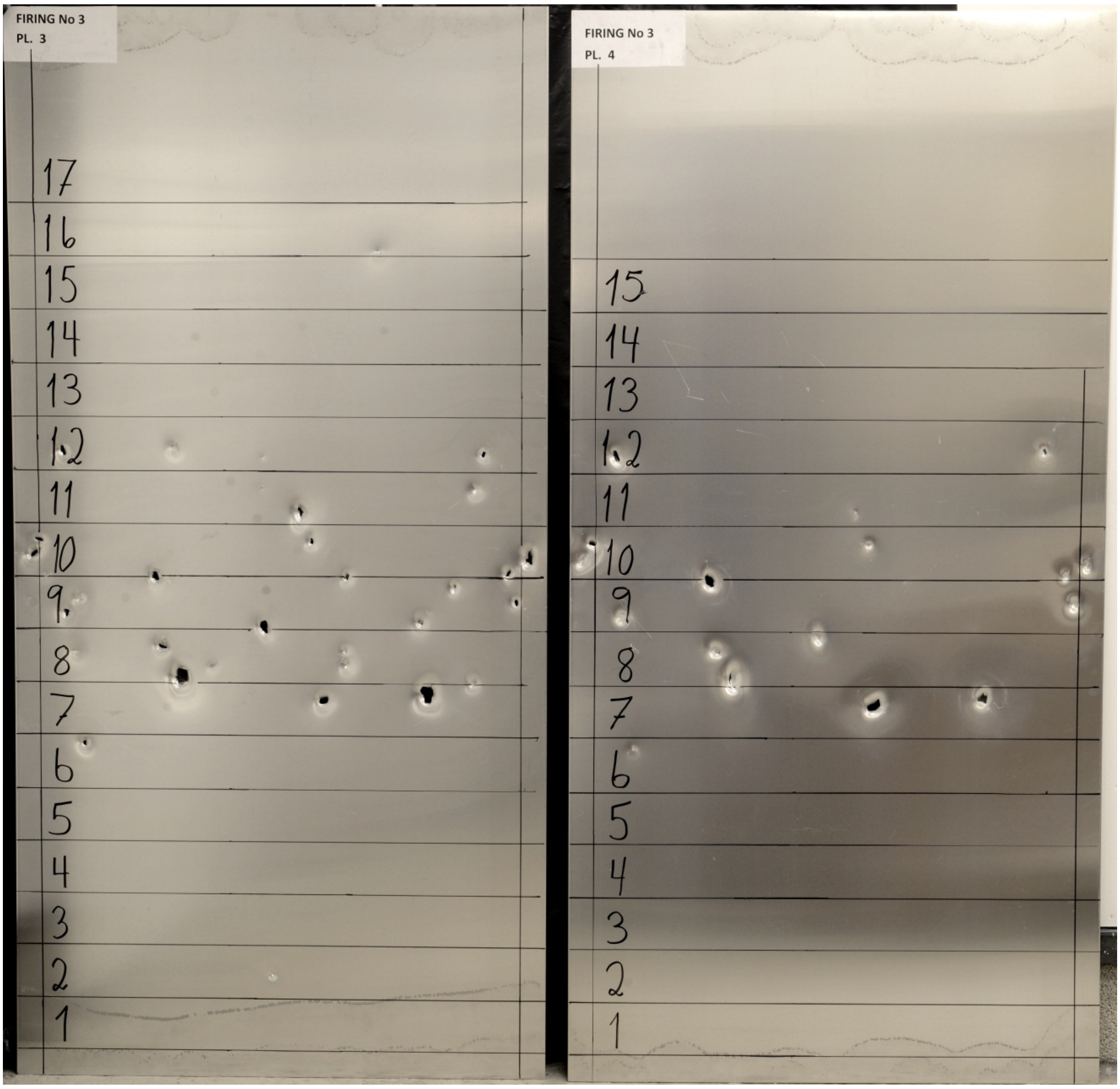

Figure App C. 14 Witness plates No 3 and No 4 from firing of shell No 4 filled with MCX-8100 composition.

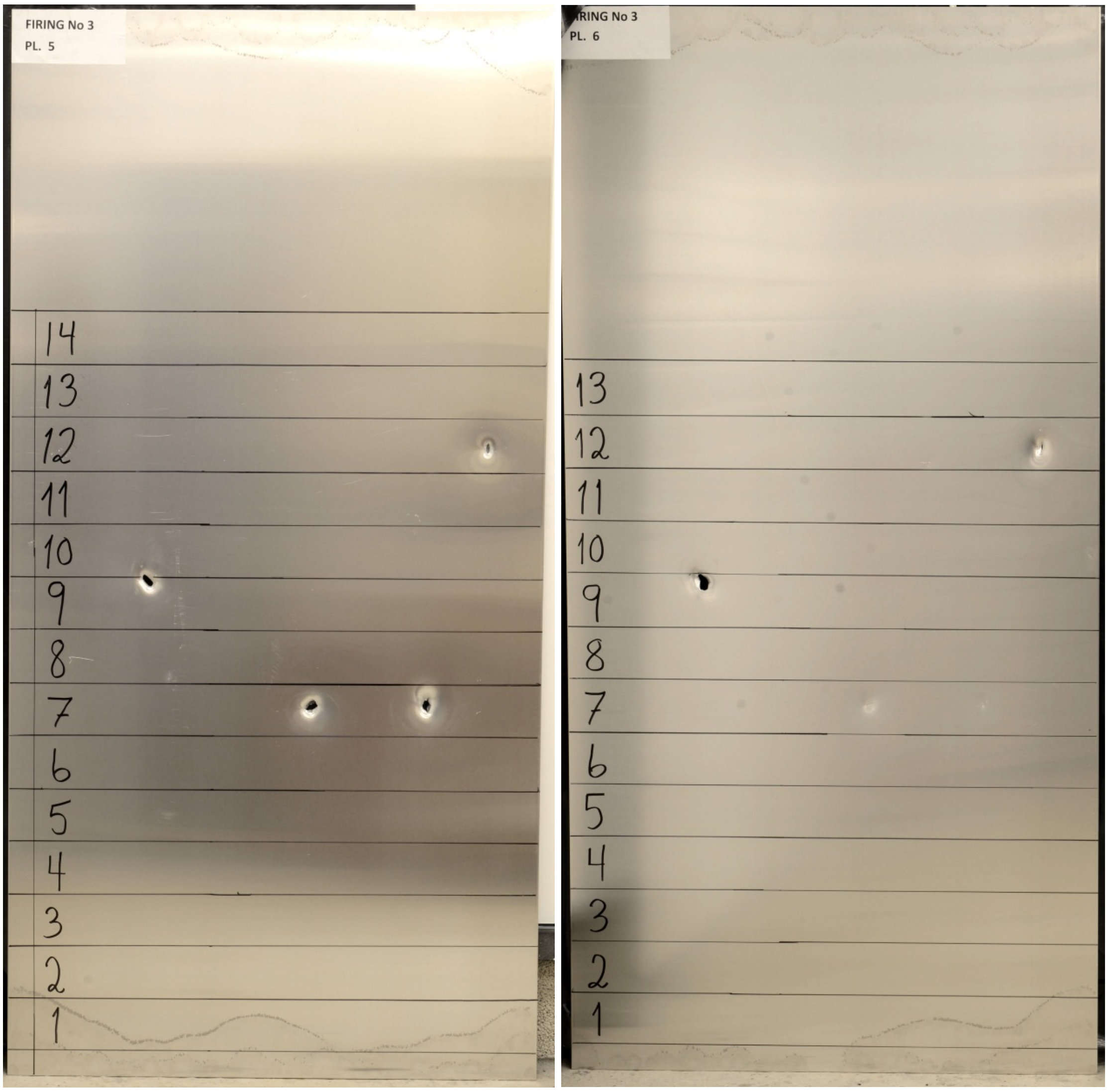

Figure App C. 15 Witness plates No 5 and No 6 from firing of shell No 4 filled with MCX-8100 composition.

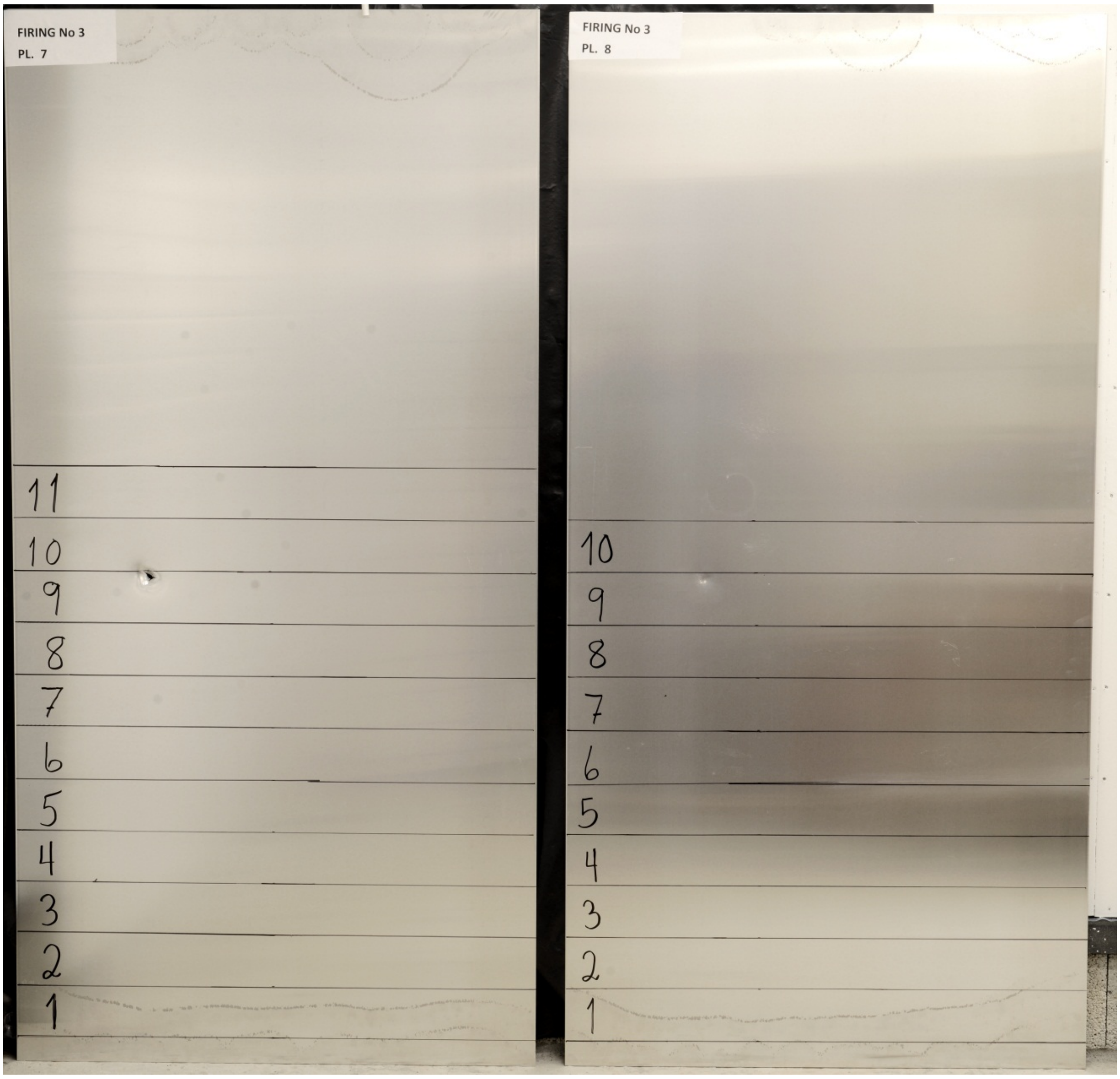

Figure App C. 16 Witness plates No 7 and No 8 from firing of shell No 4 filled with MCX-8100 composition.

C.4 Witness plates for firing No 4 with MCX-6100 composition

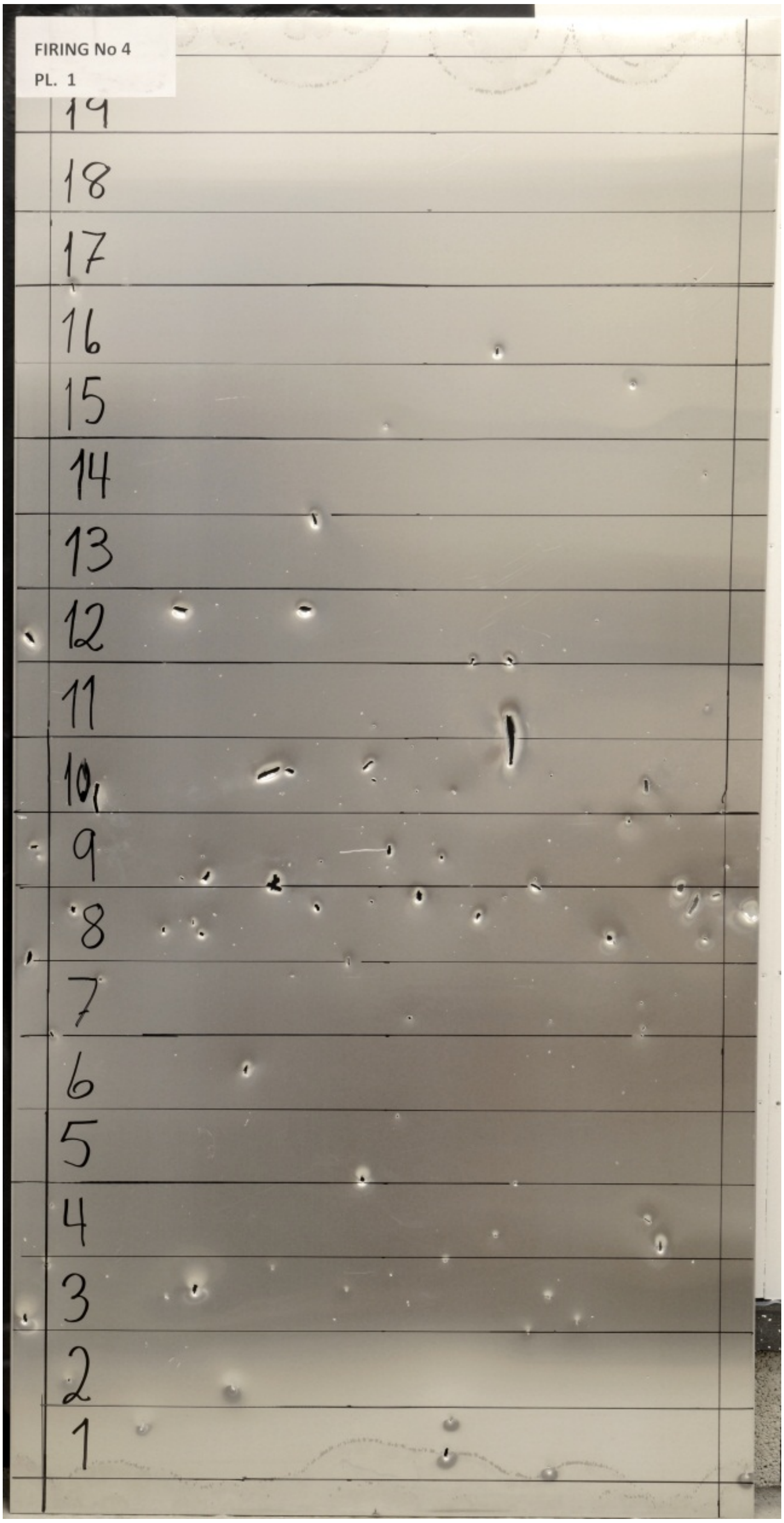

Figure App C. 17 Witness plate No 1 from firing of shell No 2 filled with MCX-6100 composition.

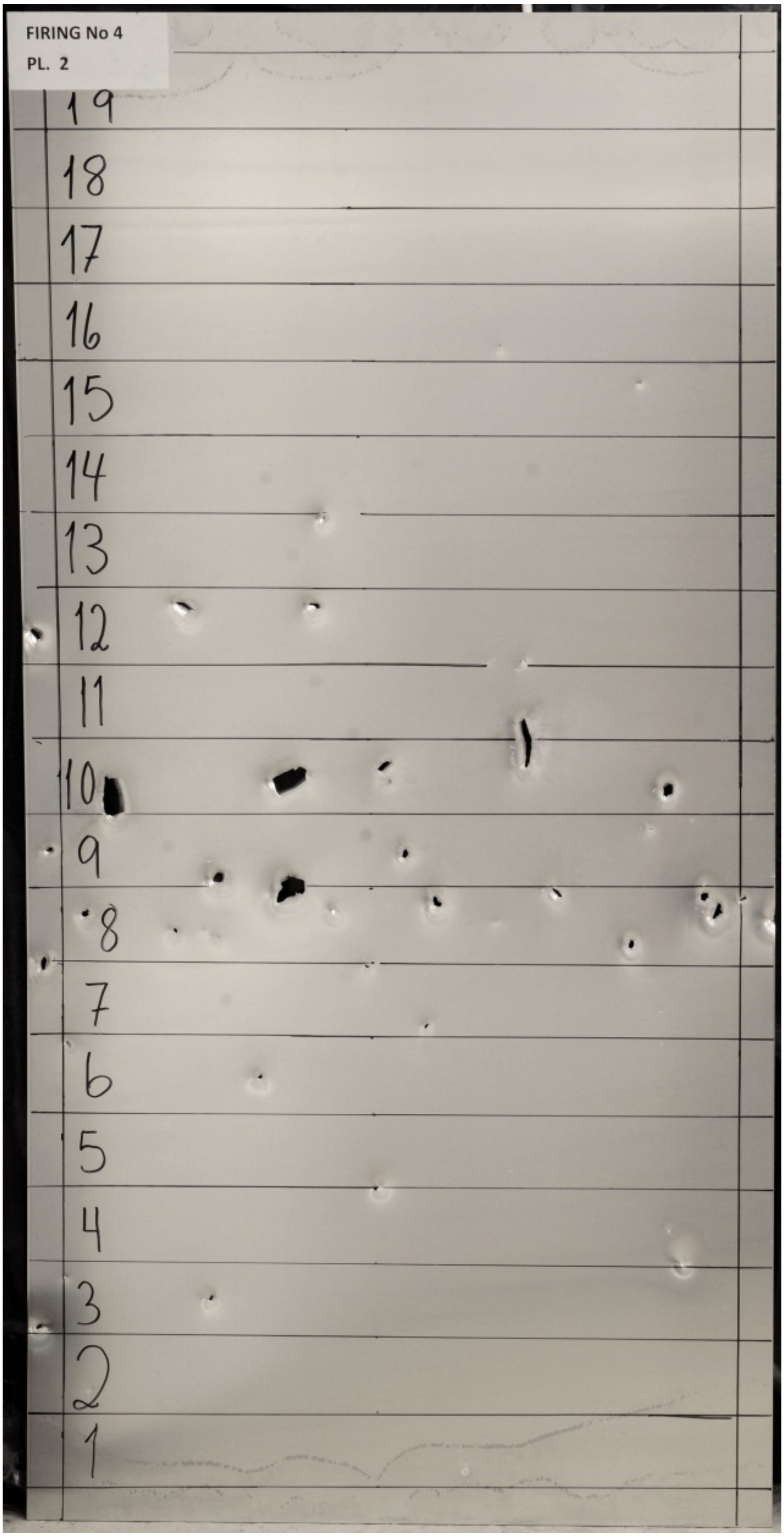

Figure App C. 18 Witness plate No 2 from firing of shell No 2 filled with MCX-6100 composition.

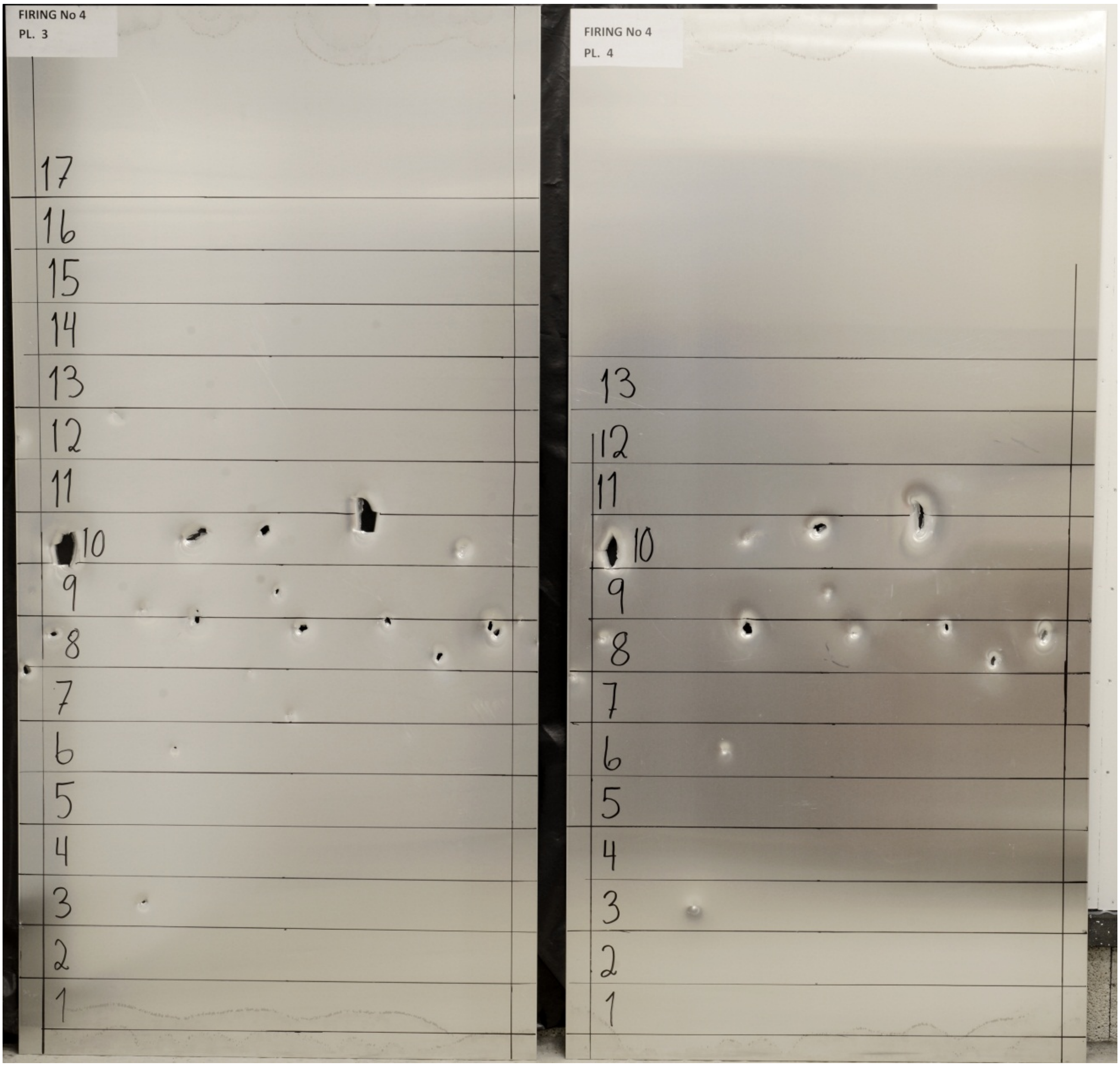

Figure App C. 19 Witness plates No 3 and No 4 from firing of shell No 2 filled with MCX-6100 composition.

Figure App C. 20 Witness plates No 5 and No 6 from firing of shell No 2 filled with MCX-6100 composition.

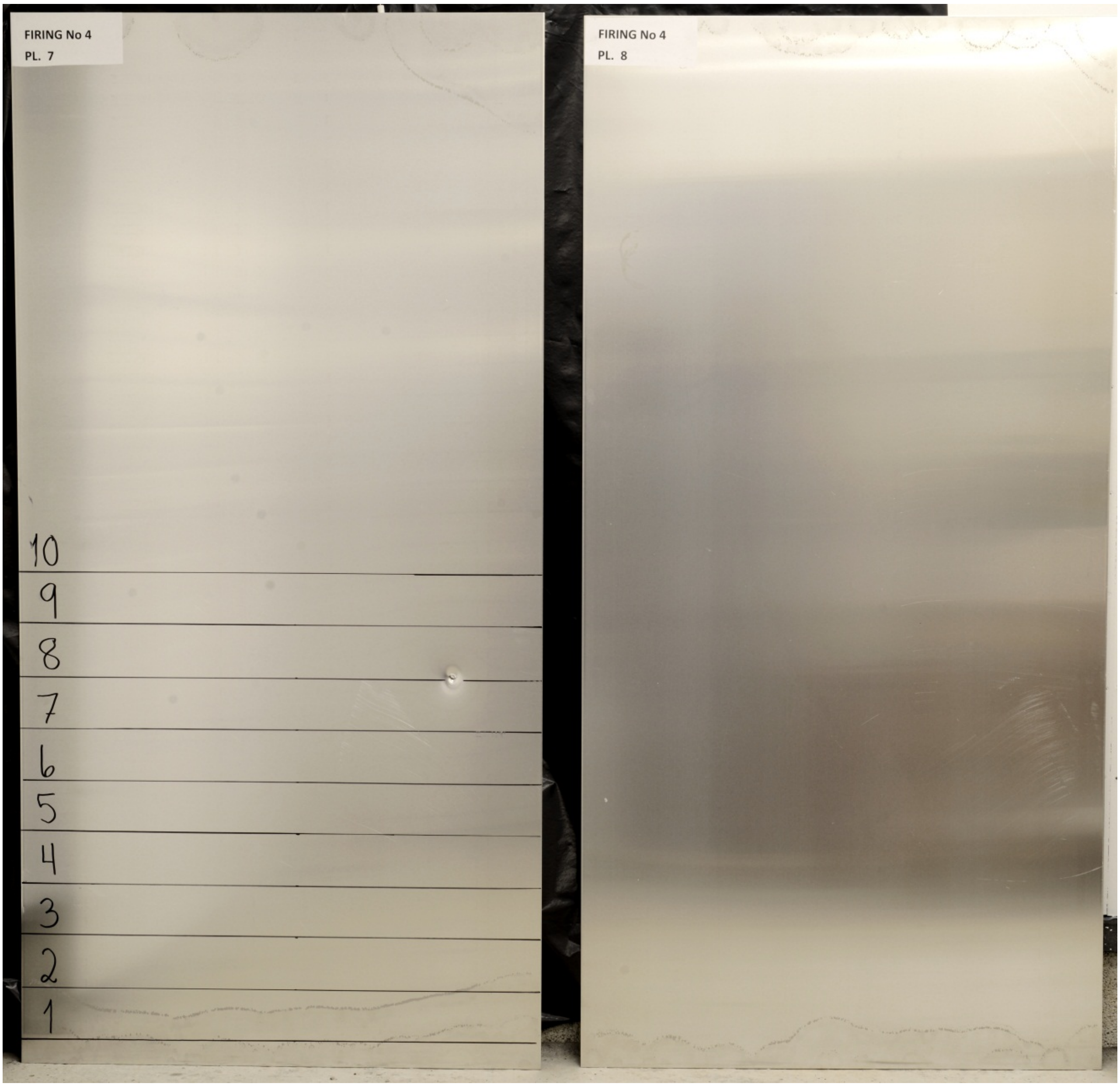

Figure App C. 21 Witness plates No 7 and No 8 from firing of shell No 2 filled with MCX-6100 composition.

C.5 Witness plates for firing No 5 with GA/BAMO/HMX composition

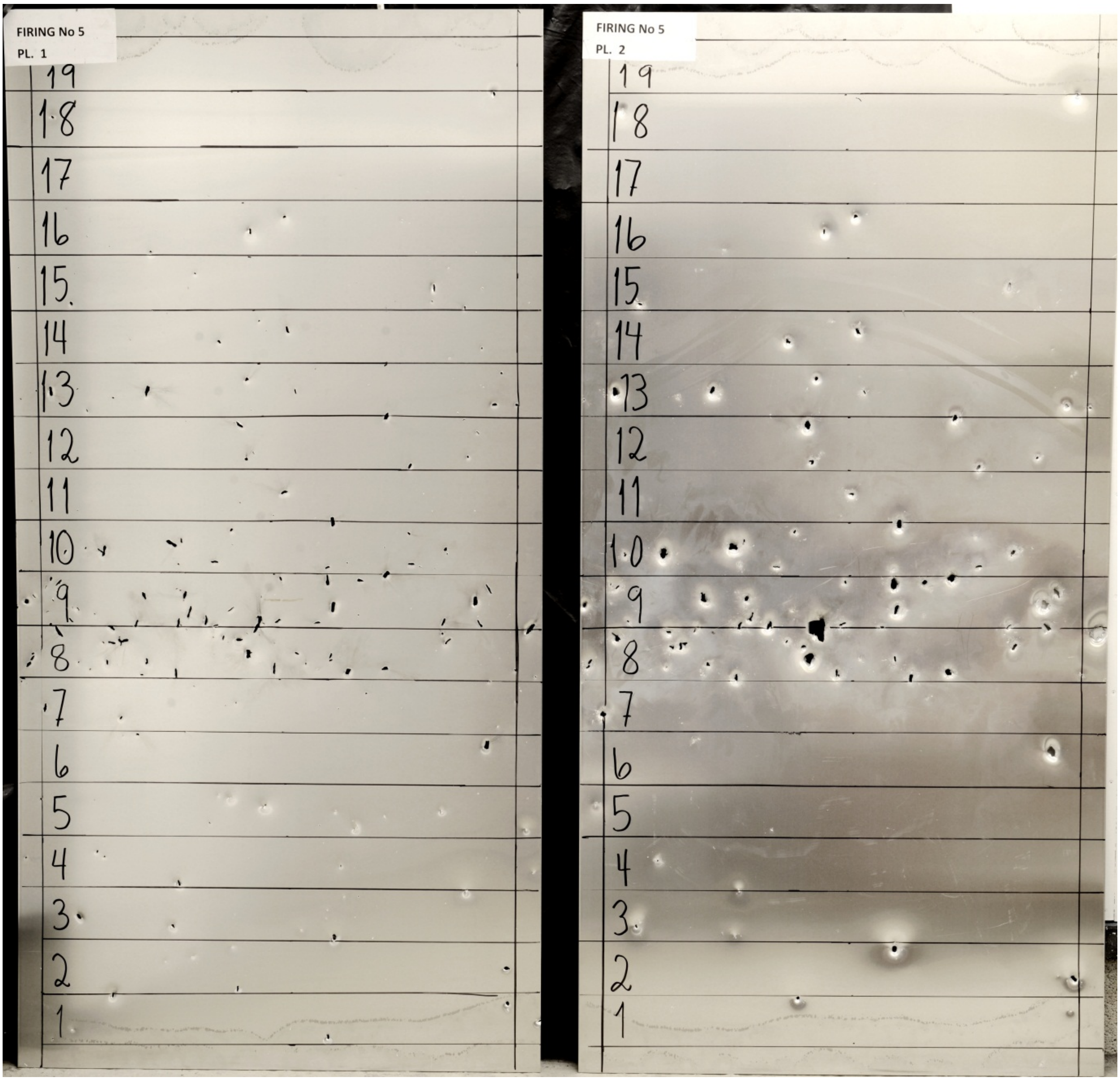

Figure App C. 22 Witness plates No 1 and No2 from firing of shell No 10 press filled with GA/BAMO/IPDI/HMX Sats 432/13 composition.

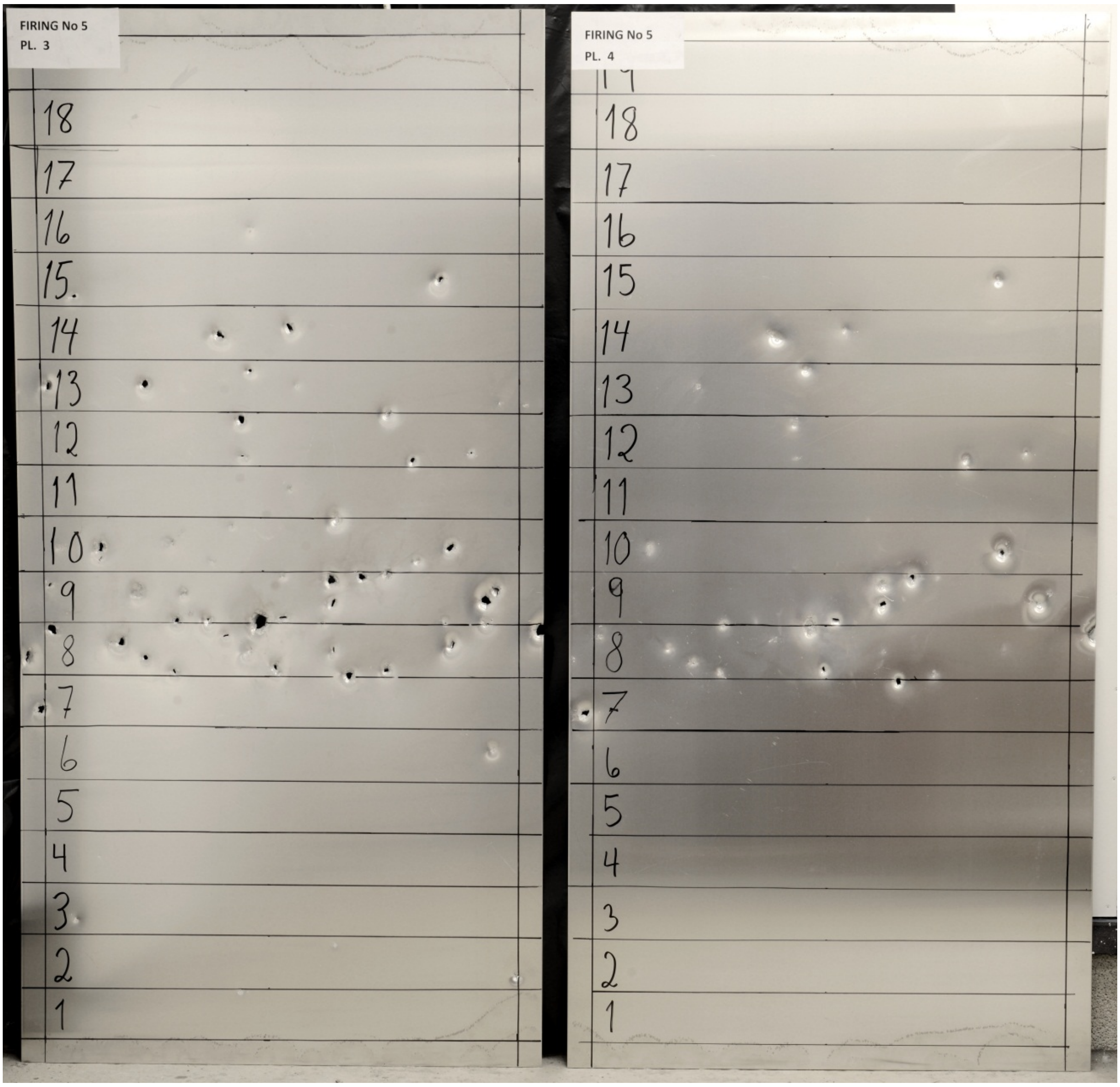

Figure App C. 23   Witness plates No 3 and No 4 from firing of shell No 10 press filled with GA/BAMO/IPDI/HMX Sats 432/13 composition.

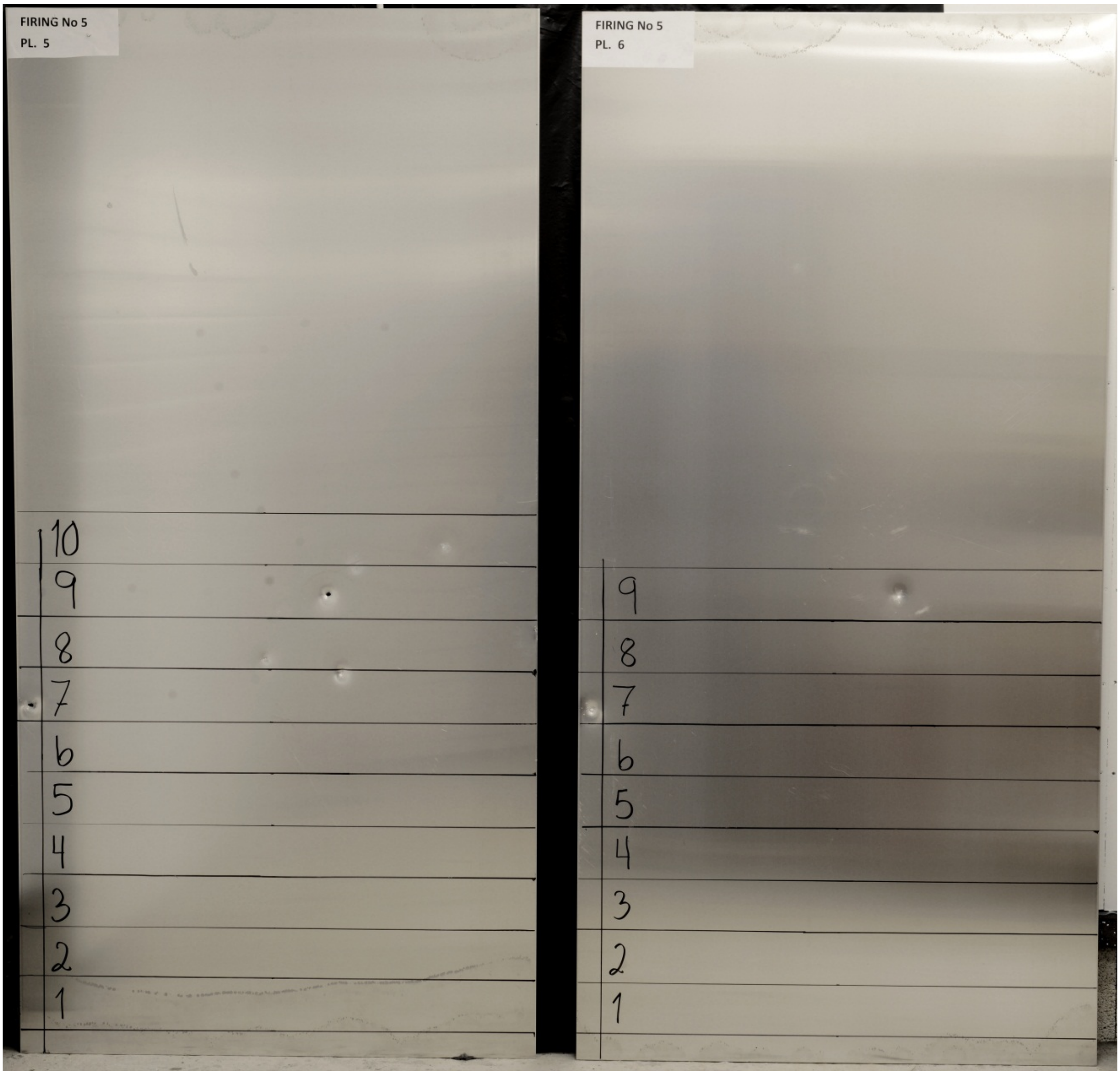

Figure App C. 24 Witness plates No 5 and No 6 from firing of shell No 10 press filled with GA/BAMO/IPDI/HMX Sats 432/13 composition.

Figure App C. 25 Witness plates No 7and No 8 from firing of shell No 10 press filled with GA/BAMO/IPDI/HMX Sats 432/13 composition.

C.6 Witness plates for firing No 6 with MCX-8001 composition

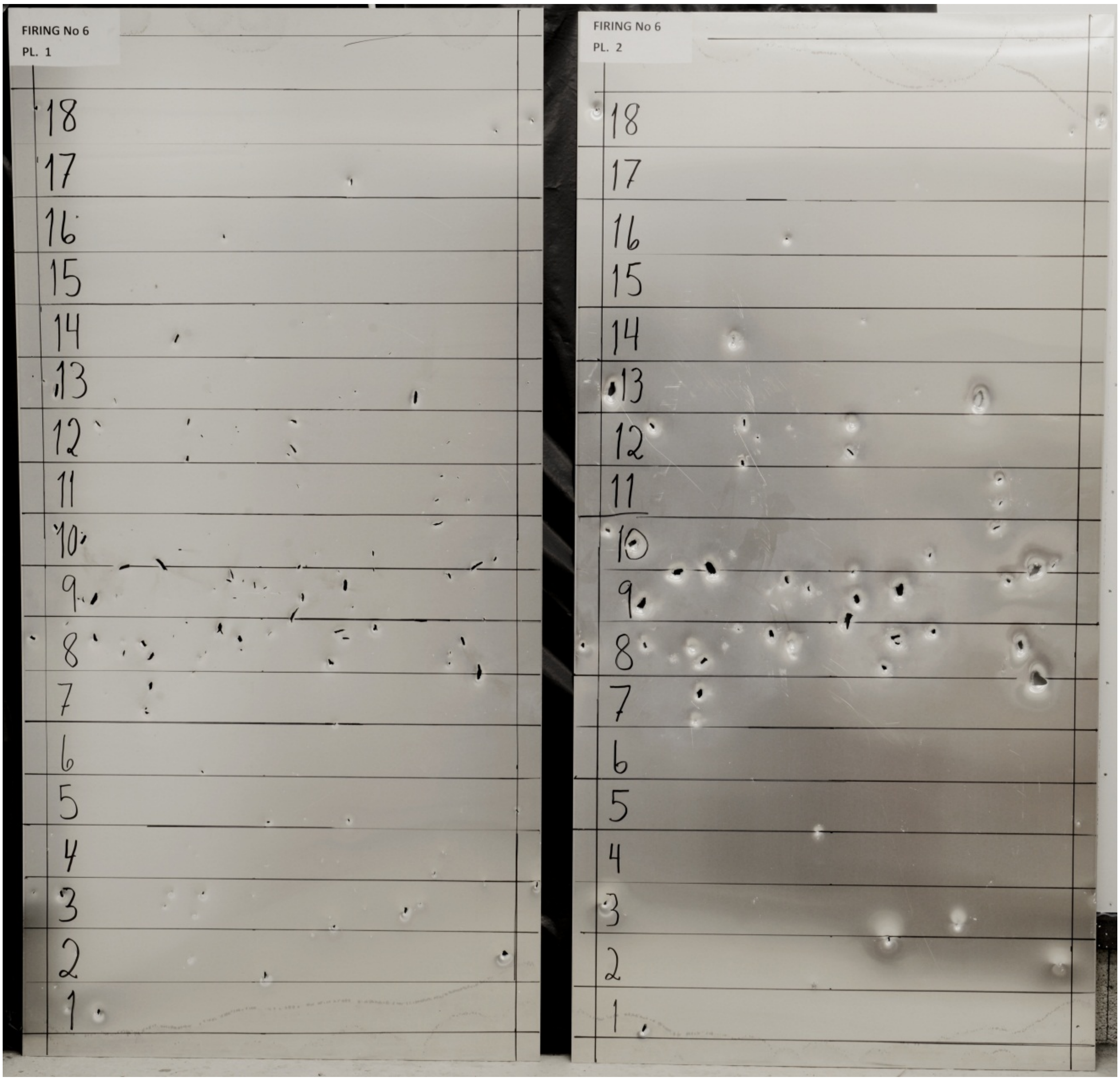

Figure App C. 26 Witness plates No 1 and No 2 from firing of shell No 7 filled with MCX-8001composition.

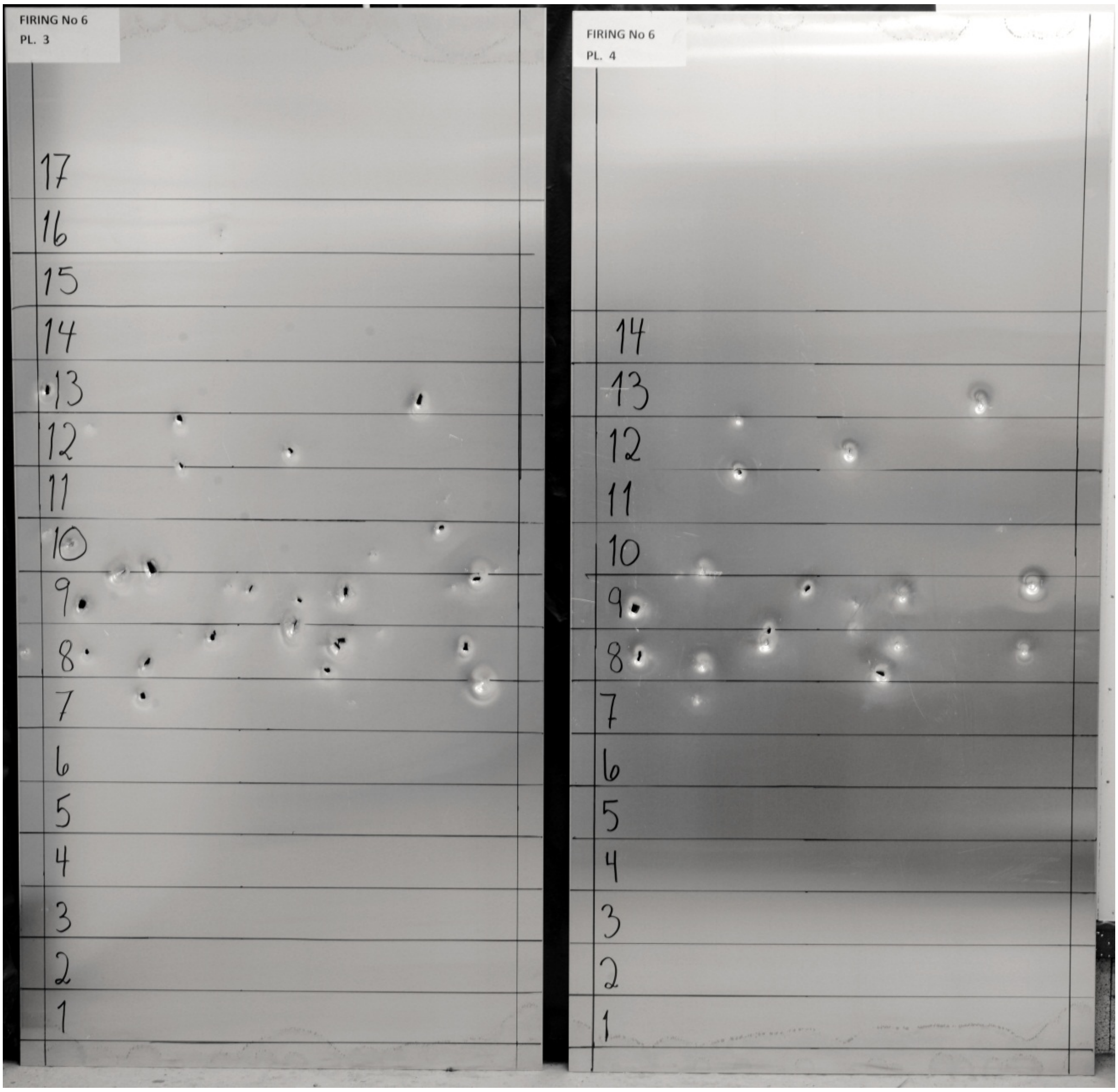

Figure App C. 27 Witness plates No 3 and No 4 from firing of shell No 7 filled with MCX-8001 composition.

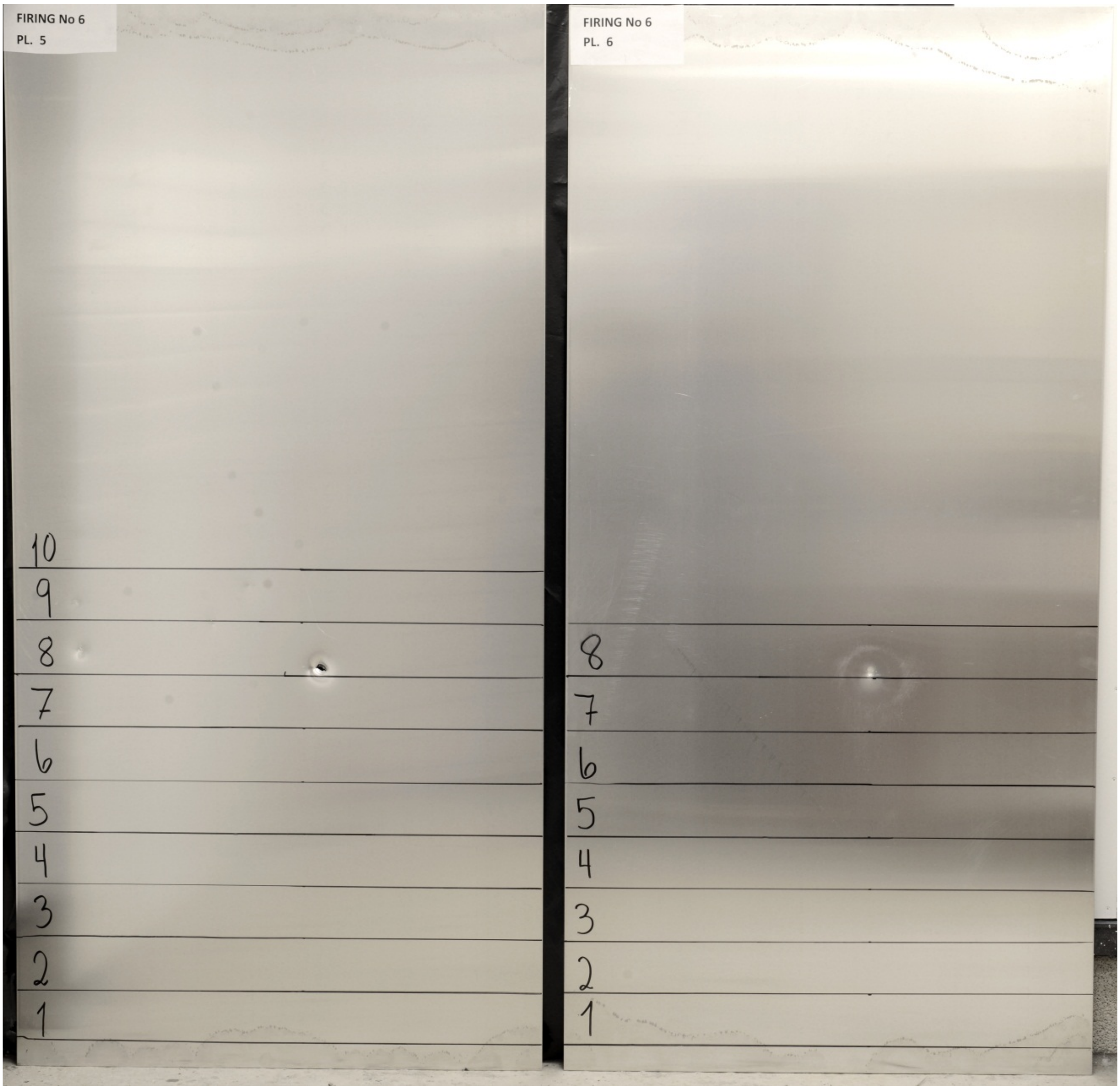

Figure App C. 28 Witness plates No 5 and No 6 from firing of shell No 7 filled with MCX-8001 composition.

Figure App C. 29 Witness plates No 7 and No 8 from firing of shell No 7 filled with MCX-8001 composition.

C.7 Witness plates for firing No 7 with MCX-6002 composition

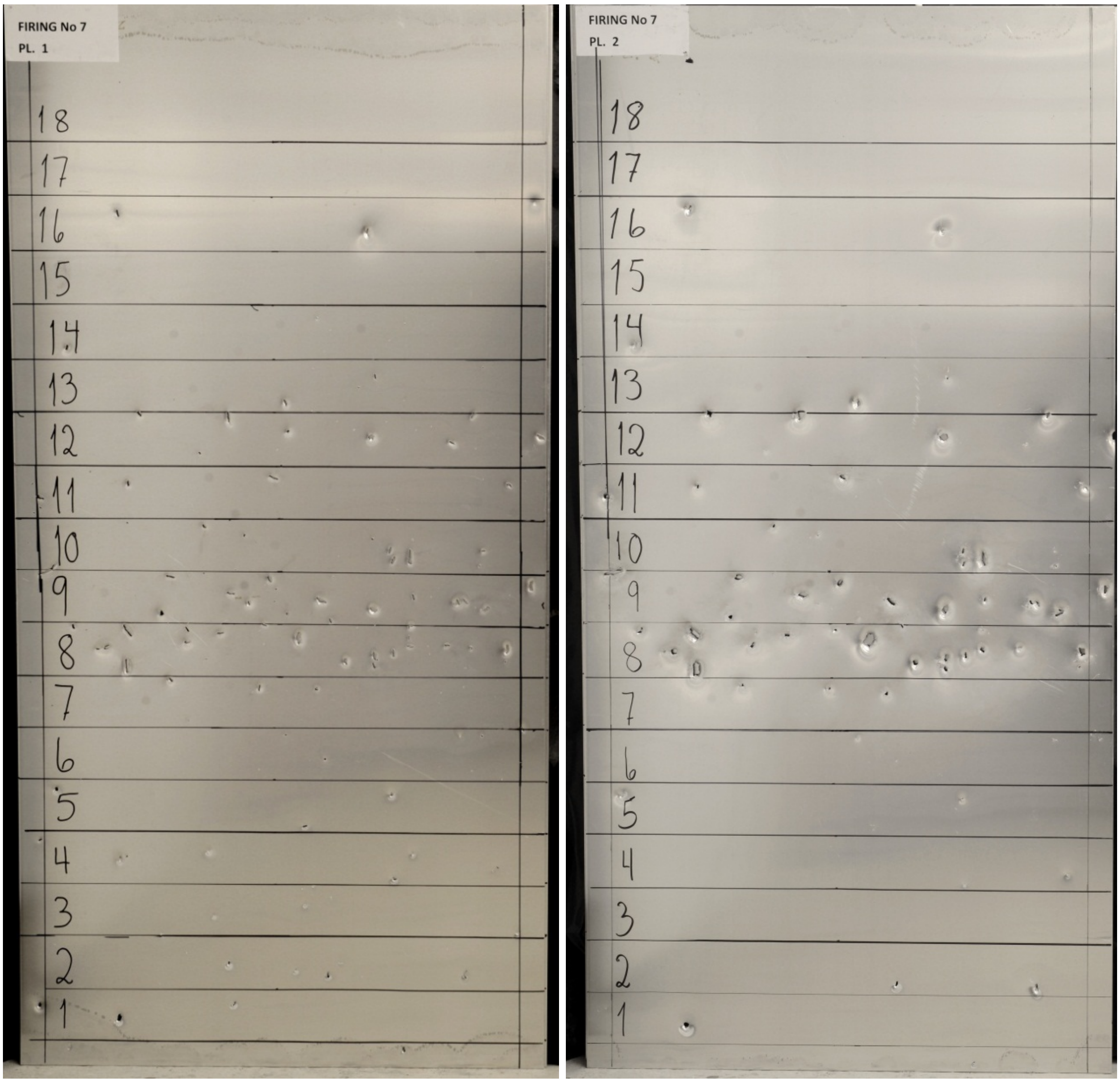

Figure App C. 30 Witness plates No 1 and No 2 from firing of shell No 5 filled with MCX-6002 composition.

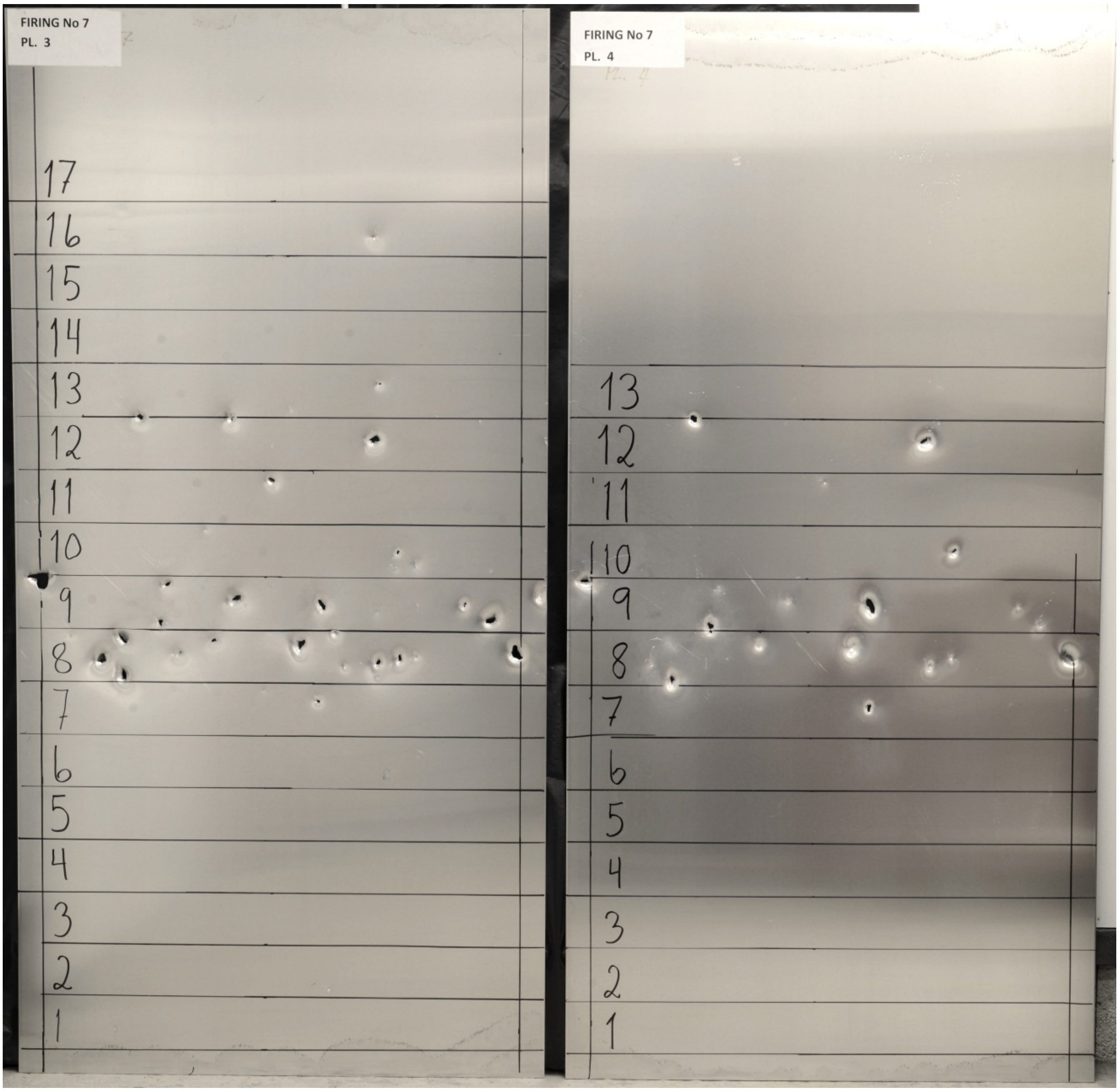

Figure App C. 31 Witness plates No 3 and No 4 from firing of shell No 5 filled with MCX-6002 composition.

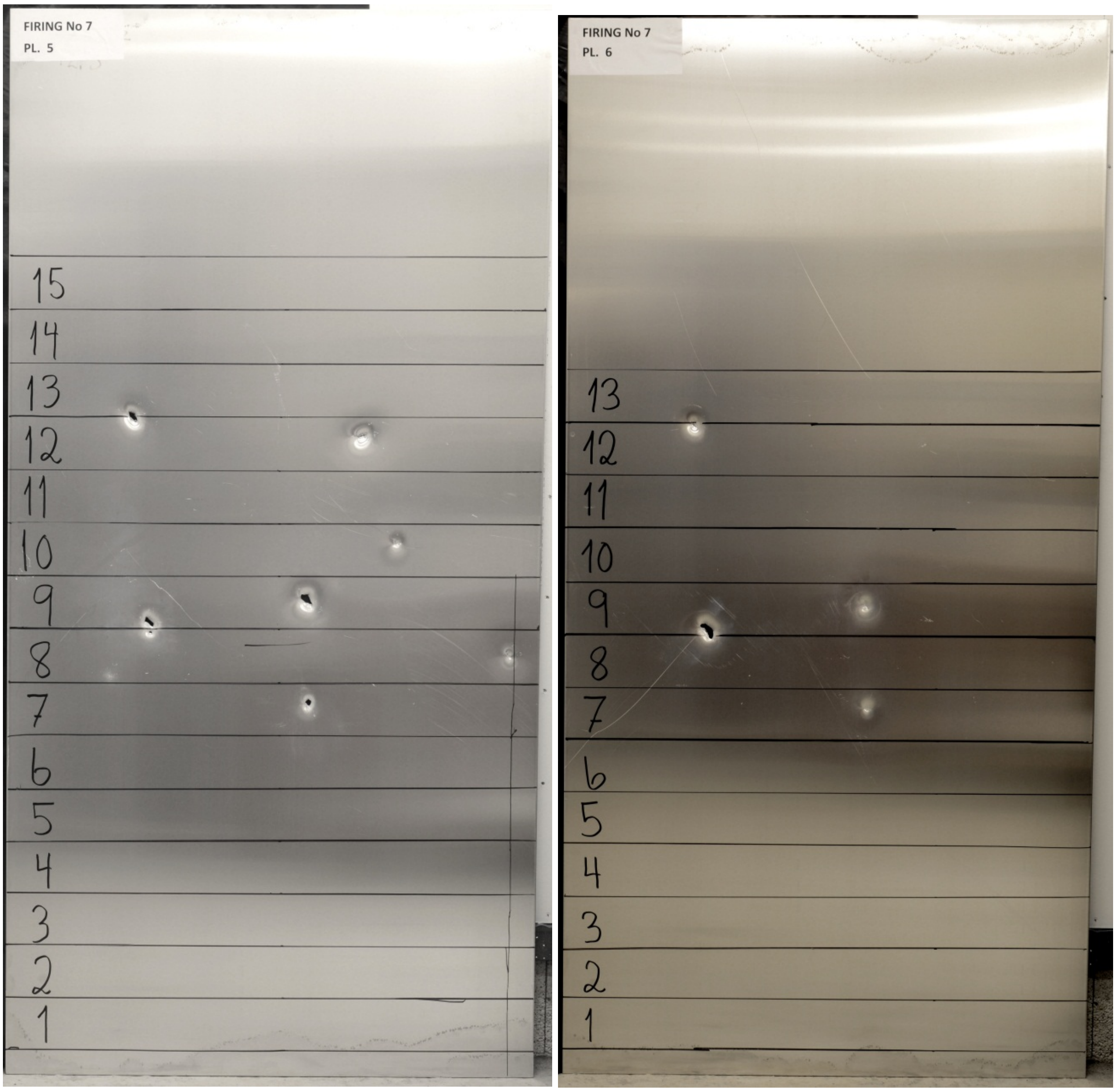

Figure App C. 32 Witness plates No 5 and No 6 from firing of shell No 5 filled with MCX-6002 composition.

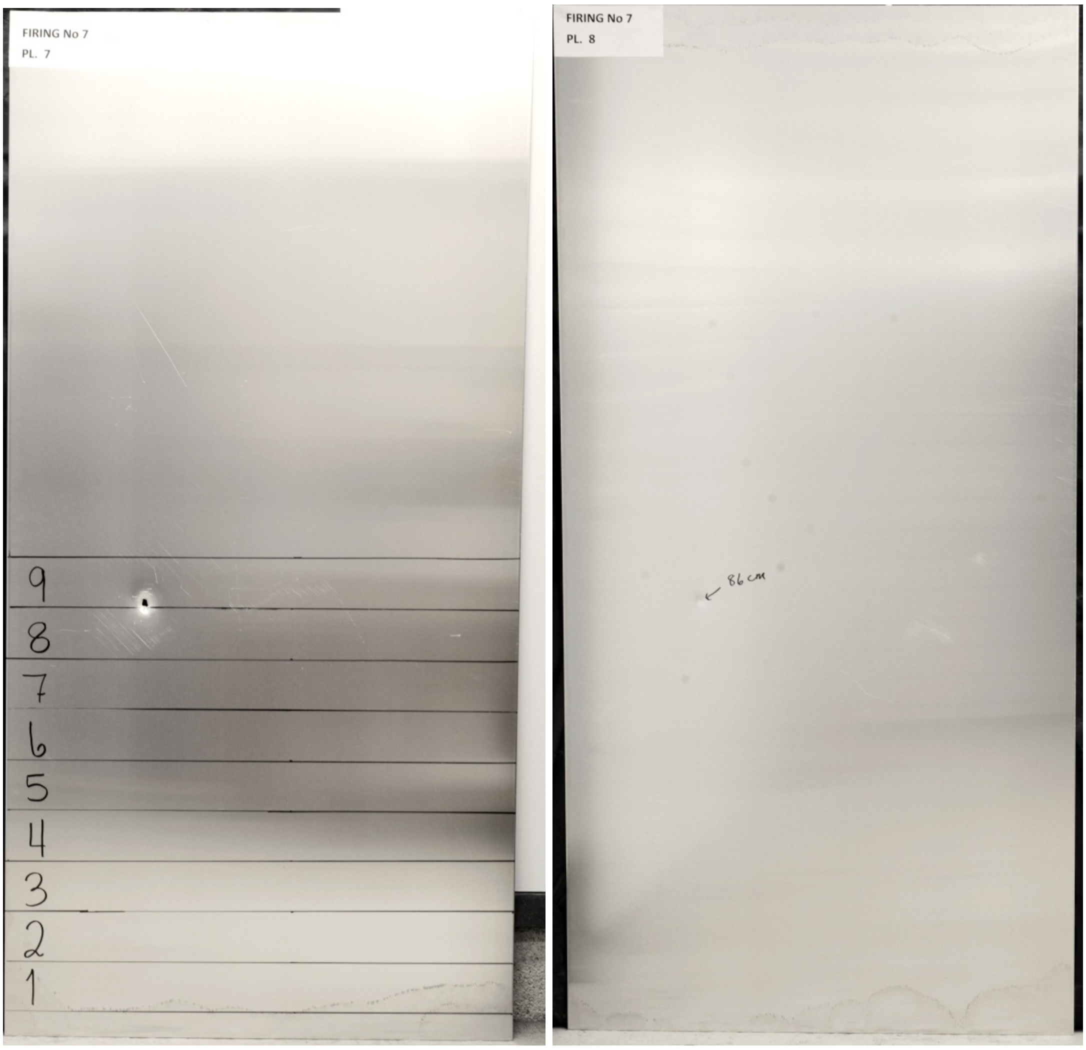

Figure App C. 33 Witness plates No 7 and No 8 from firing of shell No 5 filled with MCX-6002 composition.

C.8 Witness plates for firing No 8 with MCX-8100 composition

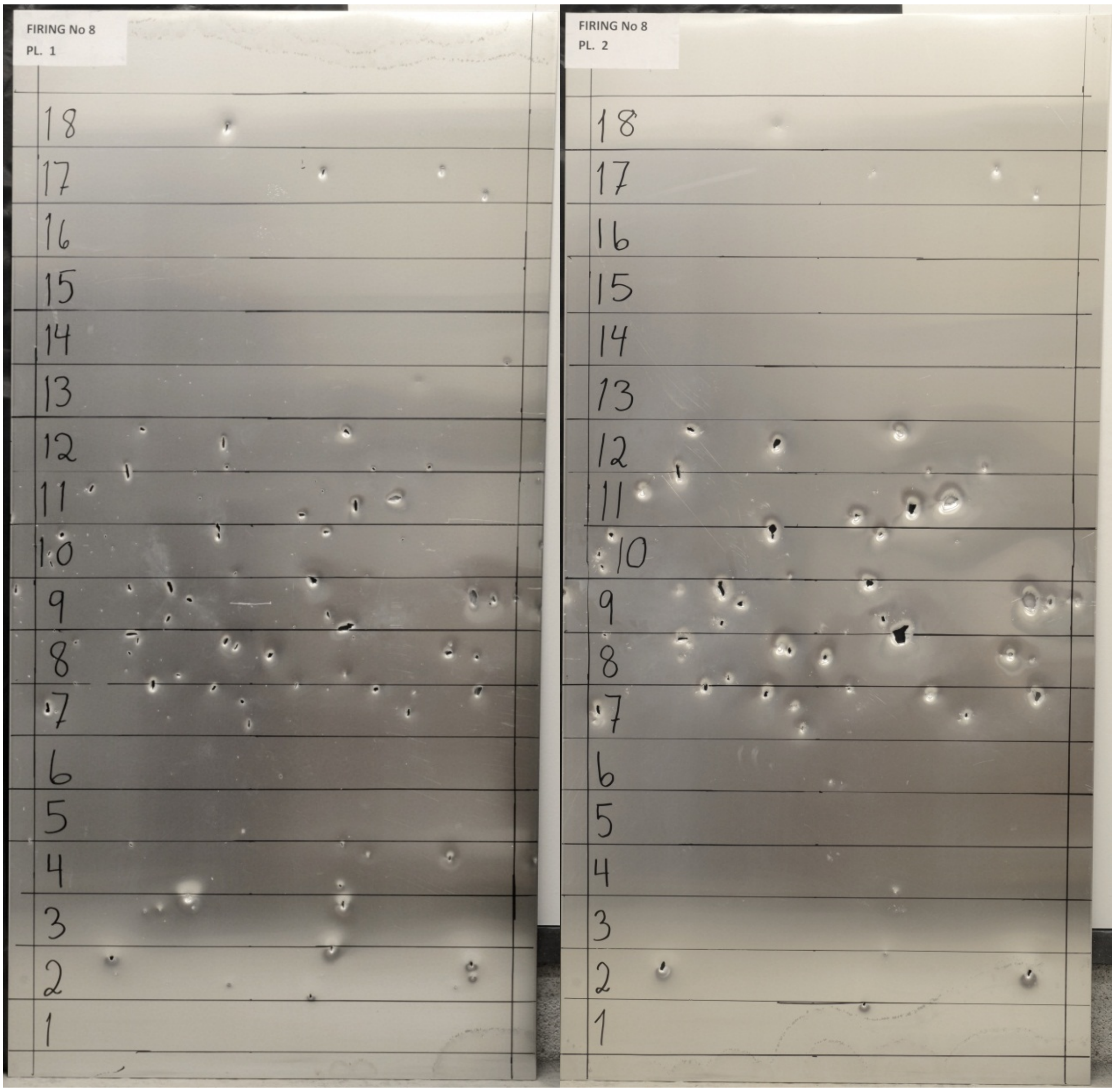

Figure App C. 34 Witness plates No 1 and No 2 from firing of shell No 3 filled with MCX-8100 composition.

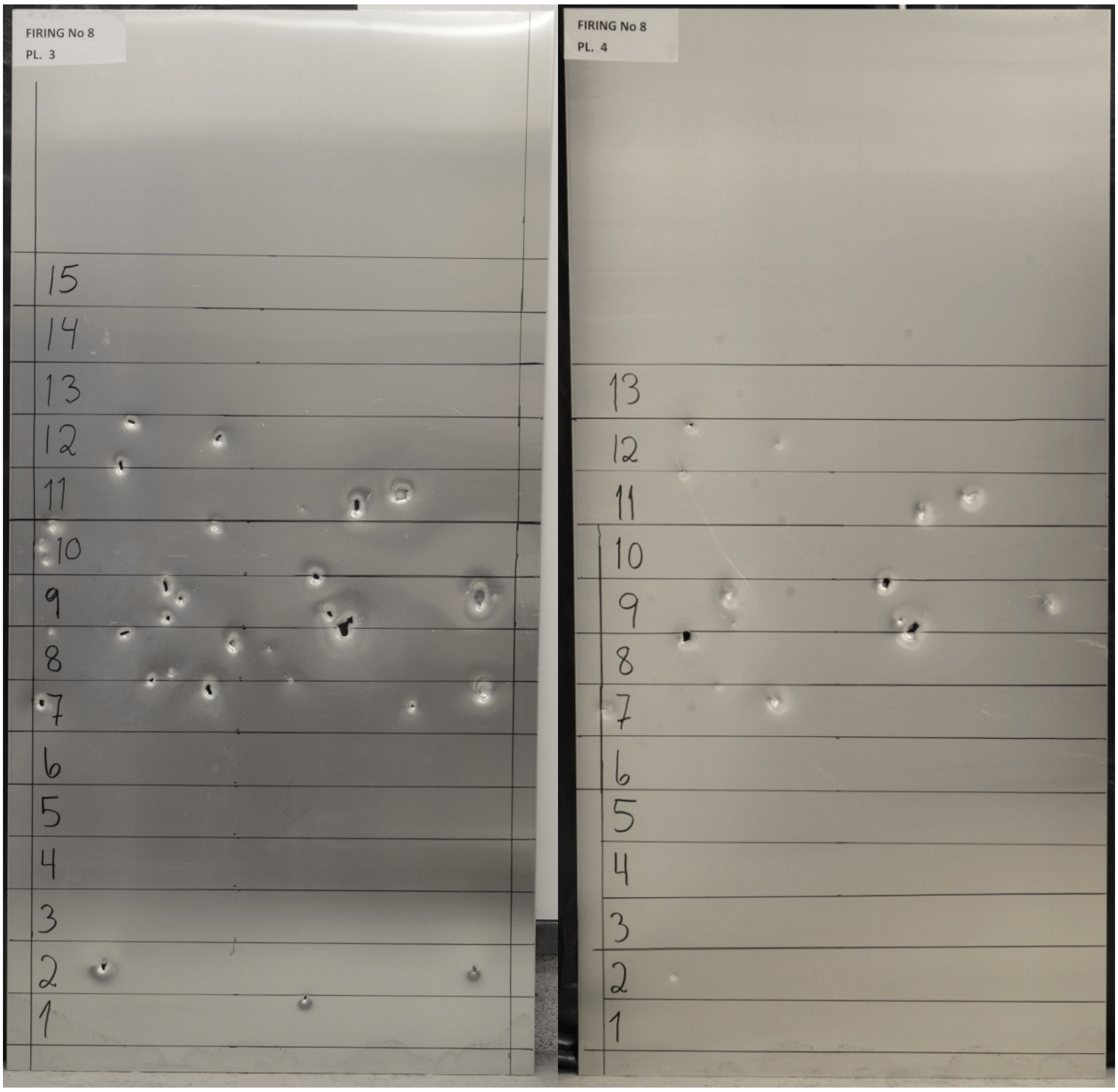

Figure App C. 35 *Witness plates No 3 and No 4 from firing of shell No 3 filled with MCX-8100 composition.*

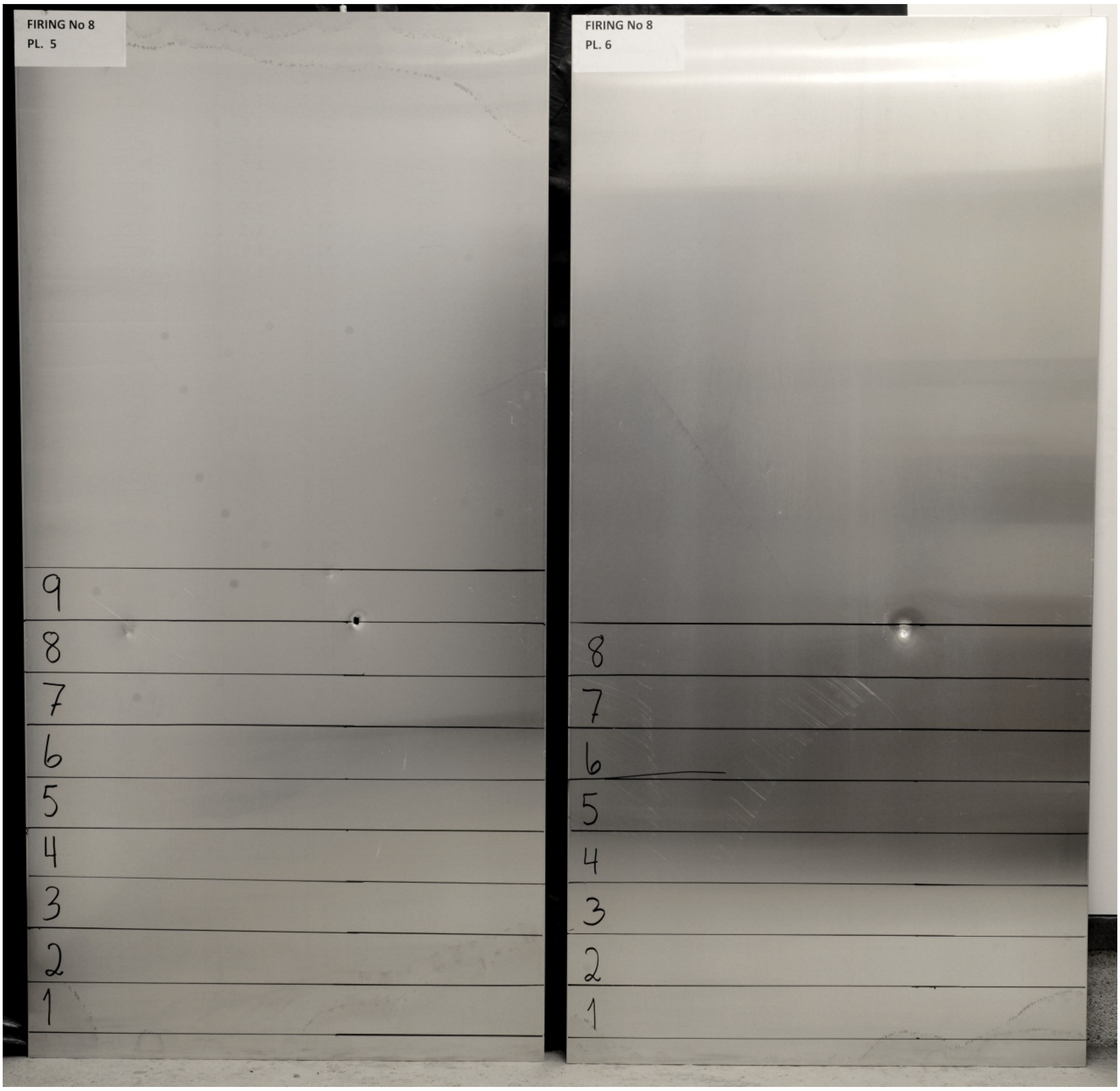

Figure App C. 36 Witness plates No 5 and No 6 from firing of shell No 3 filled with MCX-8100 composition.

Figure App C. 37 Witness plates No 7 and No 8 from firing of shell No 3 filled with MCX-8100 composition showing no fragment hits.

C.9 Witness plates for firing No 9 with MCX-6100 composition

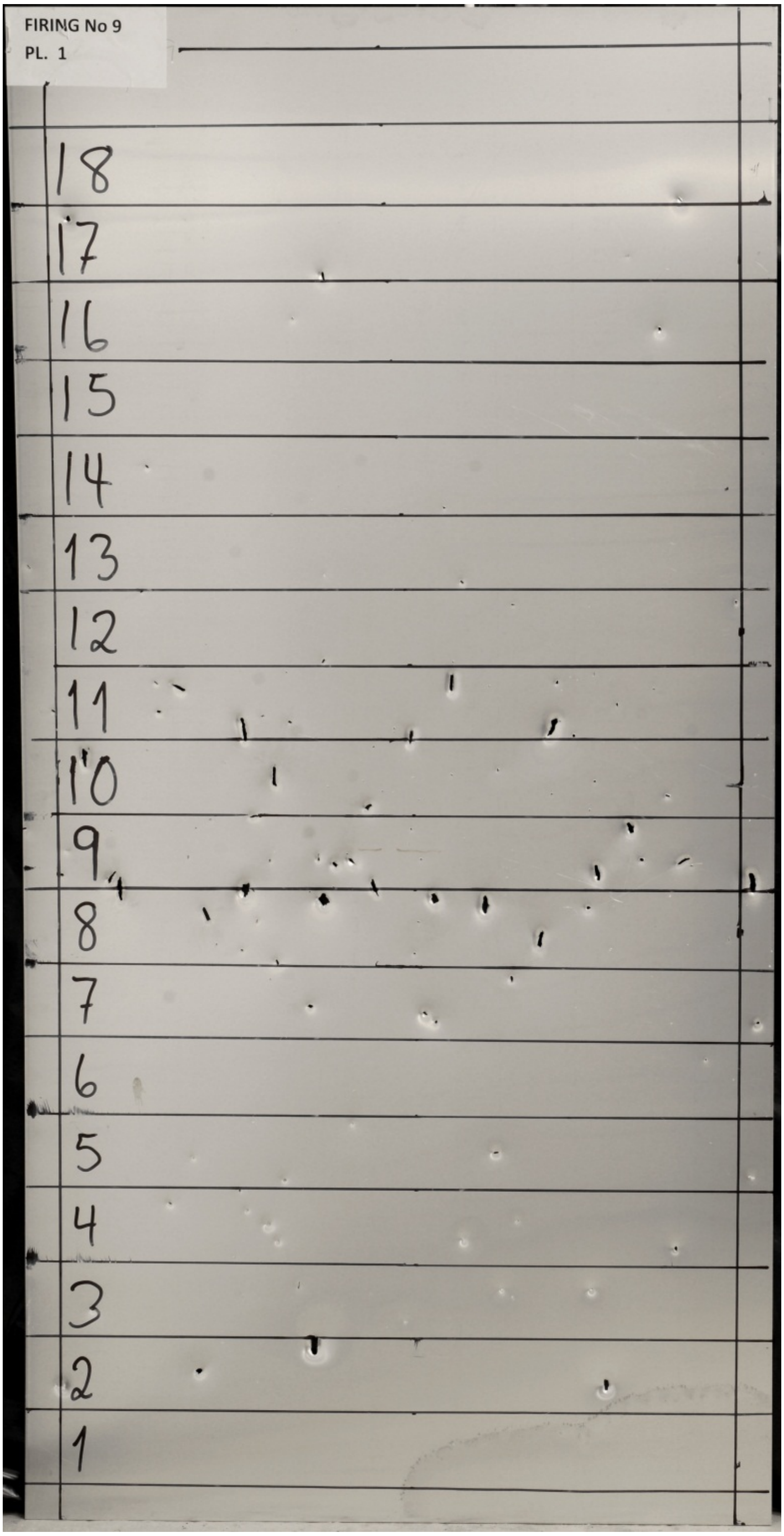

Figure App C. 38 Witness plate No 1 from firing of shell No 1 filled with MCX-6100 composition.

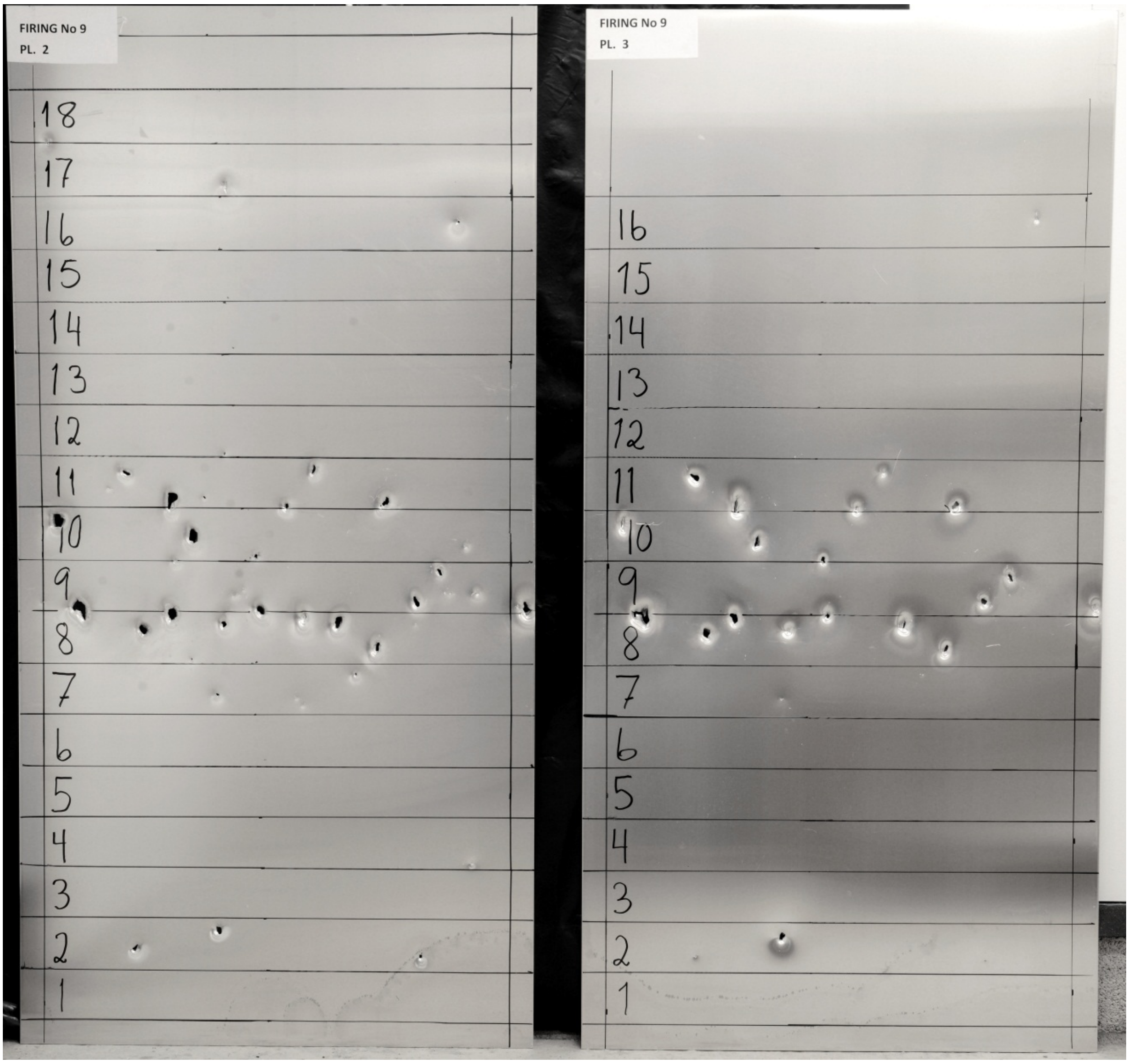

Figure App C. 39 Witness plates No 2 and No 3 from firing of shell No 1 filled with MCX-6100 composition.

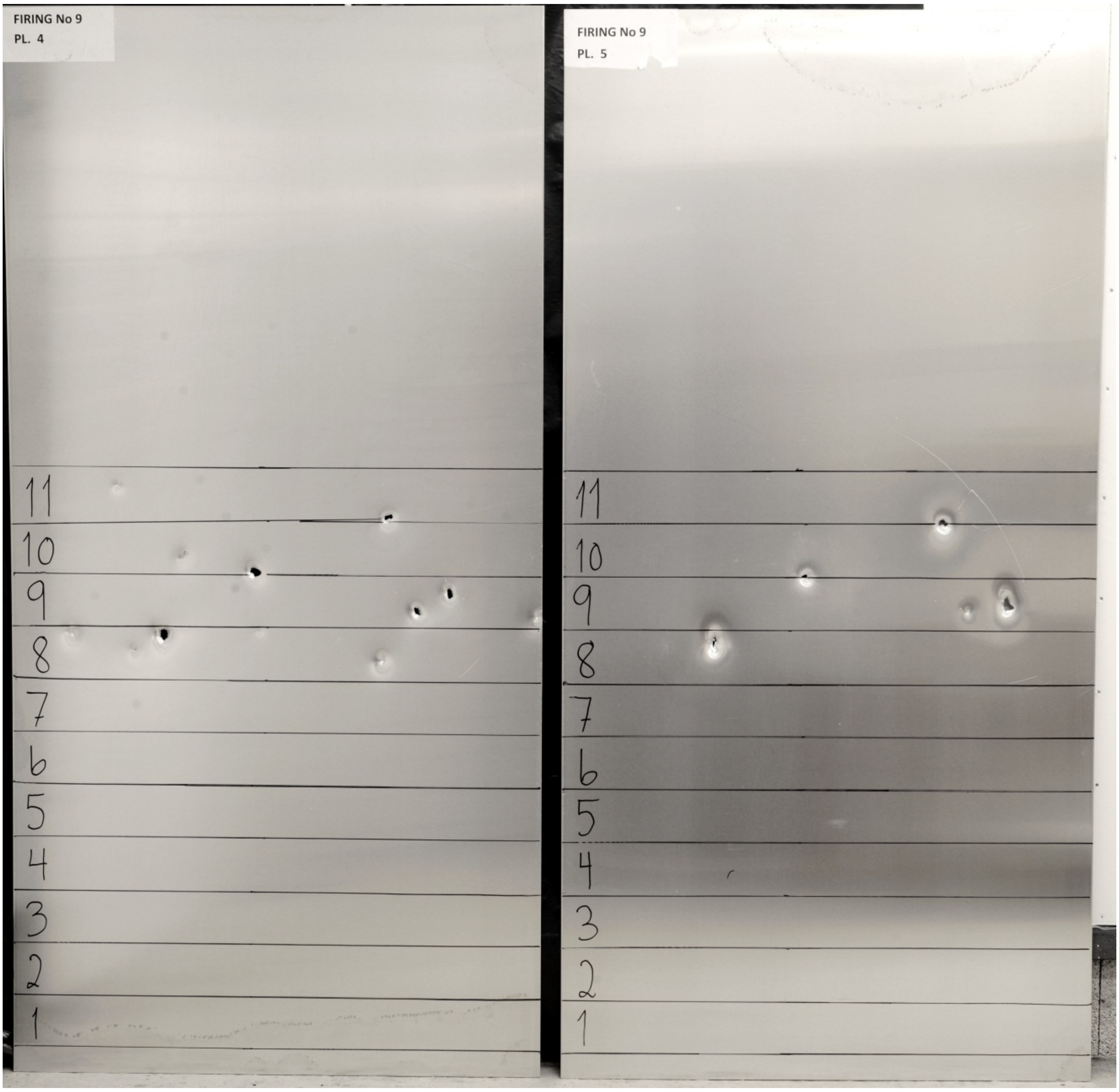

Figure App C. 40 Witness plates No 4 and No 5 from firing of shell No1 filled with MCX-6100 composition.

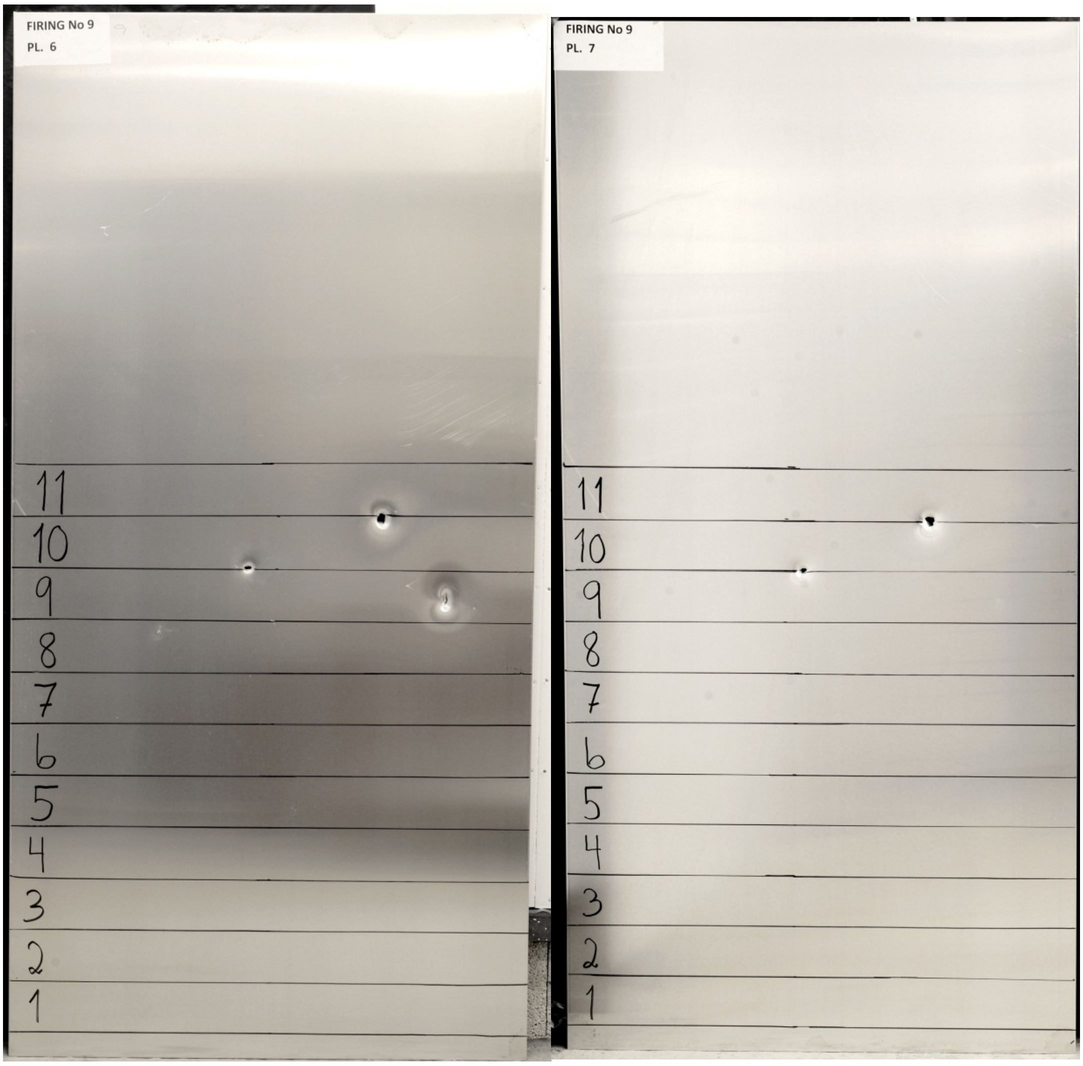

Figure App C. 41 Witness plates No 6 and 7 from firing of shell No1 filled with MCX-6100 composition.

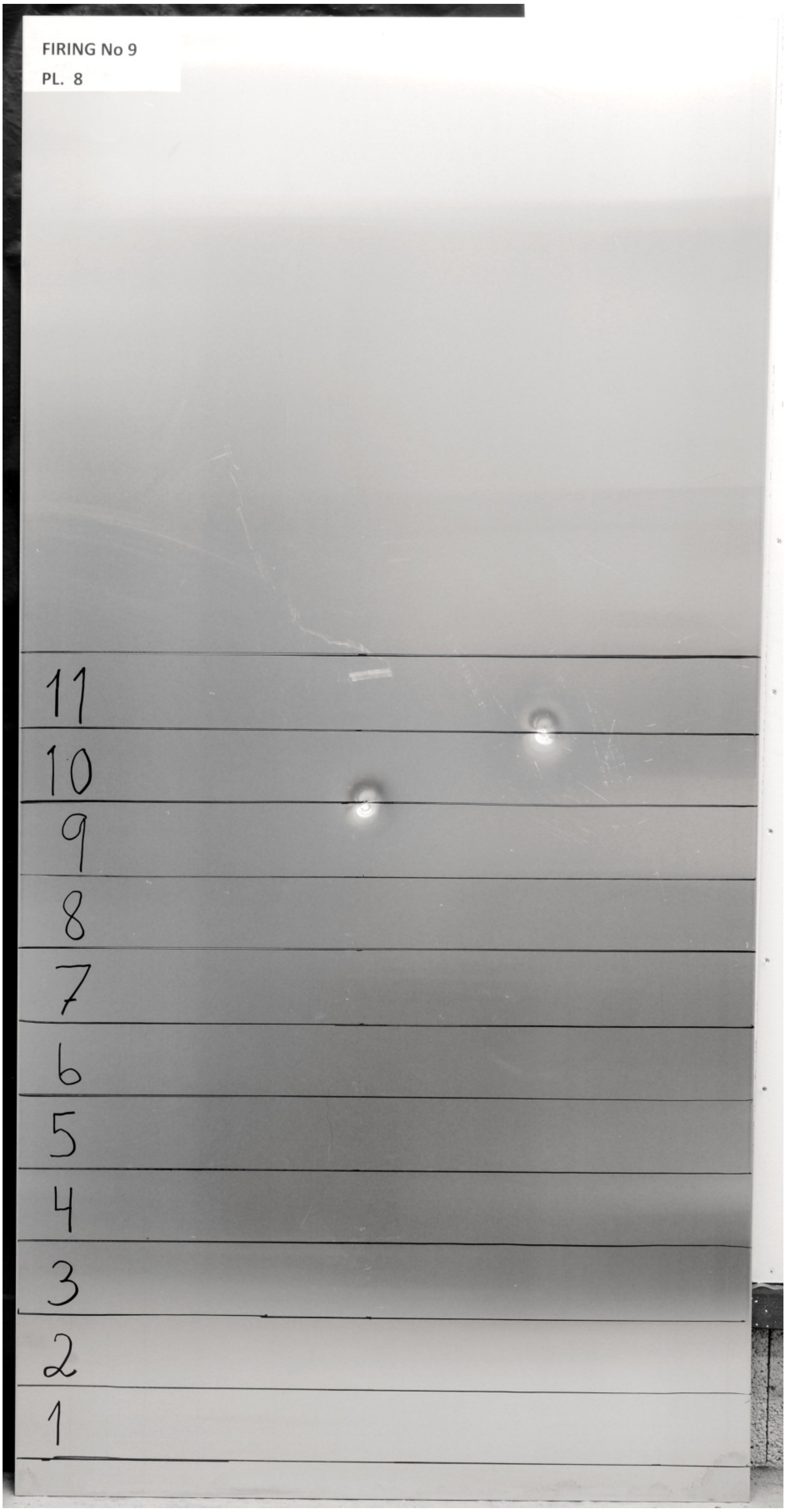

Figure App C. 42 Witness plate No 8 from firing of shell No 1 filled with MCX-6100 composition.

C.10 Witness plates for firing No 10 with GA/BAMO/HMX composition

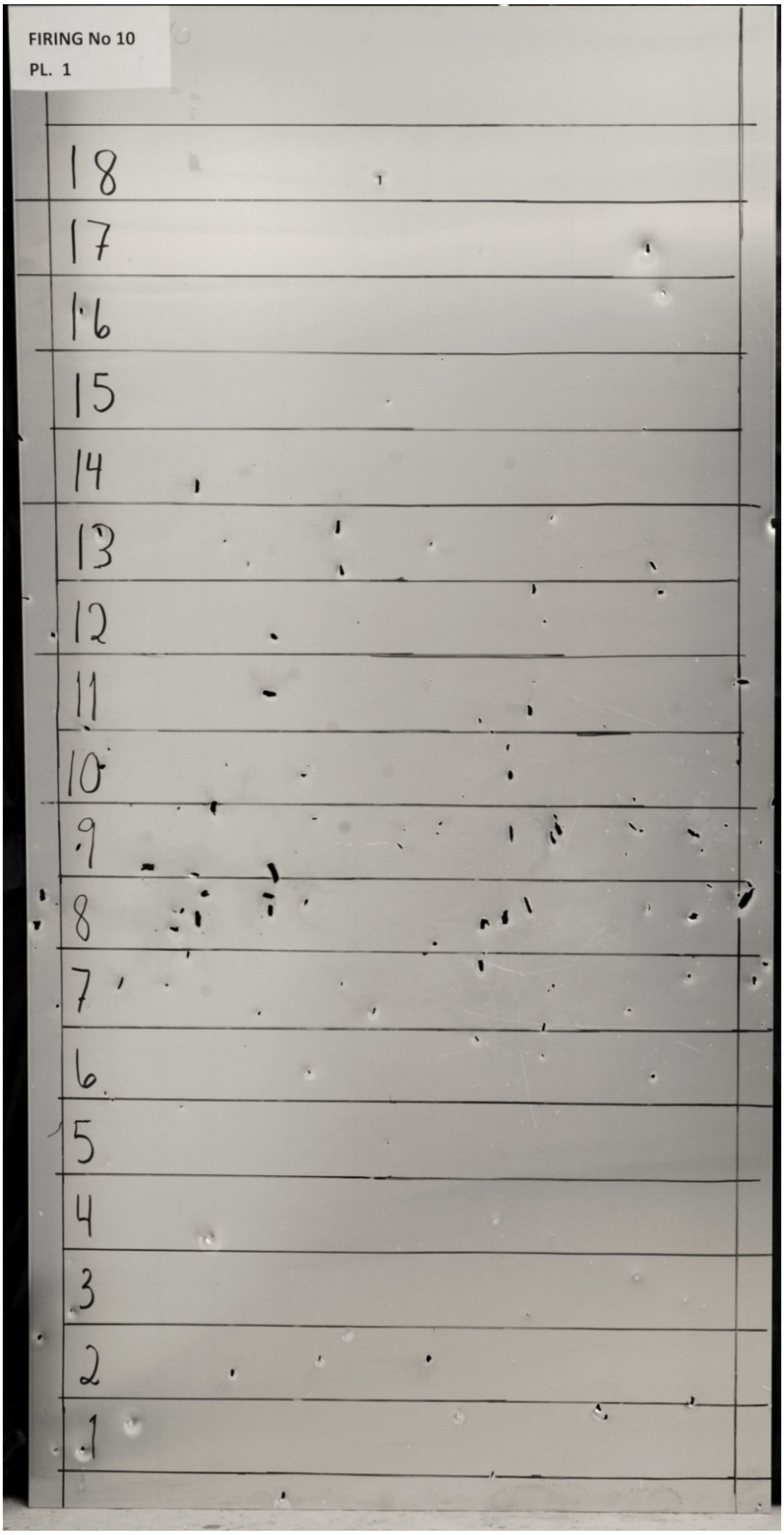

Figure App C. 43 Witness plate No 1 from firing of shell No 9 press filled with GA/BAMO/IPDI/HMX Sats 400/13 composition.

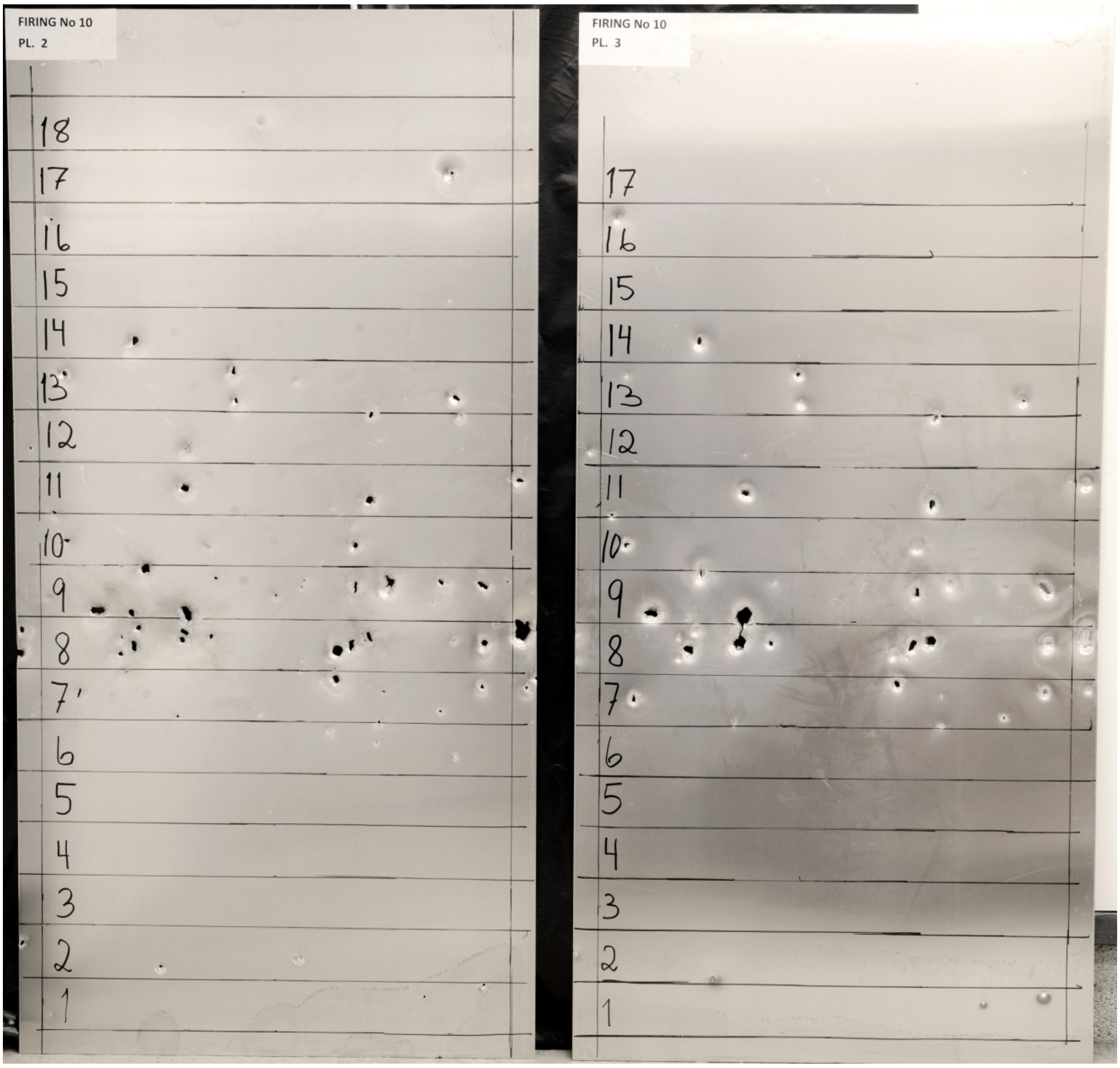

Figure App C. 44 Witness plates No 2 and No 3 from firing of shell No 9 press filled with GA/BAMO/IPDI/HMX Sats 400/13 composition.

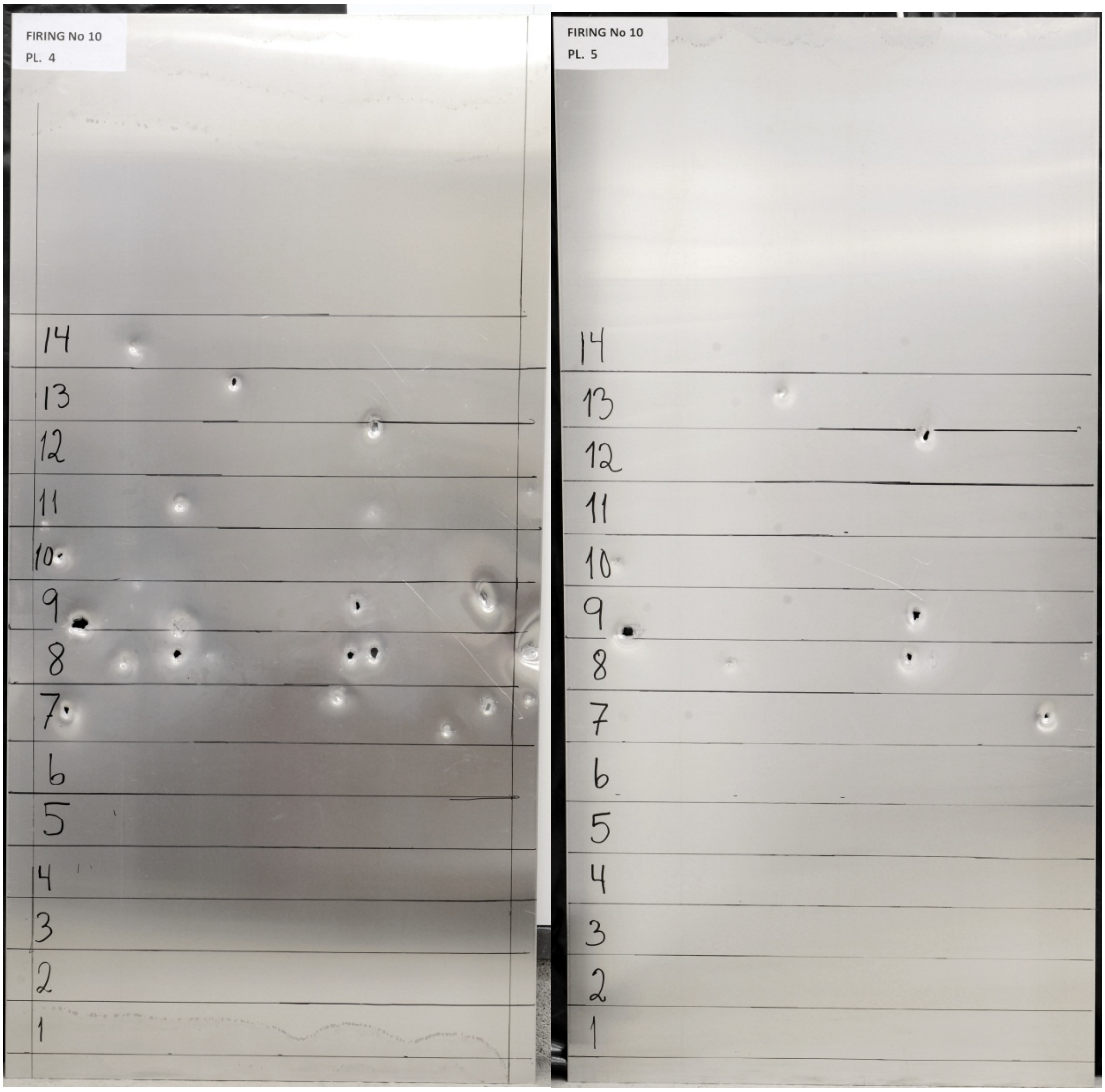

Figure App C. 45 Witness plates No 4 and No 5 from firing of shell No 9 press filled with GA/BAMO/IPDI/HMX Sats 400/13 composition.

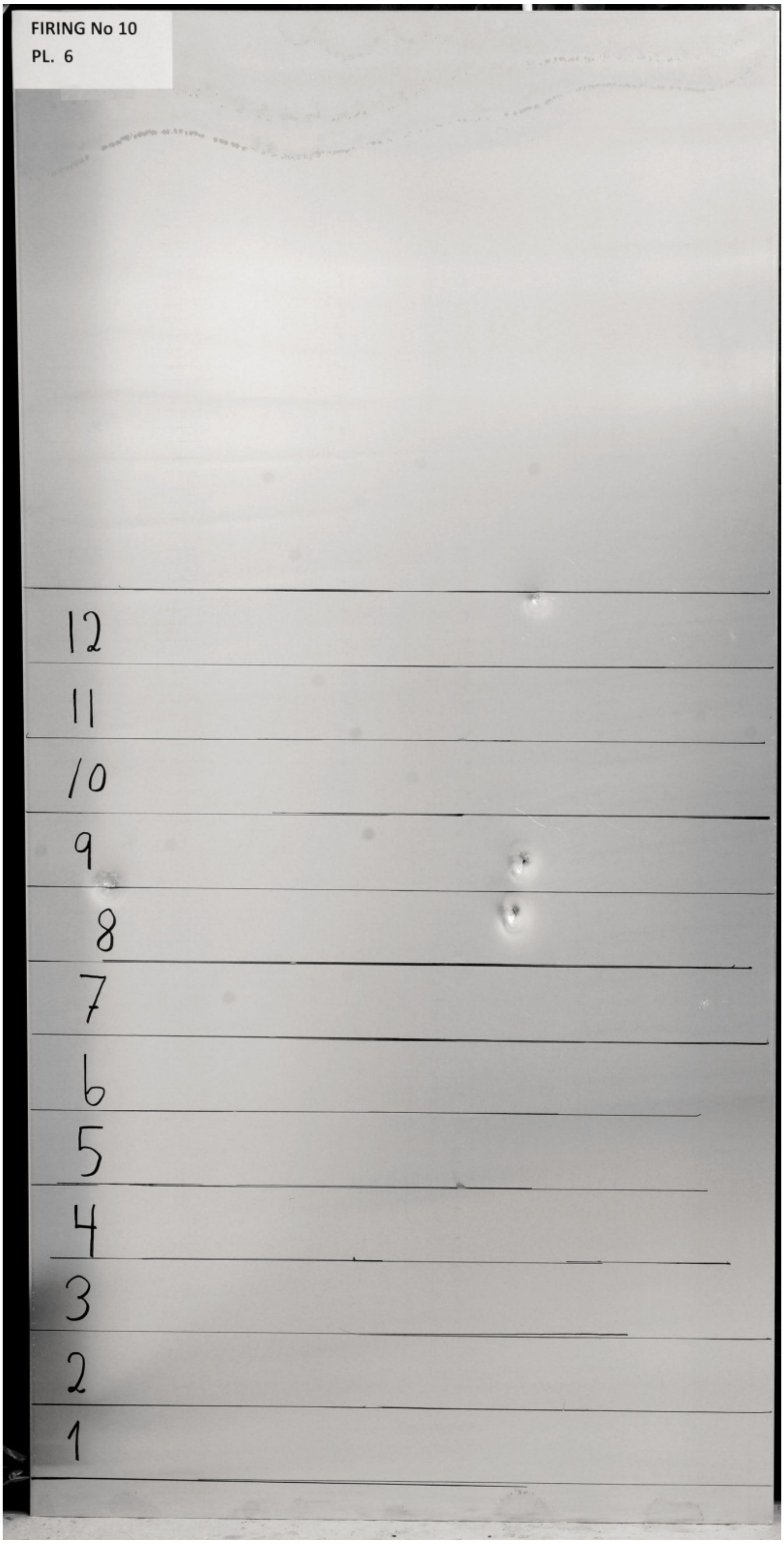

Figure App C. 46 Witness plate No 6 from firing of shell No 9 press filled with GA/BAMO/IPDI/HMX Sats 400/13 composition.

Figure App C. 47 Witness plates No 7 and No 8 from firing of shell No 9 press filled with GA/BAMO/IPDI/HMX Sats 400/13 composition.

Appendix D Cheetah Calculations for GA/BAMO/IPDI/HMX Compositions

D.1 Sats 400/13

D.1.1 TMD - 1.8571 g/cm^3

```
Product library title: bkwc
Reactant library title: # Version 2.0 by P. Clark Souers

The composition:
Name        % wt.   % mol  % vol    Heat of     Mol.    TMD
                                   formation    wt.     (g/cc)
                                   (cal/mol)
hmx          94.70  89.04  92.32    17866    296.17     1.91 c4h8n8o8
ipdi          0.30   0.38   0.53   -88910    222.28     1.06 c12h18n2o2
gap           2.00   5.62   2.87    33939     99.09     1.29 c3h5n3o1
bamo          3.00   4.97   4.29   100382    168.16     1.30 c5h8n6o1

Density  =  1.8571 g/cc   Mixture TMD =  1.8571 g/cc   % TMD = 100.0000

The C-J condition:
The pressure          =          36.43 GPa
The volume            =          0.408 cc/g
The density           =          2.450 g/cc
The energy            =           4.41 kJ/cc explosive
The temperature       =           4061 K
The shock velocity    =          9.001 mm/us
The particle velocity =          2.179 mm/us
The speed of sound    =          6.822 mm/us
Gamma                 =          3.130

Cylinder runs:             % of standards
  V/V0     Energy    TATB     PETN      HMX     CL-20   TRITON
 (rel.)   (kJ/cc)  1.83g/cc 1.76g/cc 1.89g/cc 2.04g/cc 1.70g/cc
   1.00    -1.32
   2.20    -7.10     146      112       95       78      163
   4.10    -8.47     146      110       96       80      153
   6.50    -9.02     145      109       96       81      148
  10.00    -9.37     144      108       96       82      143
  20.00    -9.78     142      107       96       82      136
  40.00   -10.08     141      106       96       83      130
  80.00   -10.30     140      105       96       83      125
 160.00   -10.48

Freezing occurred at T =     1800.0 K and relative V =   2.111
The mechanical energy of detonation =    -10.626 kJ/cc
The thermal energy of detonation    =     -0.000 kJ/cc
The total energy of detonation      =    -10.626 kJ/cc

JWL Fit results:
E0    =      -11.045 kJ/cc
A     =      1081.02 GPa, B     =     11.60 GPa, C     =         1.52 GPa
R[1] =          4.74,     R[2] =      1.07,      omega =         0.38
RMS fitting error =   0.96 %
```

D.1.2 Density 1.80 g/cm^3

```
Density  =  1.8000 g/cc   Mixture TMD =  1.8571 g/cc   % TMD = 96.9278
```

```
The C-J condition:
The pressure          =          33.70 GPa
The volume            =          0.421 cc/g
The density           =          2.376 g/cc
The energy            =           4.08 kJ/cc explosive
The temperature       =           4095 K
The shock velocity    =          8.791 mm/us
The particle velocity =          2.130 mm/us
The speed of sound    =          6.661 mm/us
Gamma                 =          3.127

Cylinder runs:             % of standards
  V/V0     Energy    TATB     PETN      HMX    CL-20   TRITON
 (rel.)   (kJ/cc)  1.83g/cc 1.76g/cc 1.89g/cc 2.04g/cc 1.70g/cc
   1.00    -1.23
   2.20    -6.72     138      106       90       74      154
   4.10    -8.05     139      104       91       76      146
   6.50    -8.59     138      104       91       77      141
  10.00    -8.94     137      103       91       78      136
  20.00    -9.35     136      102       92       79      130
  40.00    -9.64     135      102       92       79      125
  80.00    -9.87     134      101       92       80      120
 160.00   -10.04

Freezing occurred at T =     1800.0 K and relative V =   2.171
The mechanical energy of detonation =    -10.194 kJ/cc
The thermal energy of detonation    =     -0.000 kJ/cc
The total energy of detonation      =    -10.194 kJ/cc

JWL Fit results:
E0   =      -10.532 kJ/cc
A    =      1000.02 GPa, B    =    10.91 GPa, C     =         1.75 GPa
R[1] =         4.76,     R[2] =     1.11,     omega =         0.42
RMS fitting error =   0.74 %
```

D.1.3 Density 1.78 g/cm^3

```
Density  =  1.7800 g/cc   Mixture TMD =  1.8571 g/cc   % TMD = 95.8508

The C-J condition:
The pressure          =          32.79 GPa
The volume            =          0.426 cc/g
The density           =          2.350 g/cc
The energy            =           3.98 kJ/cc explosive
The temperature       =           4107 K
The shock velocity    =          8.717 mm/us
The particle velocity =          2.114 mm/us
The speed of sound    =          6.603 mm/us
Gamma                 =          3.124

Cylinder runs:             % of standards
  V/V0     Energy    TATB     PETN      HMX    CL-20   TRITON
 (rel.)   (kJ/cc)  1.83g/cc 1.76g/cc 1.89g/cc 2.04g/cc 1.70g/cc
   1.00    -1.20
   2.20    -6.58     136      104       88       73      151
   4.10    -7.91     136      102       89       75      143
   6.50    -8.45     136      102       90       76      138
  10.00    -8.80     135      101       90       77      134
  20.00    -9.20     134      100       90       77      128
  40.00    -9.49     133      100       91       78      123
  80.00    -9.72     132       99       91       79      118
 160.00    -9.89
```

```
Freezing occurred at T =     1800.0 K and relative V =   2.191
The mechanical energy of detonation =    -10.044 kJ/cc
The thermal energy of detonation    =     -0.000 kJ/cc
The total energy of detonation      =    -10.044 kJ/cc

JWL Fit results:
E0   =      -10.379 kJ/cc
A    =       972.73 GPa, B    =     10.69 GPa, C     =         1.75 GPa
R[1] =         4.77,     R[2] =      1.11,     omega =         0.42
RMS fitting error =   0.74 %
```

D.2 Sats 432/13

D.2.1 TMD – 1.853 g/cm^3

```
Product library title: bkwc
Reactant library title: # Version 2.0 by P. Clark Souers

The composition:
Name      % wt.   % mol  % vol    Heat of     Mol.   TMD
                                formation     wt.    (g/cc)
                                (cal/mol)
hmx        94.30  87.79  91.73    17866   296.17     1.91 c4h8n8o8
ipdi        0.40   0.50   0.70   -88910   222.28     1.06 c12h18n2o2
gap         2.65   7.37   3.80    33939    99.09     1.29 c3h5n3o1
bamo        2.65   4.34   3.78   100382   168.16     1.30 c5h8n6o1

Density = 1.8530 g/cc   Mixture TMD = 1.8530 g/cc   % TMD = 100.0000

The C-J condition:
The pressure          =          36.16 GPa
The volume            =          0.409 cc/g
The density           =          2.446 g/cc
The energy            =           4.38 kJ/cc explosive
The temperature       =           4054 K
The shock velocity    =          8.974 mm/us
The particle velocity =          2.175 mm/us
The speed of sound    =          6.799 mm/us
Gamma                 =          3.127

Cylinder runs:              % of standards
  V/V0     Energy    TATB     PETN      HMX    CL-20   TRITON
 (rel.)   (kJ/cc)  1.83g/cc 1.76g/cc 1.89g/cc 2.04g/cc 1.70g/cc
   1.00    -1.31
   2.20    -7.06    146      111       95       78      162
   4.10    -8.42    145      109       95       80      153
   6.50    -8.97    144      108       95       81      147
  10.00    -9.32    143      107       95       81      142
  20.00    -9.73    142      106       96       82      136
  40.00   -10.03    140      106       96       83      130
  80.00   -10.25    139      105       96       83      124
 160.00   -10.43

Freezing occurred at T =     1800.0 K and relative V =   2.112
The mechanical energy of detonation =    -10.582 kJ/cc
The thermal energy of detonation    =     -0.000 kJ/cc
The total energy of detonation      =    -10.582 kJ/cc

JWL Fit results:
E0   =      -10.927 kJ/cc
```

A = 1065.67 GPa, B = 11.46 GPa, C = 1.76 GPa
R[1] = 4.74, R[2] = 1.11, omega = 0.42
RMS fitting error = 0.72 %

D.2.2 Density 1.80 g/cm^3

Density = 1.8000 g/cc Mixture TMD = 1.8530 g/cc % TMD = 97.1399

The C-J condition:
The pressure = 33.64 GPa
The volume = 0.421 cc/g
The density = 2.376 g/cc
The energy = 4.08 kJ/cc explosive
The temperature = 4086 K
The shock velocity = 8.779 mm/us
The particle velocity = 2.129 mm/us
The speed of sound = 6.650 mm/us
Gamma = 3.124

Cylinder runs: % of standards

V/V0 (rel.)	Energy (kJ/cc)	TATB 1.83g/cc	PETN 1.76g/cc	HMX 1.89g/cc	CL-20 2.04g/cc	TRITON 1.70g/cc
1.00	-1.23					
2.20	-6.70	138	106	90	74	154
4.10	-8.04	138	104	91	76	146
6.50	-8.57	138	103	91	77	140
10.00	-8.93	137	103	91	78	136
20.00	-9.33	136	102	92	79	130
40.00	-9.63	135	101	92	79	125
80.00	-9.85	134	101	92	80	120
160.00	-10.02					

Freezing occurred at T = 1800.0 K and relative V = 2.168
The mechanical energy of detonation = -10.181 kJ/cc
The thermal energy of detonation = -0.000 kJ/cc
The total energy of detonation = -10.181 kJ/cc

JWL Fit results:
E0 = -10.591 kJ/cc
A = 999.96 GPa, B = 10.96 GPa, C = 1.51 GPa
R[1] = 4.76, R[2] = 1.07, omega = 0.38
RMS fitting error = 0.97 %

D.2.3 Density 1.78 g/cm^3

Density = 1.7800 g/cc Mixture TMD = 1.8530 g/cc % TMD = 96.0606

The C-J condition:
The pressure = 32.73 GPa
The volume = 0.425 cc/g
The density = 2.350 g/cc
The energy = 3.97 kJ/cc explosive
The temperature = 4098 K
The shock velocity = 8.705 mm/us
The particle velocity = 2.112 mm/us
The speed of sound = 6.593 mm/us
Gamma = 3.122

Cylinder runs: % of standards

V/V0 (rel.)	Energy (kJ/cc)	TATB 1.83g/cc	PETN 1.76g/cc	HMX 1.89g/cc	CL-20 2.04g/cc	TRITON 1.70g/cc
1.00	-1.20					
2.20	-6.57	135	103	88	73	151

```
   4.10    -7.89     136      102       89       75      143
   6.50    -8.43     135      102       89       76      138
  10.00    -8.78     135      101       90       76      134
  20.00    -9.19     134      100       90       77      128
  40.00    -9.48     133      100       90       78      123
  80.00    -9.70     132       99       91       79      118
 160.00    -9.87

Freezing occurred at T =     1800.0 K and relative V =   2.188
The mechanical energy of detonation =    -10.031 kJ/cc
The thermal energy of detonation    =     -0.000 kJ/cc
The total energy of detonation      =    -10.031 kJ/cc

JWL Fit results:
E0   =      -10.437 kJ/cc
A    =       972.99 GPa, B    =     10.74 GPa, C     =         1.51 GPa
R[1] =         4.76,     R[2] =      1.07,     omega =         0.38
RMS fitting error =   0.97 %
```